STANLEY, JARROD LEE, M.S. Palladium Catalyzed Dehydration of Primary Amides: A Step Economical Synthesis of Vildagliptin (2021)

Directed by Dr. Mitchell P. Croatt. 111 pp.

The development of reactions that facilitate a concise path to chemical complexity has long been a focus within the synthetic community. Specifically, the use of readily available starting materials towards efficient routes to chemically relevant molecules is imperative. These designed reactions exhibit utility to applications within synthetic, medicinal, and materials science. Herein, efforts to endow the scientific community with efficacious syntheses is realized with the step economical synthesis of Vildagliptin.

A novel Selectfluor-modified palladium catalyst enabled the dehydration of primary amides for a concise route to nitrile moieties. These reactions were studied for their unique reactivities and to elucidate mechanistic insight. Following successful manipulation of more than 20 substrates, the utility of the methodology turned to the total synthesis of Vildagliptin. Vildagliptin is a nitrile bearing anti-diabetic medication that can be formed using a primary amide precursor. Once Vildagliptin was synthesized using the dehydration methodology, a more efficacious route was desired and efforts began towards a one-pot synthesis of the medication. The capability to produce chemically relevant products in a step economical manner will benefit not only the synthetic community, but also the recipients of medications and products resulting from such developments.

PALLADIUM CATALYZED DEHYDRATION OF PRIMARY AMIDES: A STEP ECONOMICAL SYNTHESIS OF VILDAGLIPTIN

by

Jarrod Lee Stanley

A THESIS

Submitted to

the Faculty of The Graduate School at

The University of North Carolina at Greensboro

in Partial Fulfillment

of the Requirements for the Degree

Master of Science

Greensboro

2021

Approved by

_____

Committee Chair

DEDICATION

To Carson and Madison.

APPROVAL PAGE

This thesis written by Jarrod Lee Stanley has been approved by the following committee of the Faculty of The Graduate School at The University of North Carolina at Greensboro

Committee Chair Dr. Mitchell P. Croatt

Committee Members Dr. Jason J. Reddick

Dr. Robert B. Banks

4/27/2021

Date of Acceptance by Committee

4/21/2021

Date of Final Oral Examination

TABLE OF CONTENTS

LIST OF TABLES

LIST OF FIGURES

LIST OF SCHEMES

CHAPTER I: INTRODUCTION

Justification of Synthetic Achievements

Prevailing universal challenges involve two common themes: elucidating the elemental properties of our universe and extending the longevity of our existence. In response to these enigmatic quandaries, indelible synthetic achievements have contributed generously to our chemical coffers. As a cornerstone of chemistry, organic synthetic research continues to resolve the most fundamental questions about molecular interaction. These answers yield extensions to life via development of synthetic medications and comprehensive knowledge about molecular interaction.

The utility of synthetic chemistry hinges on time and step economic realization of more complex molecules.[1] With this in mind, this thesis presents the use of readily available starting materials to yield Vildagliptin (**1**), an anti-hyperglycemic medication bearing a nitrile moiety **(Figure 1.1)**.[2]

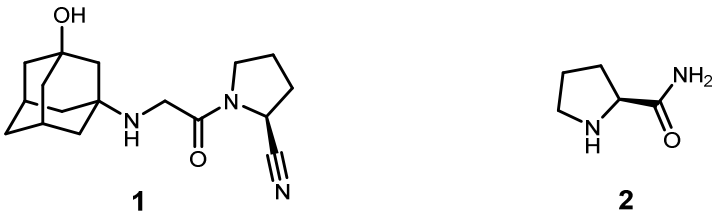

Figure 1.1: Vildagliptin, Prolinamide

This process involves a 1-step *in situ* synthesis of Vildagliptin beginning with L-prolinamide (**2**), an abundant and easily acquired molecular building block **(Figure 1.1)**.[3] L-prolinamide was acetylated, coupled with an adamantal moiety, and consequently dehydrated to form Vildagliptin. This approach was carried out in a one flask reaction utilizing *in situ* additions of components with a single purification step

Introduction to Nitriles

The importance of nitriles has significant historical precedence beginning in 1782 with C. W. Scheele's successful preparation of hydrogen cyanide.[4] Following a semi-centennial period, Wöhler and Liebig reported the first known synthesis of nitriles in 1832 producing benzyl cyanide and benzonitrile. However, it was not until 1844 that Hermann Fehling was able to characterize benzonitrile by comparison to the known synthesis of hydrogen cyanide.[5] Fehling conceived the term "nitrile" that is now used to identify the ubiquitous compound.[6] Since inception, nitriles have expanded into a myriad of applications including more than 30 nitrile containing pharmaceuticals currently prescribed.[7] Vildagliptin (**1)** is an antidiabetic medication that inhibits dipeptidyl peptidase-IV. Nitrile-containing fluoroquinolones (**Figure 1.2, 3**) have exhibited potency against Methicillin-Resistant *Staphylococcus aureus*,[8] a bacterium attributed with high mortality rates,[9] and Anastrazole (**Figure 1.2, 4**) treats osterogen-dependent breast cancer. Materials science uses nitriles to develop designer magnets[10] and high-performance thermoplastic polymers.[11] Perhaps most significant is the organocatalytic manipulation of nitriles into other functional groups such as carboxylic acids,[12] aldehydes,[13] esters,[14] heterocycles[15] and more.[16]

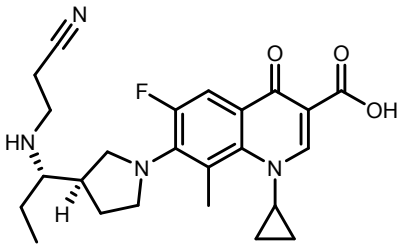

Nitrile Bearing Fluoroquinolone (**3**)

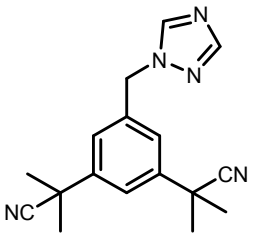

Anastrazole (**4**)

Figure 1.2: Nitrile Containing Pharmaceuticals

Synthetic methods for nitrile formation command further investigation to meet the diverse applications of the functional group.[17] New reaction designs may consider transition metal complexes. For example, typically Pd^{II} catalysts are used to hydrolyze nitriles to amides, but in 2005 Maffioli[18] reported a dehydration of primary amides to nitriles using a $PdCl_2$ catalyst in aqueous acetonitrile. In 2018 Croatt *et al* attempted to semi-synthetically improve the activity of

Alamethicin F50 **(Figure 1.3)** by fluorination using Selectfluor and $Pd(OAc)_2$, and inadvertently developed a novel dehydration methodology to produce nitriles.[19] Application of this synthetic methodology to the formation of molecules such as Vildagliptin **1** can mitigate issues inherent to nitrile installation in the presence of other functional groups.[20]

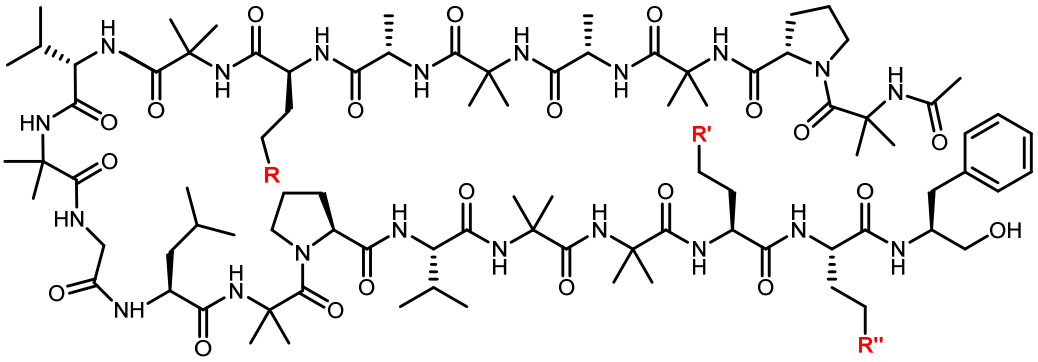

R, R', R'' = $CONH_2$, Alamethicin (**5**)
R, R', R' = CN (**6**)

Figure 1.3: Alamethicin F50 and Dehydrated Alamethicin F50

Discovery of Vildagliptin

In 1991 Novartis® began the grassroots efforts into the application of dipeptidyl peptidase IV inhibitors. Eventually this work led to the discovery of Vildagliptin (**1**) as an antidiabetic agent in 1998.[21] Vildagliptin is an aminonitrile containing drug for monotherapy or used in combination with Metformin, another type-2 diabetic medication.[22] Vildagliptin has less undesired side effects than Metformin, although slightly less effective, and functions by inhibiting dipeptidyl peptidase IV (DPP IV). The DPP IV enzyme rapidly metabolizes incretins,[23] and inhibiting the protein extends the action of incretins which increase pancreas activity for secretion of insulin, thus functioning as an antihyperglycemic treatment for type-2 diabetes. As one of the most chronic diseases in the world, type-2 diabetes requires more efficacious synthetic routes to drugs like Vildagliptin.[24]

Although initial syntheses of Vildagliptin remain patent protected, a 2003 publication by E.B. Villhauer[25] reports a 3-step synthesis in which L-prolinamide (**2**) is first acetylated **(Figure 1.4)**, and then dehydrated to yield the nitrile (**8**) from its respective amide (**7**). The resulting (*S*)-1-(2-

chloroacetyl)pyrrolidine-2-carbonitrile (**8**) is then coupled to 3-amino-1-adamantanol (**9**) to yield Vildagliptin (**1**) in 14-23% yield.

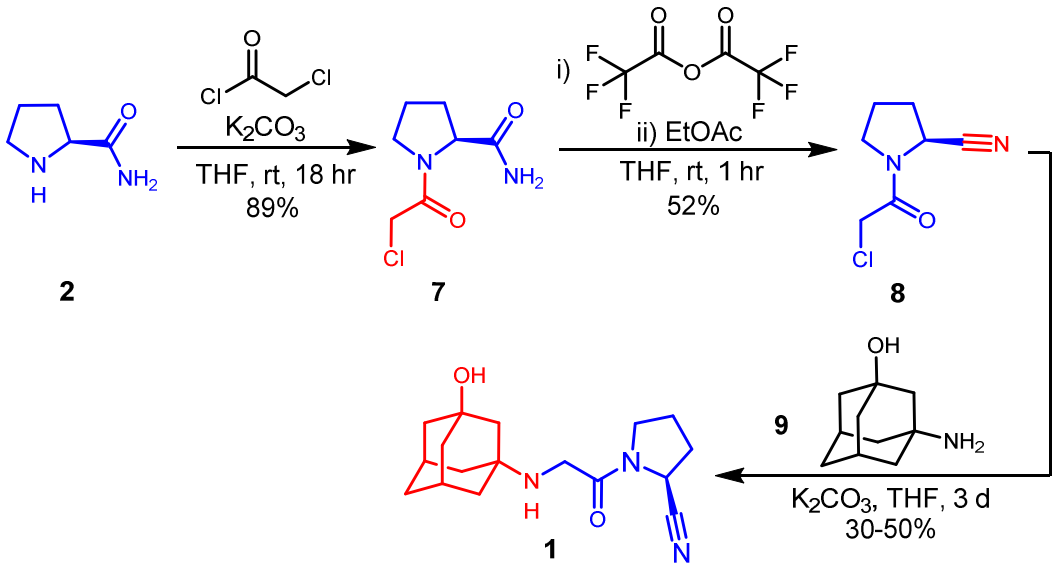

Figure 1.4: Villhauer Approach to Vildagliptin

Pharmaceutical interest in Vildagliptin encouraged other synthetic routes including a 3-step synthesis in 2013 from Glenmark employing Vilsmeier's reagent, gold, and $SOCl_2$.[26] In 2014, Deng used L-proline starting material in a 4-step synthesis that improved typical yields to 59%.[27] Notably, Deng employed Finkelstein conditions when adding the adamantal moiety to promote decreased reaction times.[28] In 2015, Novartis adapted the Vildagliptin synthesis to flow chemistry reactors to streamline the production and maintained a 3-step synthetic route.[29] Adapting reaction conditions to continuous flow and batch technologies implements safer practices for industrial environments and prevents time lost to isolation of materials over multiple steps. In context of this advantage, the authors determined isolation of (*S*)-1-(2-chloroacetyl)pyrrolidine-2-carbonitrile (**8**) was essential prior to attaching the adamantal moiety. This is a significant impediment to the flow chemistry process, and formation of the nitrile intermediate continues to be a point of contention in the full synthesis of Vildagliptin.

Seeking to resolve synthetic obstacles to Vildagliptin, the Croatt group has developed a synthetic strategy to potentially afford Vildagliptin in a single pot. Converting L-prolinamide to Vildagliptin in a single pot has attractive complexity in both industrial and academic fields. Use

of the Croatt group's previously developed dehydration conditions provides the ability to rearrange the synthetic pathway and mitigate complications with formation or isolation of nitrile intermediate **8.** Also important is the ability to dehydrate natural products to cyano-bearing structural analogs. Nitrile-containing enzymes are studied for synthetic applications[30] and more than 120 nitrile-containing natural products are currently known.[31] Understanding the influence of nitrile-containing natural products on the bacterial community is an urgent target,[32] and a synthetic method for nitrile installation can facilitate elucidation of their biological role.[33]

CHAPTER II: DEVELOPMENT AND UTILIZATION OF A PALLADIUM CATALYZED DEHYDRATION OF PRIMARY AMIDES TO FORM NITRILES

This article was published in the Journal of Organic Chemistry and is presented as published. My personal contributions to this manuscript include optimization of the dehydration conditions, synthesis of primary amides, subsequent dehydrations, qualitative and quantitative analysis. I also contributed to the writing of the manuscript, including development of the supporting information.

Al-Huniti, M. H.; Rivera-Chávez, J.; Colón, K. L.; Stanley, J. L.; Burdette, J. E.; Pearce, C. J.; Oberlies, N. H.; Croatt, M. P. Development and Utilization of a Palladium-Catalyzed Dehydration of Primary Amides To Form Nitriles. *Org. Lett.* **2018**, *20* (19), 6046–6050.

[†]Department of Chemistry and Biochemistry, University of North Carolina at Greensboro, 435 Sullivan Science Building, Greensboro, North Carolina 27402, USA

[‡]Institute of Chemistry, Universidad Nacional Autónoma de México, Circuito Exterior s/n, Coyacán, Mexico City 04510, Mexico

[§]Department of Medicinal Chemistry and Pharmacognosy, University of Illinois at Chicago, 900 A. Ashland Ave., Chicago, IL 60607, USA

[I]Mycosynthetix, Inc., Suite 103, 505 Meadowlands Drive, Hillsborough, NC 27278, USA

Abstract

A palladium(II) catalyst, in the presence of Selectfluor, enables the efficient and chemoselective transformation of primary amides into nitriles. The amides could be attached to aromatic rings, heteroaromatic rings, or aliphatic side chains, and the reactions tolerated steric bulk and electronic modification. Dehydration of a peptaibol containing three glutamine groups afforded

structure-activity relationships for each glutamine residue. Thus, this dehydration can act similarly to an alanine scan for glutamines via synthetic mutation.

In the area of new reaction design and development, the chemoselective interconversion of functional groups is highly sought after.[34] Two noteworthy examples include 1) the selective methylation of the carboxylic acid of amphotericin B in the presence of seven alkenes, nine secondary alcohols, a hemiacetal, and a primary amine[35] and 2) the C-H oxygenation of a bryostatin analogue with DMDO in the presence of eleven similar C-H bonds, an alkene, an acetal, and three carboxyl groups.[36] The first case represents the conversion of a carboxylic acid to an ester, a relatively simple transformation that modifies reactivity, but the conversion in amphotericin B is complicated by the other functional groups surrounding it. For example, typical Fisher esterification using strong acid is not compatible with this molecule. Similarly, the dehydration of a primary amide to form a nitrile, which has been previously explored,[18] is often complicated by the presence of other functional groups.[24] Transition metal catalyzed dehydration reactions typically utilize acetonitrile[18,37] or *N*-methyl-*N*-(trimethylsilyl)trifluoroacetamide (MSTFA)[38,39,40] as a dehydrating agent (Scheme 2.1). These reactions generate acetamide as a byproduct from acetonitrile or *N*-methyltrifluoroacetamide and hexamethyldisiloxane from MSTFA. For reactions involving MSTFA, high reaction temperatures and excess amounts of MSTFA are required. Non-aqueous acetonitrile reactions require excess amounts of lithium and silver salts.[37] On the other hand, reactions involving water as co-solvent can proceed at room temperature,[18] but are limited to substrates that are stable and soluble under aqueous conditions (Scheme 2.1, a)

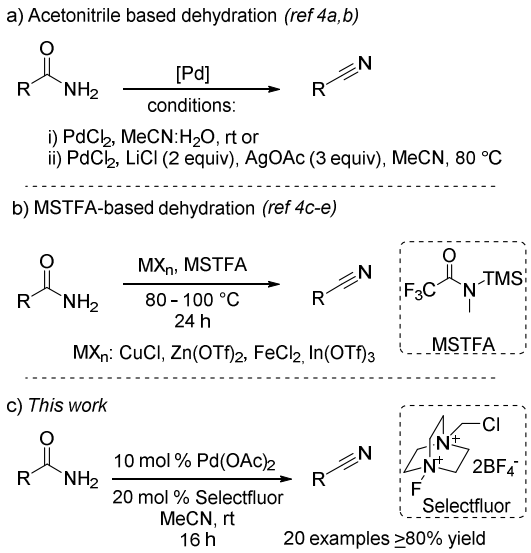

Scheme 2.1: Methods to Convert Primary Amides to Nitriles

During our studies to semi-synthetically improve the activity of natural products, typically by incorporating fluorine into the molecule,[41] we attempted to fluorinate alamethicin F50, a 20-mer peptaibol containing an acetylated N-terminus, a C-terminal phenylalaninol, and three glutamine (Gln) residues (Gln7, Gln18-19; Scheme 2.2).[42] Although our fluorination attempts were unsuccessful,[43] it was determined that all three glutamine residues were dehydrated in the presence of $Pd(Oac)_2$ and Selectfluor. This led to the formation of tricyano product 2, along with semi-dehydrated analogues (3-8; *vide infra*). This transformation was efficient and completely chemoselective without modifying the primary alcohol or any of the secondary or tertiary amides. Herein, we describe the further optimization and exploration of this dehydration reaction and utilize the dehydration of alamethicin F50 to illustrate the benefits of this reaction as a quick method to functionalize and determine the biological effects of the glutamine residues in the peptaibol

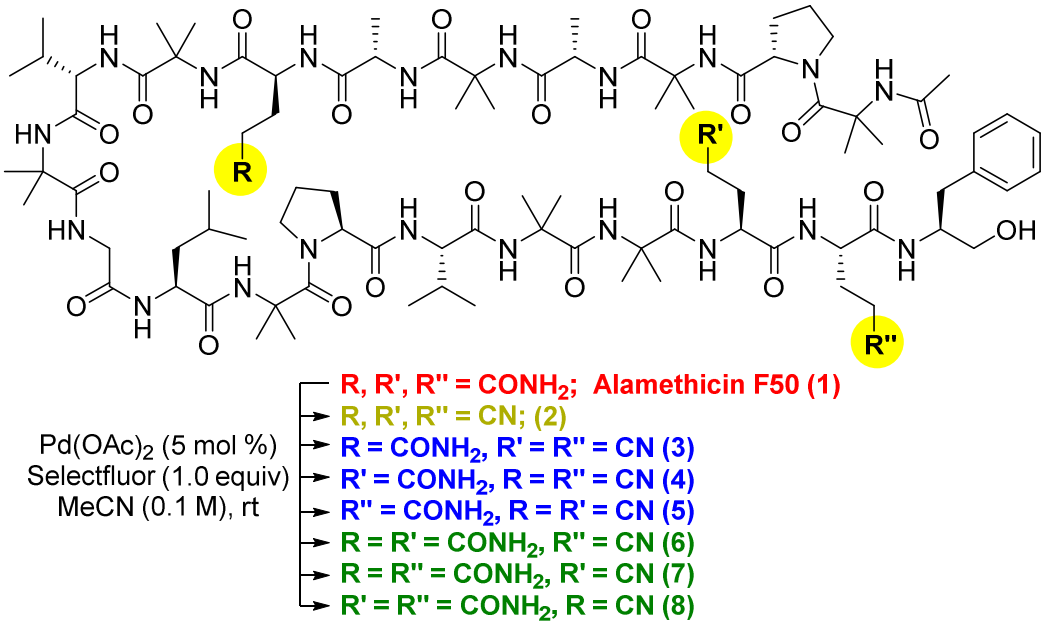

Scheme 2.2: Identification of a Chemoselective Dehydration

To examine the optimal conditions of the dehydration of primary amides, 4-methoxybenzamide was used as a model substrate in the presence of catalytic amounts of various metal salts and Selectfluor. The reaction gave excellent yields of the nitrile product in the presence of Pd(II) or Pd(0); contrasting results were observed with Zn(II) or Cu(II) catalyzed reactions (Table 2.1, entries 1-5). Although the $Pd_2(dba)_3$ reaction appears faster than that with $Pd(Oac)_2$, the purification was complicated by the dba (dibenzylideneacetone) ligand. Thus, catalyst loading and Selectfluor stoichiometry were examined using the $Pd(Oac)_2$ catalyst. Using 5 mol % of catalyst, the reaction yielded 71% of the desired nitrile after 16 h (Table 2.1, entry 6). Increasing the amount of Selectfluor to 40% gave nitrile **10a**, in addition to the fluorinated nitrile derivative (Table 2.1, entry 8). Reactions performed in the absence of Selectfluor or in the presence of DABCO instead of Selectfluor yielded no nitrile product. Although Selectfluor is a non-hygroscopic reagent, we examined the requirement for water using $Pd(Oac)_2$ in the absence of Selectfluor (Table 2.1, entries 11-13). Increasing the amount of water in the reaction improved the reaction yield (68% was observed with 2.0 equiv of water). For comparison, the addition of water to the reaction conditions with Selectfluor was not beneficial. A previous report by Maffioli[18] found that the palladium-catalyzed dehydration requires water. We verified their results in the absence of Selectfluor, which indicates that Selectfluor is modifying the catalytic

cycle,[37] such that water is no longer required. After screening a variety of conditions, the optimal conditions were determined to be using 10 mol % $Pd(Oac)_2$ and 20 mol % Selectfluor in acetonitrile (entry 1)

Table 2.1: Optimization of Palladium-Catalyzed Dehydration with Selectfluor

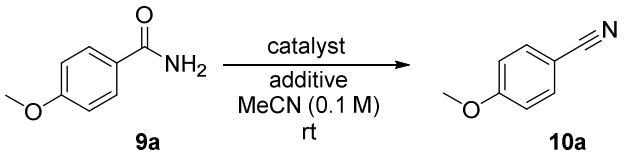

entry	cat. (mol %)	additive (mol %)	time (h)	yield (%)[a]
1	$Pd(Oac)_2$ (10)	Selectfluor (20)	16	96
2	$PdCl_2$ (10)	Selectfluor (20)	16	82
3	$Pd_2(dba)_3$ (5)	Selectfluor (20)	13	91
4	$ZnBr_2$ (10)	Selectfluor (20)	24	trace
5	$Cu(Otf)_2$ (10)	Selectfluor (20)	24	26
6	$Pd(Oac)_2$ (5)	Selectfluor (20)	16	71
7	$Pd(Oac)_2$ (10)	--	24	trace
8	$Pd(Oac)_2$ (10)	Selectfluor (40)	16	93[b]
9	$Pd(Oac)_2$ (10)	Selectfluor (5)	24	88
10	$Pd(Oac)_2$ (10)	DABCO (20)	24	NR[c]
11	$Pd(Oac)_2$ (10)	H_2O (50)	16	31
12	$Pd(Oac)_2$ (10)	H_2O (100)	16	42
13	$Pd(Oac)_2$ (10)	H_2O (200)	16	68

[a] Isolated yield. [b] 7% Fluorinated 4-methoxybenzonitrile was observed. [c] No reaction.

With the optimal conditions in hand, a series of primary amides were synthesized from their respective carboxylic acids and screened in the dehydration conditions (Scheme 2.3). The substrate scope is broad, with high yields for both aliphatic and aryl amides to generate aliphatic and aryl nitriles. High yields were observed from reactions involving non-, mono-, and di-substituted benzamides (10a-c and 10e-g; 80-96% yields). The lower yield for compound 10d (4-trifluoromethylbenzamide, 42% yield) was likely due to electronic factors. However, the effect was negligible on cinnamide derivatives (10h-10j). Several aliphatic amides were also converted to their corresponding primary, secondary, and tertiary nitriles in good yields. Importantly, the cyclopropyl moiety in amides (9t-9v) has been preserved under the reaction conditions to

generate cyclopropyl nitriles (10t-10v) in excellent yields (86-93%). In total, 22 substrates were screened, and it was determined that this reaction tolerates the presence of alkenes, aromatic rings, heteroaromatic rings, nitro groups, cyclopropanes, and halides. To further test the chemoselectivity of the reaction, we ran the dehydration of 9a in the presence of either salicylaldehyde or 4-phenylbutyric acid. These reactions gave desired product 10a (93% and 95% yield, respectively) with a quantitative recovery of salicylaldehyde and 4-phenylbutyric acid, illustrating that phenols, aldehydes, and carboxylic acids are also tolerated.

Based on our results and the similarity of conditions to prior reports,[18] the reaction mechanism (Scheme 2.4) might involve the formation of a mixed imidic anhydride (**B**) that undergoes proton transfer and coordination of acetate (**C**) followed by an elimination to yield the desired nitrile and acetamide (**D**), as has been proposed previously.[37] The role of Selectfluor remains uncertain, but one potential option is that it accelerates the catalytic cycle by formation of a Pd(IV) catalyst, as has been reported by others.[43,44] Additional evidence in support of a Pd(IV) mechanism is the observation of a signal at -181 ppm in the ^{19}F NMR when $Pd(Oac)_2$ is added to Selectfluor (^{19}F NMR signals for SelectFluor are 48 (N-F) and -151 (BF_4) ppm, Supporting Information (SI)). A more resolved mechanism for this reaction is still being examined and will be published in due course.

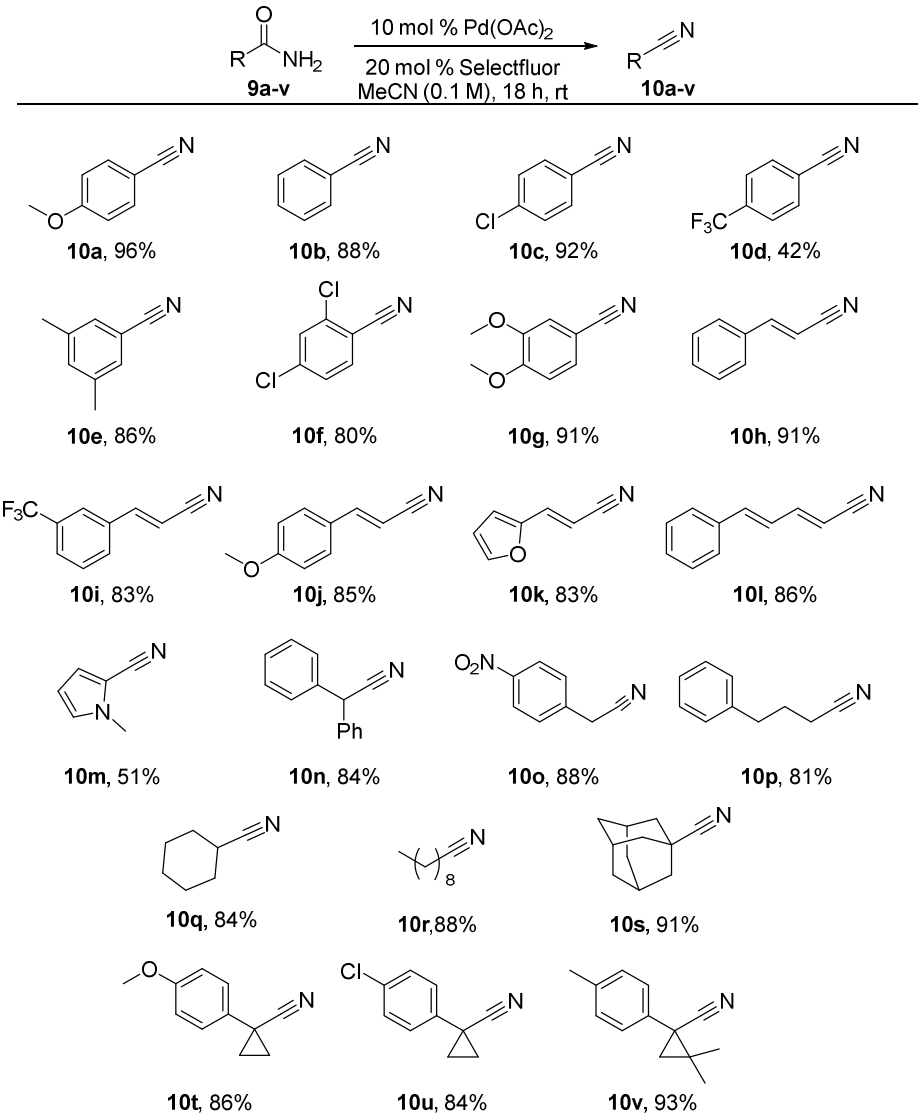

Scheme 2.3: Various Substrates for Primary Amide Dehydration

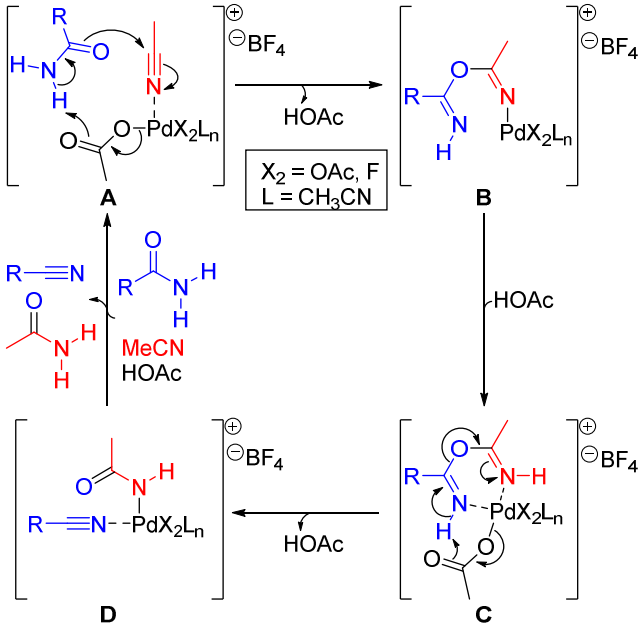

Scheme 2.4: Postulated Mechanism for Dehydration

To further establish the utility of the dehydration, alamethicin F50 was re-examined as a starting material (**1; Scheme 2.5**), with an approach focused on the exploration of the structure-activity relationship of the different primary amides. The reaction of compound **1** with SelectFluor (1.0 equiv) and $Pd(Oac)_2$ (5 mol %) in MeCN (0.1 M) at room temperature for 12 h gave the tricyano peptaibol derivative (**2**; 47% yield after purification), along with the dicyano product (**3**) where the glutamines at positions 18 and 19 were dehydrated (13% yield after purification). The structures of compounds **2** and **3** were confirmed by ^{1}H and ^{13}C NMR spectroscopy and HRESIMS/MS data (SI).

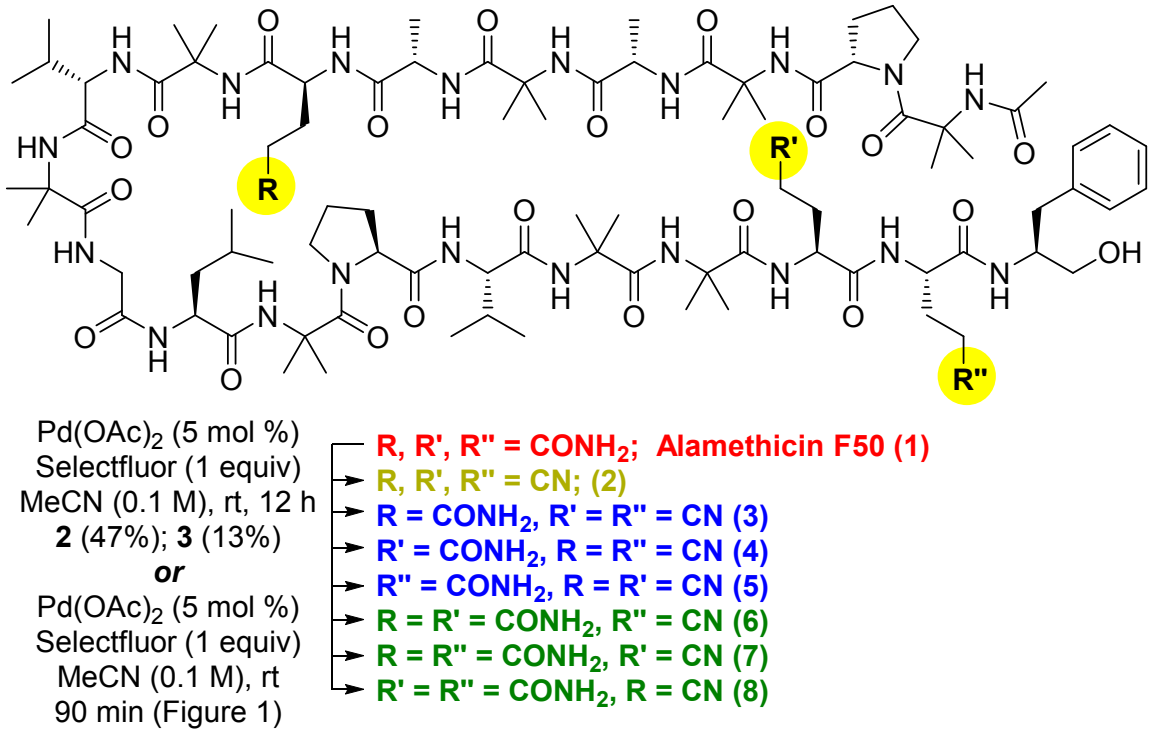

Scheme 2.5: Synthesis of mono-, di- and tri-cyano alamethecin F50 analogues

Scaling up of the reaction with SelectFluor in acetonitrile permitted the isolation, structural characterization, and biological evaluation of dehydrated analogues **2-8**. The structures of these analogues were established through analyses of their HRESIMS/MS spectra (SI). Importantly, these seven analogues were all accessed by a single reaction using **1** as the starting material instead of designing and developing seven different approaches or through the use of protecting groups.[45] Furthermore, in contrast to the more typically used alanine scan,[46] this method has a minimal change in the overall sterics of the sidechain since there is no deletion of carbon over the course of the reaction.

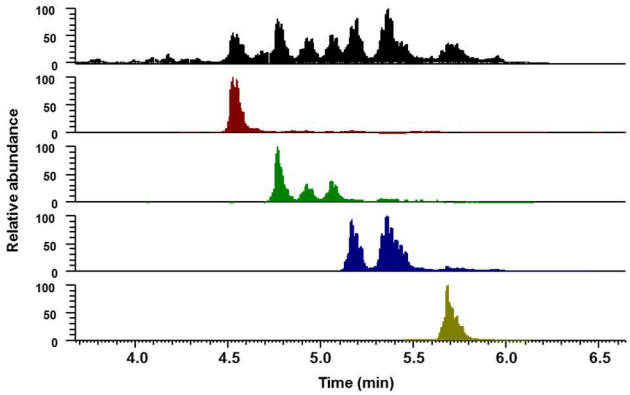

Figure 2.1: HRESIMS spectra of the reaction of **1** (10 mg, 5.9 µmol) with SelectFluor (2.1 mg, 5.9 µmol) and $Pd(Oac)_2$ (0.011 mg, 0.05 µmol) in MeCN (0.1M) at 25 °C after 90 min. In black is the base peak chromatogram, in maroon the extracted ion chromatogram for the staring material (**1**) at m/z 1963.0, in green the extracted ion chromatogram at m/z 1945.0 for the monocyano products (**6-8**), in navy the extracted ion chromatogram at m/z 1927.0 for the dicyano products (**3-5**), and in yellow the extracted ion chromatogram at m/z 1909.0 for the tricyano product (**2**).

Alamethicin F50 (**1**) is known to be antibacterial, antifungal, anthelmintic, and cytotoxic.[42,47] Based on our groups' attempts to generate anticancer leads,[41,48,49] we decided to determine the impact of the glutamine residues on the bioactivity in a panel of cancer cell lines (Table 2.2). The cytotoxicity data indicated that the glutamine at position seven was crucial for maintaining the cytotoxic properties of the molecule. This was determined since the analogue dehydrated exclusively at position seven (**8**) was inactive, whereas monocyano **6** and **7** were active. Similarly, dicyano **5** and **4**, both of which had position seven dehydrated, were inactive or much less active, respectively. Dehydration of glutamine 18 and/or 19 led to analogues that had similar activities. These results give unique insight into the impact of each glutamine residue on the cytotoxic properties of **1** and show that position seven is crucial to the observed cytotoxicity.

Table 2.2: Cytotoxicity of Alamethicin F50 and Dehydrated Analogues

compound	MDA-MB-435	MDA-MB-231	OVCAR3
1	4.4	3.7	7.8
2; R,R',R'' = CN	>25	>25.0	>25
3; R',R'' = CN	2.6	1.2	3.0
4; R,R'' = CN	3.1	8.7	13.4
5; R,R' = CN	>25	22.3	>25
6; R'' = CN	2.2	1.3	4.6
7; R' = CN	2.8	2.0	3.9
8; R = CN	>25	>25	>25
Taxol	0.0005	0.009	0.002

[a] IC_{50} values in the indicated cell lines were determined as the concentration required to reduce cellular proliferation by 50% relative to the untreated controls following 72 h of continuous exposure.

Several techniques, including X-ray diffraction,[50] NMR,[42,51,52] CD,[53] Raman, and molecular dynamics,[42,54] have been used to characterize the α-helical conformation of alamethicin F50 (**1**) in both solution and solid states.[42] In an attempt to gain information about the conformational changes induced by the dehydration of the glutamine residues in **1**, the CD spectrum for each analogue was recorded in MeCN (Figure **2.2**). The far UV/CD spectra, 260-180 nm, with absorbances attributed to the peptide bond, is the most extensively used spectroscopic readout to determine the secondary structures of peptides in solution (α-helix, β-pleated sheet, and random coil).[55] The right handed α-helix is reported to give two negative Cotton effects at 222 and 208 nm, while the β-pleated sheet shows one negative and one positive Cotton effect at 217 nm and 198 nm, respectively.[55]

Analysis of the experimental CD data obtained for alamethicin F50 (**1**) and its analogues (**2-8**) indicated that the mono- and dicyano compounds (**3-8**) predominantly retained the α-helical conformation, with a minor population of 3_{10}-helix, as previously reported by Peggion et al.[56] However, the CD spectrum for tricyano **2** indicated that the conformation was modified, increasing the population of the 3_{10}-helix conformer (Figure 2.2 and SI). Surprisingly, the helical nature of the different peptaibol analogues did not have a strong correlation with the cytotoxicity data (compare Figure 2.2 and Table 2.2). In Figure 2.2, the UV/CD spectra of alamethicin F50 (**1**) is most similar to that of monocyano analogues **6-8**, but analogue **8** is inactive. Likewise, there is a grouping in the spectra of dicyano analogues **3-5**, but analogue **3** is active, whereas

analogue **5** is inactive and compound **4** has decreased activity. These data indicate that the cytotoxicity of alamethicin F50 is dependent on the presence of a glutamine residue at position seven, and that the activity is not simply a stabilization of the α-helix conformation of the peptaibol

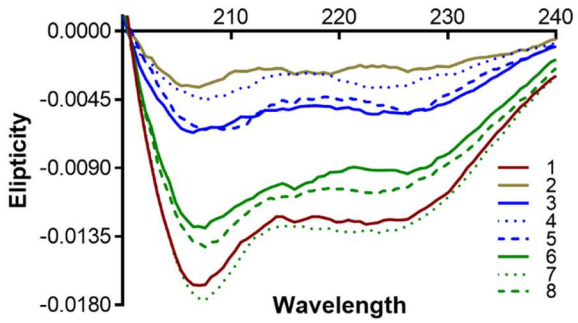

Figure 2.2: Far UV/CD-spectra for alamethicin F50 (**1**) and its dehydrated analogues (**2-8**).

In summary, a Selectfluor-modified palladium catalyst was shown to enable the chemoselective dehydration of primary amides to generate nitriles. The reaction tolerates the presence of primary alcohols, primary amides, secondary amides, aldehydes, carboxylic acids, nitro groups, alkenes, heteroaromatic rings, halides, and cyclopropanes and is efficient with aromatic and aliphatic amides, with little impact by the electronics or sterics of the system. The application of the dehydration method facilitated the synthesis of the seven possible dehydrated analogues of alamethicin F50 (**1**). Importantly, all the peptaibol derivatives were generated in a single reaction in sufficient amounts for purification, characterization, and biological evaluation. The application of this methodology allowed us to generate data that highlight the importance of each individual glutamine residue on the bioactivity and conformation of **1**. We hypothesize that this primary amide dehydration methodology may be used as an alternative to alanine scanning to assess the implications of glutamine and possibly asparagine residues in the activity and 3D structure of peptides

Associated Content

SUPPORTING INFORMATION

Experimental information and spectral data for all compounds and cytotoxicity data for compounds **1-8**

The Supporting Information is available free of charge on the ACS Publications website.

Author Information

CORRESPONDING AUTHOR

*mpcroatt@uncg.edu

AUTHOR CONTRIBUTIONS

All authors have given approval to the final version of the manuscript.

Acknowledgement

This research was supported in part by P01 CA125066 from the National Cancer Institute/NIH, Bethesda, MD, USA. The authors thank Drs. Franklin J. Moy and Daniel A. Todd (both from UNCG) for assistance with NMR and high-resolution mass spectrometry data, respectively

CHAPTER III: SYNTHESIS OF VILDAGLIPTIN AND APPLICATION OF DEHYDRATION METHODOLOGY

Probing the Synthetic Route to Vildagliptin

Tandem reactions were used for the synthesis of Vildagliptin from commercially available starting materials in one step, which is at least two fewer steps compared to previously reported syntheses (Scheme 3.1).[25] The synthesis described herein rearranges a traditional pathway to Vildagliptin resulting in a final dehydration step.

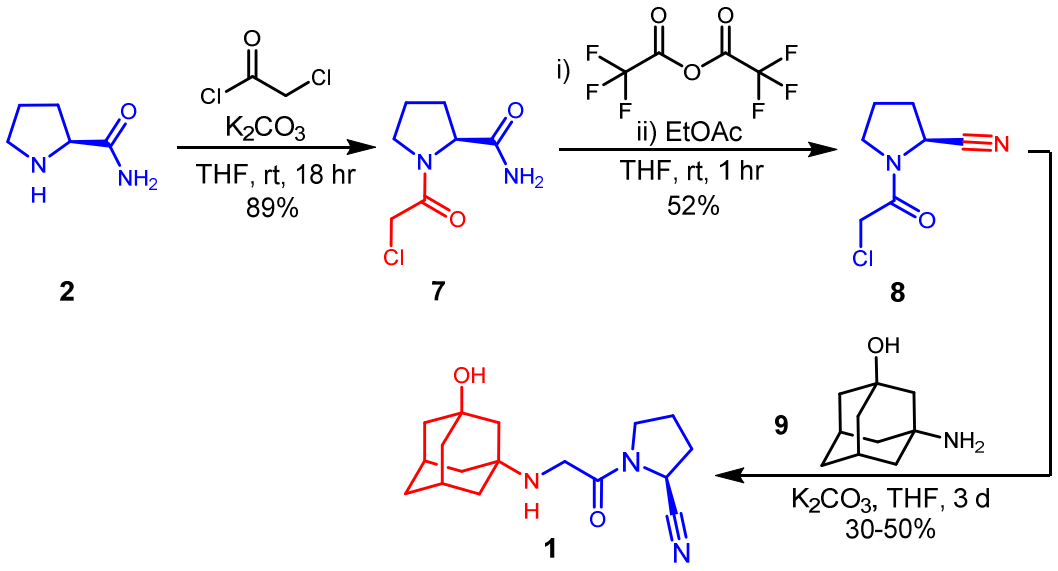

Scheme 3.1: Villhauer Approach to Vildagliptin

The route in Scheme 3.2 begins with the acetylation of L-prolinamide (**2**) using K_2CO_3 as a base and acetonitrile as a solvent.[57] After stirring under N_2 atmosphere at 30 °C for 15 hours the acetylated L-prolinamide (**7**) is afforded. In the same pot, 3-amino-1-adamantanol (2 eq), NaI (2 eq), and K_2CO_3 (2 eq) are added with CH_3CN (0.9 M). Introducing Finkelstein conditions promotes the formation of iodinated intermediate **10** yielding *N*-(3-hydroxy-1-adamantanol)glycyl-L-prolinamide (**11**) after stirring under N_2 at 35 °C for 15 hours. In the same pot the crude mixture is then subjected to dehydration conditions using $Pd(OAc)_2$ (10 mol %)

and Selectfluor (20 mol %) with aqueous CH_3CN as the solvent. After stirring under N_2 at room temperature for 12 hours the target molecule Vildagliptin **1** may be isolated.

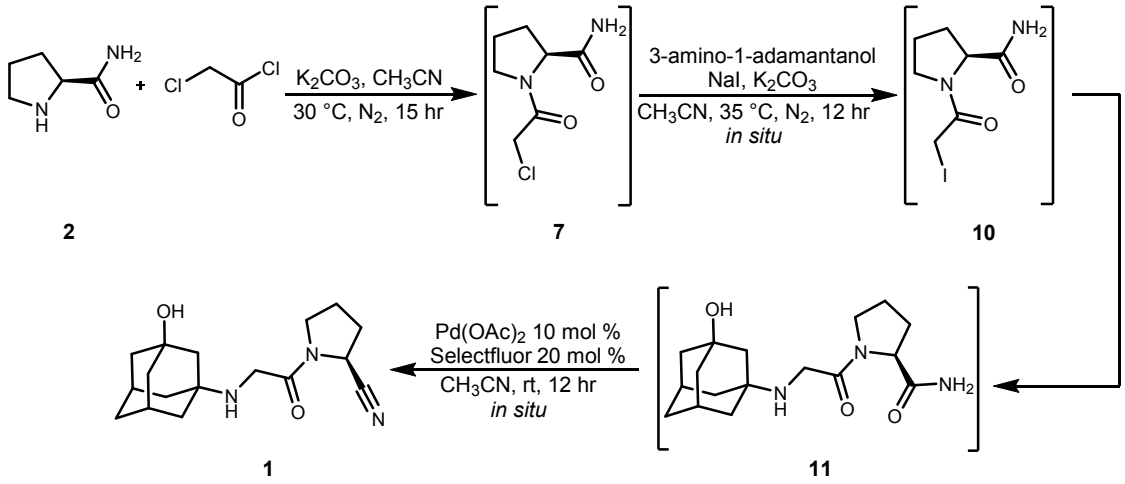

Scheme 3.2: One-pot Synthesis of Vildagliptin

Variations of the synthetic path to Vildagliptin were probed prior to realizing the one-pot route in Scheme 3.2. Efforts to acetylate L-prolinamide were initially facilitated with Et_3N (2 eq), DMAP (1 mol %), and DMF (Scheme 3.3). Problematic purification (removal of DMF), lengthy reaction times, and low yields resulted in divergent conditions with K_2CO_3 as base and CH_3CN for solvent as seen in Scheme 3.2

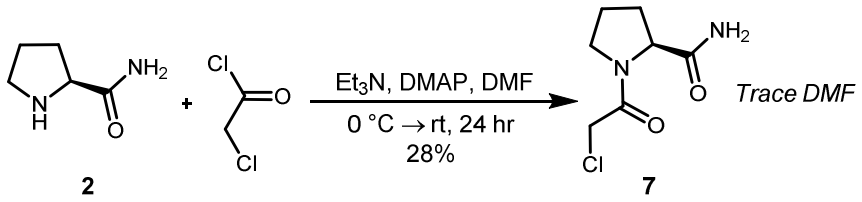

Scheme 3.3: Preliminary Conditions for Acylation of L-prolinamide

Also investigated was the dehydration of L-prolinamide using $Pd(OAc)_2$ (10 mol %) and Selectfluor (**13**) (20 mol %) with CH_3CN as solvent (**Scheme 3.4**). The unsuccessful dehydration (**A**) led to an investigation (**B**) that determined Selectfluor was oxidizing the amine of L-prolinamide to yield 3,4-dihydro-2H-pyrrole-5-carboxamide (**12**).

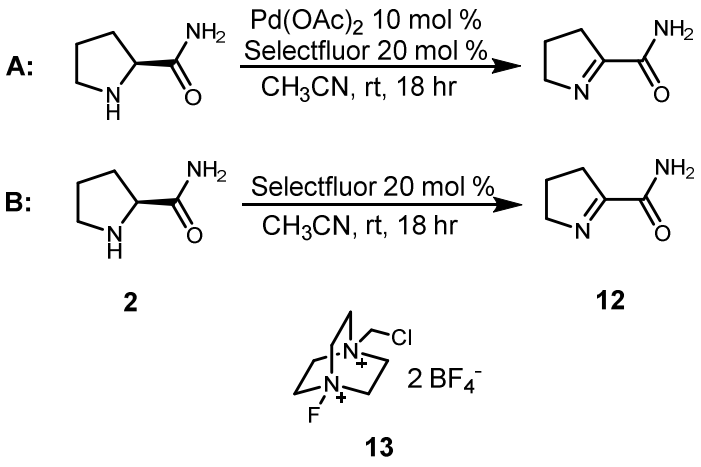

Scheme 3.4: Dehydration of L-prolinamide

In an alternate pathway, 1-chloroacetyl-2-(*S*)-pyrrolidinecarboxamide (**7**) was isolated and subsequently dehydrated to yield (*S*)-1-(2-chloroacetyl)pyrrolidine-2-carbonitrile (**8**) (**Scheme 3.5**) prior to installing the adamantal moiety to yield Vildagliptin (**1**). When converting the amide product **7** to the nitrile derivative **8** the oxidation of the amine is less favored due to the reactivity of the primary amide.

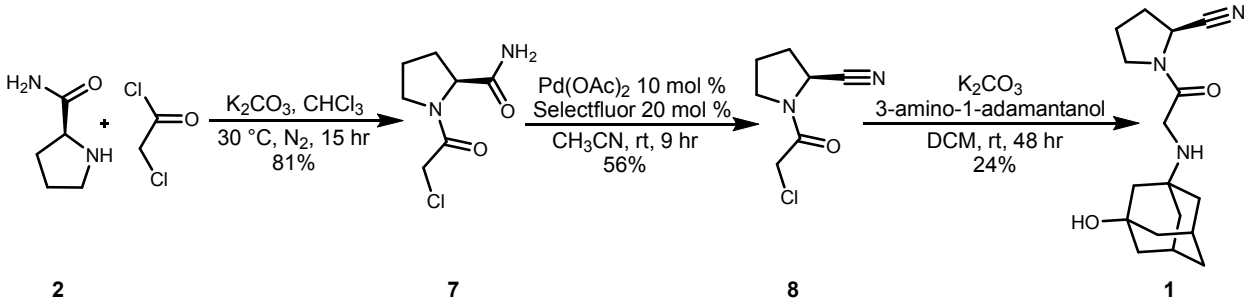

Scheme 3.5: Initial Route to Vildagliptin

Although the synthetic route exhibited in Scheme 3.5 was viable, the desire for enhanced chemical complexity in fewer steps remained a focal point for the synthesis of Vildagliptin. Consequently, a one-component solvent system was investigated for single-pot compatibility. Due to its required use for dehydration of **7** to its respective nitrile (**8**), acetonitrile was deemed a suitable solvent for tandem *in situ* reactions. To probe this, the solvent used for acylation of L-prolinamide in Scheme 3.5 ($CHCl_3$) was substituted with acetonitrile. Upon actualization, 1-

chloroacetyl-2-(*S*)-pyrrolidinecarboxamide (**7**) was subsequently reacted with 3-amino-1-adamantanol (**9**) *in situ* to yield *N*-(3-hydroxy-1-adamantanol)glycyl-L-prolinamide (**11**) (**Scheme 3.2**). These results indicated acetonitrile as a workable solvent as well as the ability to install an adamantal moiety prior to dehydration of **7**. With this knowledge in hand Scheme 3.2 was developed.

Challenges to Dehydration

Inaugural efforts to convert the primary amide of *N*-(3-hydroxy-1-adamantanol)glycyl-L-prolinamide (**11**) to a nitrile did not yield target molecule **1** by NMR analysis. The reaction utilized unpurified starting material in accordance with *in situ* conditions. To this crude solution $Pd(OAc)_2$ (20.9 mg, 0.093 mmol, 10 mol %) was added and the solution assumed a light brown color. Subsequently Selectfluor was added (67 mg, 0.19 mmol, 20 mol %). Upon addition of Selectfluor the reaction exhibited an intense color change from light brown to a dark red-orange. Similar color changes were observed from the oxidation of L-prolinamide in Scheme 3.4. Considering the possibility of oxidation at the secondary amine of **11**, a control experiment was performed without $Pd(OAc)_2$ (**Scheme 3.6 B**). This reaction returned the same results in the absence of $Pd(OAc)_2$, indicating the Pd was likely not entering the catalytic cycle, and Selectfluor was modifying the starting materials in lieu of the $Pd(OAc)_2$.

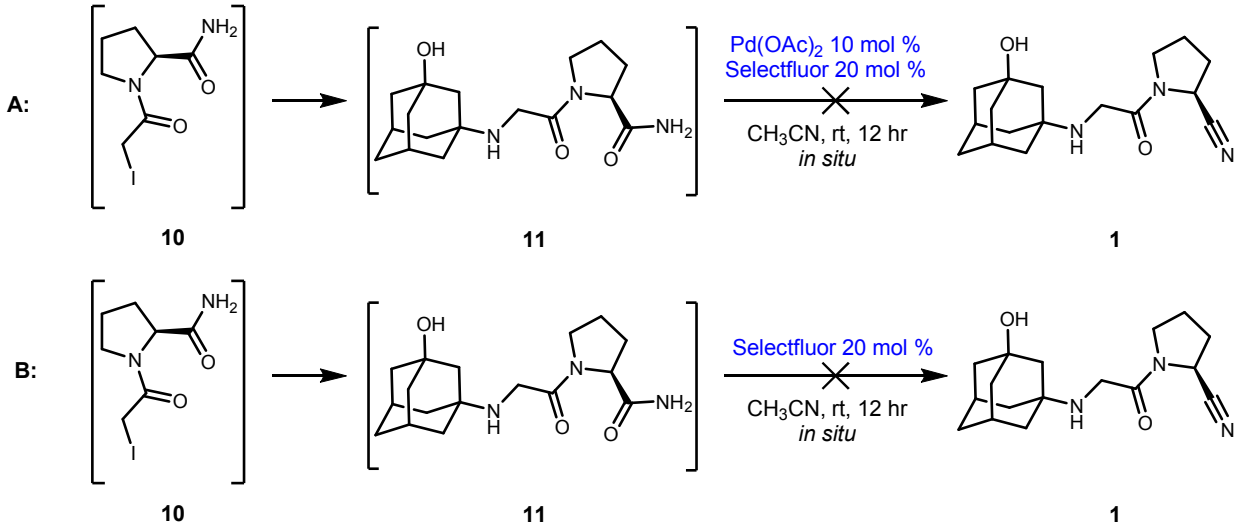

Scheme 3.6: Probing the Dehydration Reaction

This knowledge is valuable to the developed dehydration methodology[19], and indicates limitations for substrates possessing secondary amines. To mitigate the Selectfluor promoted oxidation of *N*-(3-hydroxy-1-adamantanol)glycyl-L-prolinamide **11**, efforts were made to stir $Pd(OAc)_2$ with Selectfluor prior to addition to the reaction mixture. In a 4 mL vial $Pd(OAc)_2$ (10 mol %) and Selectfluor (20 mol %) were combined and stirred in CH_3CN (10 minutes) before injecting the catalytic mixture into the reaction vessel. Ostensibly, the Selectfluor would promote a higher oxidation state of $Pd(OAc)_2$, which would in turn react with the substrate **11.** Unfortunately, similar results to Scheme 3.6 were obtained and none of the target molecule was recovered.

After discerning the oxidative relationship between Selectfluor and **11,** it was decided to interrogate the impact of the crude *in situ* mixture on $Pd(OAc)_2$. In order to do this *N*-(3-hydroxy-1-adamantanol)glycyl-L-prolinamide (**11**) was synthesized and purified. The expectation was to expose pure **11** to the dehydration conditions to determine if the crude reaction mixture was indeed hindering the catalytic cycle. The pure *N*-(3-hydroxy-1-adamantanol)glycyl-L-prolinamide (50.0 mg, 0.16 mmol, 1 eq) was placed in a 4 mL vial with 1 mL CH_3CN. In a separate 4 mL vial $Pd(OAc)_2$ (180 µL: 20 mg/mL CH_3CN, 3.59 mg, 0.016 mmol, 10 mol %) and Selectfluor (532 µL: 20 mg/mL CH_3CN, 10.63 mg, 0.03 mmol, 20 mol %) were stirred for 10 minutes, and then injected into the reaction vial. After stirring for 24 hours the reaction mixture was heterogenous, and the starting material unconsumed. It was determined that isolating *N*-(3-hydroxy-1-adamantanol)glycyl-L-prolinamide from the crude *in situ* solution results in a compound no longer soluble in CH_3CN.

Due to the time and effort required to synthesize *N*-(3-hydroxy-1-adamantanol)glycyl-L-prolinamide, it was decided to use a sample substrate to further investigate the effects of a crude *in situ* mixture on the dehydration methodology. To create a model substrate 3,4-dimethoxybenzoic acid **14** was used to form 3,4-dimethoxybenzamide **15** (**Scheme 3.7**) which was subsequently probed for *in situ* compatibility.

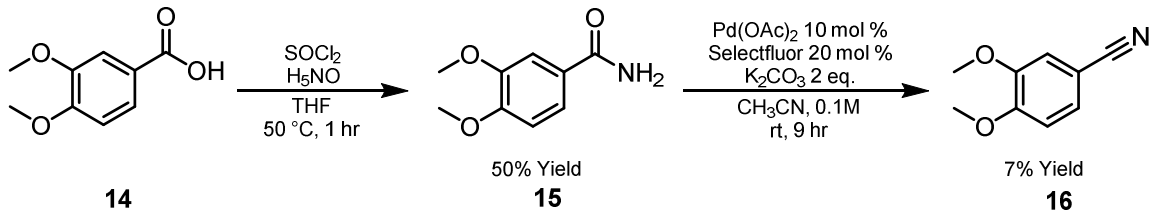

Scheme 3.7: Synthesis of 3,4-dimethoxybenzonitrile

As seen in Scheme 3.7 the dehydration of amide **11** to the nitrile bearing Vildagliptin **1** is carried out via *in situ* addition of palladium acetate and Selectfluor. The previous stage of the reaction scheme involves the addition of K_2CO_3 (2 equivalents). Previous syntheses indicate the need for isolation of intermediates and removal of K_2CO_3 prior to realizing **1**,[29]and indicate residual carbonate within the reaction mixture may inhibit the final dehydration reaction to yield target molecule **1**. To investigate this possibility the palladium catalyzed dehydration of 3,4-dimethoxybenzamide in Scheme 3.12 was performed with the addition of K_2CO_3 (2 equivalents). Previous results for this reaction experienced a 96% yield[19], however in the presence of K_2CO_3 a much lower 7% yield was observed. Thus, support for potassium carbonate hindering the reaction was revealed. Compelled to thwart this issue, another reaction was conducted to determine if the residual salts or carbonate in solution was culpable (**Scheme 3.8**).

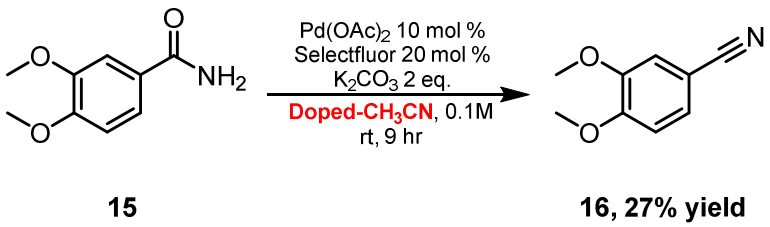

Scheme 3.8: Doped CH_3CN Dehydration

The solvent (CH_3CN) was first stirred with K_2CO_3 for 2 hours before filtering the solids and using the "doped" solvent for the dehydration reaction. The product was recovered in 27% yield. Literature values for this reaction are very good at ~ 97% yield, indicating that the carbonate in the solvent is hindering the reaction mechanism. However, the dramatic increase in yield indicates the solids from K_2CO_3 may also serve an inhibitory role. One hypothesis is K_2CO_3 creates a more basic solution where a less oxidized Pd^0 species is preferred, as promoted by Pourbaix.[58]This reduced Pd species does not subscribe to the purported catalytic mechanism for

the dehydration of primary amides to nitriles[19], and may indicate limitations to the substrate scope.

Conclusions and Future Work

This work sought to achieve a concise synthesis of Vildagliptin, a commercially produced anti-hyperglycemic medication. The work also focused on developing a one pot *in situ* synthesis through application of a previously developed palladium catalyzed dehydration of primary amides to nitriles. The very mild and highly chemoselective nature of the dehydration methodology indicates broad utility for various substrates and was conducive to achieving a short 3-step synthesis of Vildagliptin.

Achieving a one-pot *in situ* synthesis of Vildagliptin is not yet successful due to the nature of intermediate products, organization of synthetic steps, and a component-driven catalytic inhibition of dehydration. Intermediate nitrile bearing products once isolated became insoluble in the solvent system and were not productive to sequential reactions. The developed scheme for synthesizing Vildagliptin requires *in situ* addition of successive materials and a single-component solvent system. This approach mitigates the solubility issues observed, but presents other calamities resulting from K_2CO_3 used in the one-pot system. Obstruction of the catalytic path by K_2CO_3 shunts the purported relationship between $Pd(OAc)_2$ and Selectfluor in the reaction. This in turn promotes the oxidation of the substrate at the secondary amine. Discovering this potential oxidation is vital to further applications of the dehydration methodology. Dehydrating a substrate scope containing a variety of amines may yield clarification. For this work, rearranging the synthetic path to Vildagliptin may present solutions to this issue, but after probing a myriad of routes to an *in situ* synthesis this is likely not practical. Future work should include the stoichiometric manipulation of Selectfluor in the reaction to determine if excess Selectfluor is effectively oxidizing the substrate.

In conclusion, readily available starting materials were used to efficiently synthesize Vildagliptin in 3-steps by converting an amide intermediate to the nitrile bearing product. The 3-step synthesis validates a developed palladium catalyzed dehydration with application for generating medications that include nitrile moieties. Efforts to further consolidate the production to a one-

pot *in situ* synthesis were not fruitful, but proffered valuable information indicating limits of the dehydration methodology with regards to K_2CO_3 salts and/or secondary amines.

CHAPTER IV: EXPERIMENTAL DATA

General Information

All anhydrous reactions were performed with dry solvents in oven dried glassware under a nitrogen atmosphere. Unless otherwise noted, all solvents and reagents were obtained from commercial sources and used without further purification. Chromatographic purification was performed using silica gel (60 Å, 32-63 μm). NMR spectra were recorded using a JEOL ECA spectrometer (500 and 400 MHz for ^{1}H, 125 and 100 MHz for ^{13}C). Coupling constants, *J*, are reported in hertz (Hz) and multiplicities are listed as singlet (s), doublet (d), triplet (t), quartet (q), doublet of doublets (dd), triplet of triplets (tt), multiplet (m), etc. IR data was obtained with a Perkin Elmer FTIR spectrometer with ATR sampling accessory with frequencies reported in cm^{-1}. High Resolution Mass Spectra were acquired on a ThermoFisher Scientific LTQ Orbitrap XL MS system.

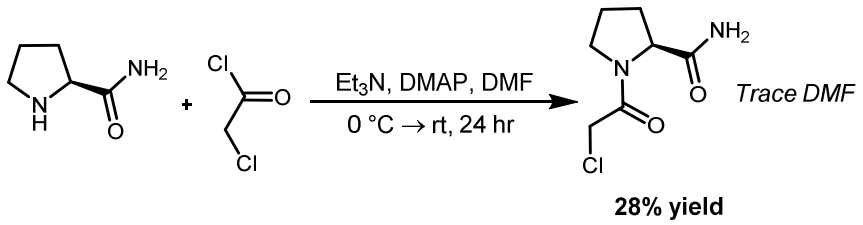

Scheme 4.1: Preliminary Acetylation of L-prolinamide25

L-prolinamide (50.0 mg, 0.44 mmol, 1 eq) was placed into an oven dried 25 mL round bottom flask with a magnetic stir bar. The flask was placed into an ice bath before adding 1.0 mL of DMF. Ice-chilled chloroacetyl chloride (54.7 mg, 0.48 mmol, 1.1 eq) was slowly added to an aliquot of DMF (1.0 mL) in a separate vessel, exhibiting white smoke. This solution was then injected dropwise into the reaction flask. Pre-cooled Et_3N (90.0 mg, 0.88 mmol, 2 eq at 0 °C) was then added dropwise to the reaction flask. Subsequently DMAP (0.54 mg, 0.004 mmol, 1 mol%) was added to the reaction flask which was then capped and stirred as the ice bath proceeded to room temperature. After stirring for 27 hours the crude mixture was extracted with EtOAc (3 x

25 mL). The combined organic layers were washed with H_2O (3 x 25 mL) and then once with brine (25 mL). The combined organic layers were dried over sodium sulfate and concentrated under reduced atmosphere. Product was a tan foam (23.0 mg, 28% yield) with residual DMF observed.

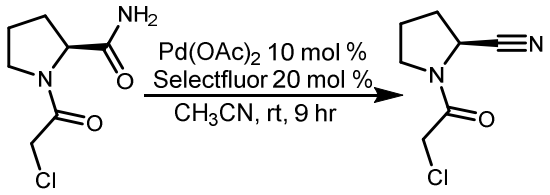

Scheme 4.2: General Procedure for Palladium Catalyzed Dehydration (1-chloroacetyl-2-(*S*)-pyrrolidinecarboxamide shown).[19]

In an oven dried 20 mL vial 1-chloroacetyl-2-(*S*)-pyrrolidinecarboxamide (20.0 mg, 0.10 mmol, 1 eq), palladium acetate (0.23 g, 0.01 mmol, 10 mol%), Selectfluor (7.4 mg, 0.02 mmol, 20 mol %) and a magnetic stir bar were combined. The dark yellow solution was stirred at room temperature for 9 hours before purification on a silica gel column (100 mL 70% EtOAc:Hex). The product was an off-white foam (10 mg, 56% yield).

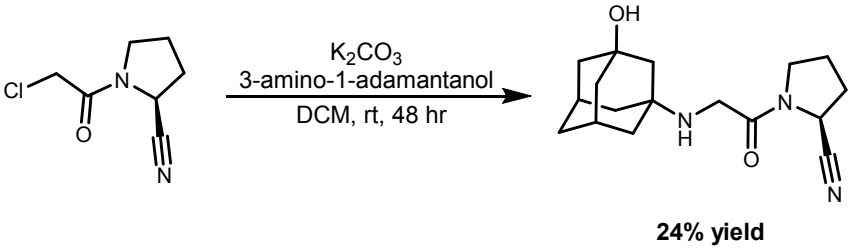

Scheme 4.3: Addition of adamantal moiety to (*S*)-1-(2-chloroacetyl)pyrrolidine-2-carbonitrile[25]

In an oven dried 20 mL vial (*S*)-1-(2-chloroacetyl)pyrrolidine-2-carbonitrile (10 mg, 0.06 mmol, 1 eq), 3-amino-1-adamantanol (12 mg, 0.07 mmol, 1.2 eq), and K_2CO_3 (45 mg, 0.32 mmol, 5.5 eq) were combined in DCM (2.0 mL) with a magnetic stir bar. After stirring for 48 hours the salts were filtered from the reaction mixture and rinsed with DCM (5.0 mL). The filtrate was concentrated under reduced atmosphere before purification on a silica gel column (Gradient, 50% MeOH to 100% MeOH). The product, Vildagliptin, was a white solid (4.3 mg, 24% yield).

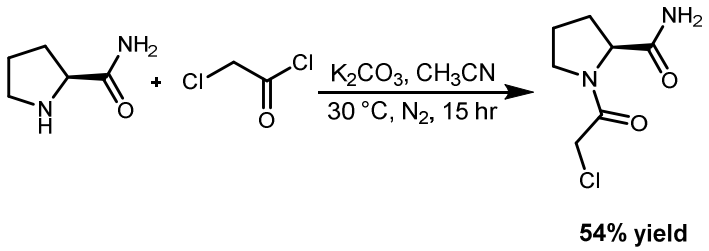

Scheme 4.4: General procedure for Acetylation of L-prolinamide[57]

In a 10 mL oven dried vial L-prolinamide (0.1 g, 0.88 mmol, 1 eq), K_2CO_3 (240 mg, 1.8 mmol, 2 eq) and a magnetic stir bar were combined in 3.2 mL CH_3CN. The vial was placed under N_2 atmosphere and in an oil bath at 30 °C. A solution of chloroacetyl chloride (110 µL in 0.8 mL CH_3CN, 0.15 g, 1.4 mmol, 1.5 eq) was injected to the reaction flask dropwise over the span of 1.5 hours. The resulting light-yellow mixture was stirred overnight before filtering the salts, drying the filtrate over sodium sulfate, and subsequent concentration under reduced atmosphere. The resulting yellow oil was purified on a silica gel column (30 mL 5% CH_3CN: EtOAc, 30 mL 10% CH_3CN:EtOAc, 30 mL 100% CH_3CN, 50 mL 100% MeOH), yielding a slightly yellow oil. The oil was sonicated in CH_3CN (0.2 mL) and then concentrated under reduced vacuum. After removing the solvent, the oil was placed under high-vacuum to instantly yield a white solid foam (90 mg, 54% yield.)

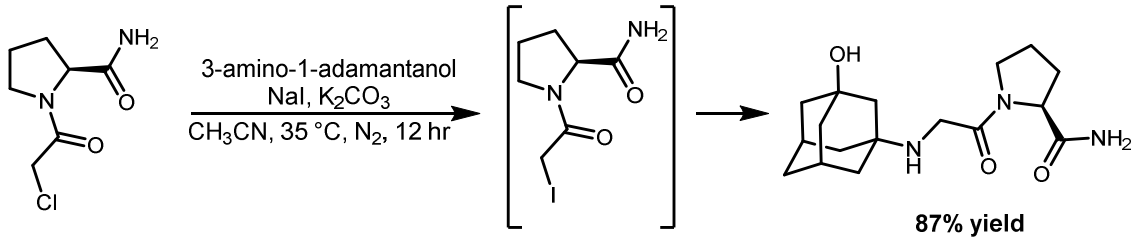

Scheme 4.5: Addition of adamantal moiety to 1-chloroacetyl-2-(*S*)-pyrrolidinecarboxamide[25]

In a 25 mL oven dried vial 1-chloroacetyl-2-(*S*)-pyrrolidinecarboxamide (0.33 g, 1.8 mmol, 1 eq), 3-amino-1-adamantanol (0.56 g, 3.5 mmol, 2 eq), NaI (0.52 g, 3.5 mmol, 2 eq), and K_2CO_3 (0.49 g, 3.5 mmol, 2 eq) were combined in CH_3CN (18 mL, 0.1 M) with a magnetic stir bar. The reaction vial was capped, flushed with N_2, and heated in an oil bath (35 °C, overnight). The salts were filtered from the reaction mixture and rinsed with CH_3CN (10 mL). The filtrate was dried over sodium sulfate and concentrated under reduced atmosphere. The resulting yellow oil was

purified on a silica gel column (200 mL 50% CH_3CN : EtOAc) yielding an off white-yellow solid (0.49 g, 87 % yield).

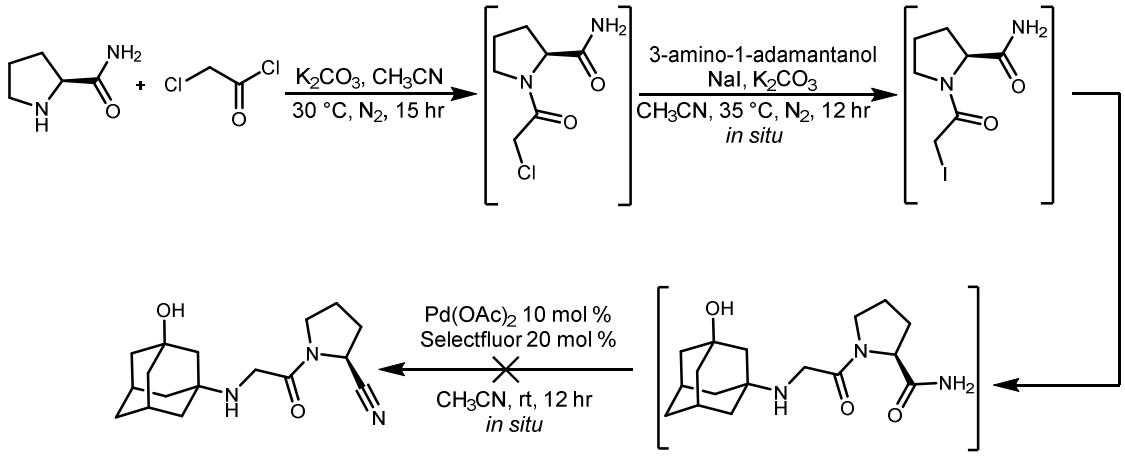

Scheme 4.6: General tandem *in situ* reactions in one-pot towards Vildagliptin

In a 25 mL oven dried vial L-prolinamide (0.1 g, 0.9 mmol, 1 eq), K_2CO_3 (0.24 g, 1.8 mmol, 2 eq) and a magnetic stir bar were combined in 4.0 mL CH_3CN. The vial was placed under N_2 atmosphere and in an oil bath at 30 °C. A solution of chloroacetyl chloride (110 µL in 0.8 mL CH_3CN, 0.15 g, 1.4 mmol, 1.5 eq) was injected to the reaction flask dropwise over the span of 1.5 hours. The resulting light-yellow mixture was stirred overnight. Next, 3-amino-1-adamantanol (0.3 g, 1.8 mmol, 2 eq), and NaI (0.26 g, 1.8 mmol, 2 eq), K_2CO_3 (0.24 g, 1.8 mmol, 2 eq), and additional CH_3CN (2.0 mL, 0.1 M) were added to the reaction flask. The reaction vial was recapped, flushed with N_2, and heated in an oil bath (35 °C, overnight). To the same pot palladium acetate (21 mg, 0.09 mmol, 10 mol %), and Selectfluor (67 mg, 0.19 mmol, 20 mol %) were added and stirred for 12 hours before filtering the salts. After rinsing the salts with CH_3CN (6 mL) the filtrate was dried over sodium sulfate and concentrated to yield a dark orange oil. TLC and ^1H NMR analysis exhibited no product formation.

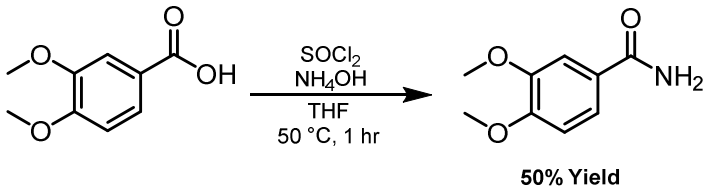

Scheme 4.7: Amidation of 3,4-dimethoxybenzoic acid[19]

In a 20 mL oven dried round bottom flask 3,4-dimethoxybenzoic acid (0.5 g, 2.7 mmol, 1 eq) was dissolved in THF (13 mL) with a magnetic stir bar. To this was added thionyl chloride (0.3 mL, 0.5 g, 4.1 mmol, 1.5 eq) in dropwise fashion. After stirring for 10 minutes the reaction flask was heated in an oil bath (50 °C, 1 hr) before cooling to room temperature and then placing in an ice bath for 10 minutes. Ice-cold ammonium hydroxide (30%, 3.0 mL, 2.6 g, 0.08 mmol, 0.03 eq) was slowly injected into the chilled reaction flask, exhibiting large volumes of white smoke. After stirring for 5 minutes the solution (and a white precipitate) were extracted with $CHCl_3$ (3 x 35 mL). The combined organic layers were dried over sodium sulfate and concentrated. The resulting solid was soaked with hexane and collected by vacuum filtration. The product was an off-white solid (250 mg, 50% yield). A significant portion of the reaction mixture was lost to the benchtop during transfer and likely contributed to a lower-than-expected yield

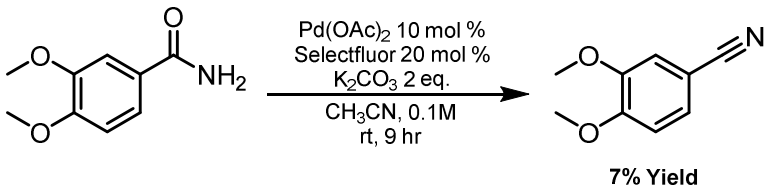

Scheme 4.8: Palladium catalyzed dehydration of 3,4-dimethoxybenzamide[19]

In an oven dried 50 mL round bottom flask 3,4-dimethoxybenamide (0.10 g, 0.55 mmol, 1 eq), palladium acetate (12 mg, 0.06 mmol, 10 mol %), Selectfluor (39 mg, 0.11 mmol, 20 mol %), and K_2CO_3 (150 mg, 1.1 mmol, 2 eq) were combined in CH_3CN (18 mL) with a magnetic stir bar. The solution was stirred for 9 hours before the salts were filtered, and the filtrate dried over sodium sulfate before concentration under reduced atmosphere. The resulting solid was purified by silica gel column (150 mL, 5% EtOAc: Hex), yielding an off-white solid (6.5 mg, 7% yield).

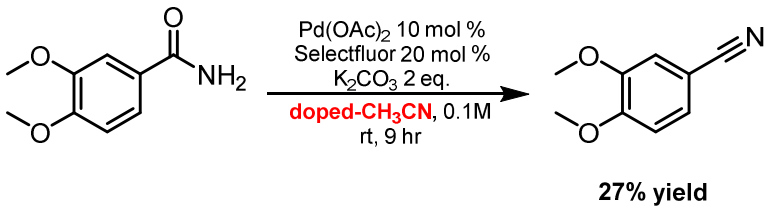

Scheme 4.9: Doped Solvent Dehydration of 3,4-dimethoxybenzamide

In an oven dried 25 mL round bottom flask, K_2CO_3 (0.15 g, 1.1 mmol, 2 eq) and CH_3CN (5.0 mL) were stirred (2 hours) before filtering the solids from the solution. The filtrate was returned to the solid-free reaction flask before adding palladium acetate (12 mg, 0.06 mmol, 10 mol %), and Selectfluor (39 mg, 0.11 mmol, 20 mol %). After stirring (5 minutes) 3,4-dimethoxybenzamide (0.1 g, 0.55 mmol, 1 eq) was added to the reaction flask. The dark orange solution was stirred for 9 hours before drying over sodium sulfate and concentration under reduced atmosphere. The dark orange oil was purified by silica gel column (150 mL, 100% EtOAc) to yield an off white solid (25 mg, 27% yield).

REFERENCES

(1) Wender, P. A.; Verma, V. A.; Paxton, T. J.; Pillow, T. H. Function-Oriented Synthesis, Step Economy, and Drug Design. *Accounts of Chemical Research*. American Chemical Society January 2008, pp 40–49.

(2) Mathieu, C.; Degrande, E. Vildagliptin: A New Oral Treatment for Type 2 Diabetes Mellitus. *Vascular Health and Risk Management*. Dove Press 2008, pp 1349–1360.

(3) Sundararaju, K.; Chidambaram, R.; Narayanaswamy, R. Synthesis, Characterization, And Molecular Docking Analysis Of Proline (Pyrrolidine 2-Carboxylic Acid) And Prolinamide (Pyrrolidine 2-Carboxylic Acid Amide) Isomers As Bacterial Collagenase Inhibitors. *Asian J. Pharm. Clin. Res.* **2019**, *12* (1), 1–4.

(4) Mowry, D. T. The Preparation of Nitriles. *Chem. Rev.* **1948**, *42* (2), 189–283.

(5) Fehling, H. Ueber Die Zersetzung Des Benzoësauren Ammoniaks Durch Die Wärme. *Ann. der Chemie und Pharm.* **1844**, *49* (1), 91–97.

(6) Hamad Elgazwy, A.-S. S.; Refaee, Mahmoud, M. R. The Chemistry of Alkenyl Nitriles and Its Utility in Heterocyclic Synthesis. *Org. Chem. Curr. Res.* **2013**, *2* (2), 1–2.

(7) Fleming, F. F.; Yao, L.; Ravikumar, P. C.; Funk, L.; Shook, B. C. Nitrile-Containing Pharmaceuticals: Efficacious Roles of the Nitrile Pharmacophore. *J. Med. Chem.* **2010**, *53* (22), 7902–7917.

(8) Murphy, S. T.; Case, H. L.; Ellsworth, E.; Hagen, S.; Huband, M.; Joannides, T.; Limberakis, C.; Marotti, K. R.; Ottolini, A. M.; Rauckhorst, M.; et al. The Synthesis and Biological Evaluation of Novel Series of Nitrile-Containing Fluoroquinolones as Antibacterial Agents. *Bioorganic Med. Chem. Lett.* **2007**, *17* (8), 2150–2155.

(9) Blot, S. I.; Vandewoude, K. H.; Hoste, E. A.; Colardyn, F. A. Outcome and Attributable Mortality in Critically Ill Patients with Bacteremia Involving Methicillin-Susceptible and Methicillin-Resistant Staphylococcus Aureus. *Arch. Intern. Med.* **2002**, *162* (19), 2229–2235.

(10) Miller, J. S.; Manson, J. L. Designer Magnets Containing Cyanides and Nitriles. *Acc. Chem. Res.* **2001**, *34* (7), 563–570.

(11) You, Y.; Zhan, C.; Tu, L.; Wang, Y.; Hu, W.; Wei, R.; Liu, X. Polyarylene Ether Nitrile-Based High- k Composites for Dielectric Applications. *International Journal of Polymer Science*. Hindawi Limited 2018, p 15.

(12) Ishikawa, T. 6.7 C–C Bond Formation: Cyanation. In *Comprehensive Chirality*; Elsevier, 2012; Vol. 6, pp 194–213.

(13) Ji, H. H.; Jin, H. A.; Duk, K. A. Selective Reduction of Aromatic Nitriles to Aldehydes by Lithium Diisobutylpiperidinohydroaluminate (LDBPA). *Bull. Korean Chem. Soc.* **2006**, *27* (1), 121–122.

(14) Tamura, M.; Tonomura, T.; Shimizu, K. I.; Satsuma, A. CeO2-Catalysed One-Pot Selective Synthesis of Esters from Nitriles and Alcohols. *Green Chem.* **2012**, *14* (4), 984–991.

(15) Yeung, K. S.; Farkas, M. E.; Kadow, J. F.; Meanwell, N. A. A Base-Catalyzed, Direct Synthesis of 3,5-Disubstituted 1,2,4-Triazoles from Nitriles and Hydrazides. *Tetrahedron Lett.* **2005**, *46* (19), 3429–3432.

(16) Ganesan, M.; Paramathevar, N. Recent Developments in Dehydration of Primary Amides to Nitriles. *Org. Chem. Front.* **2020**, 1–2.

(17) Preiml, M.; Hönig, H.; Klempier, N. Biotransformation of β-Amino Nitriles: The Role of the N-Protecting Group. In *Journal of Molecular Catalysis B: Enzymatic*; Elsevier, 2004; Vol. 29, pp 115–121.

(18) Maffioli, S. I.; Marzorati, E.; Marazzi, A. Mild and Reversible Dehydration of Primary Amides with PdCl 2 in Aqueous Acetonitrile. *Org. Lett.* **2005**, *7* (23), 5237–5239.

(19) Al-Huniti, M. H.; Rivera-Chávez, J.; Colón, K. L.; Stanley, J. L.; Burdette, J. E.; Pearce, C. J.; Oberlies, N. H.; Croatt, M. P. Development and Utilization of a Palladium-Catalyzed Dehydration of Primary Amides To Form Nitriles. *Org. Lett.* **2018**, *20* (19), 6046–6050.

(20) Carlier, P. R.; Lo, K. M.; Lo, M. M. C.; Lo, P. C. K.; Lo, C. W. S. Synthetic Optimization and Structural Limitations of the Nitrile Aldol Reaction. *J. Org. Chem.* **1997**, *62* (18), 6316–6321.

(21) Foley, J. E.; Ahrén, B. The Vildagliptin Experience - 25 Years since the Initiation of the Novartis Glucagon-like Peptide-1 Based Therapy Programme and 10 Years since the First Vildagliptin Registration. *Eur. Endocrinol.* **2017**, *13* (2), 56–61.

(22) Profit, L.; Chrisp, P.; Nadin, C. Vildagliptin: The Evidence for Its Place in the Treatment of Type 2 Diabetes Mellitus. *Core Evidence*. Dove Press 2008, pp 13–30.

(23) Page, R. C. L. 42 Insulin, Other Hypoglycemic Drugs, and Glucagon. In *Side Effects of Drugs Annual*; Elsevier, 2008; Vol. 30, pp 494–506.

(24) Castaldi, M.; Baratella, M.; Menegotto, I. G.; Castaldi, G.; Giovenzana, G. B. A Concise and Efficient Synthesis of Vildagliptin. *Tetrahedron Lett.* **2017**, *58* (35), 3426–3428.

(25) Villhauer, E. B.; Brinkman, J. A.; Naderi, G. B.; Burkey, B. F.; Dunning, B. E.; Prasad, K.; Mangold, B. L.; Russell, M. E.; Hughes, T. E. 1-[[(3-Hydroxy-1-Adamantyl)Amino]Acetyl]-2-Cyano-(S)-Pyrrolidine: A Potent, Selective, and Orally Bioavailable Dipeptidyl Peptidase IV Inhibitor with Antihyperglycemic Properties. *J. Med. Chem.* **2003**, *46* (13), 2774–2789.

(26) Bhirud, Shekhar Bhaskar; Bhushan, Kumar Hari; Thanedar, Amit Anant; Raut, Changdev Namdev; Chand, P. Improved Process for the Synthesis of Vildagliptin by Using a Nitrile Solvent in the Preparation of (S)-1-(2-Chloroacetyl)Pyrrolidine-2-Carboxamide Intermediate. WO 2013-IN787, 2013.

(27) Deng, Y.; Wang, A.; Tao, Z.; Chen, Y.; Pan, X.; Hu, X. A Facile and Economical Method to Synthesize Vildagliptin. *Lett. Org. Chem.* **2014**, *11* (10), 780–784.

(28) Żaczek, S.; Gelman, F.; Dybala-Defratyka, A. A Benchmark Study of Kinetic Isotope Effects and Barrier Heights for the Finkelstein Reaction. *J. Phys. Chem. A* **2017**, *121* (12), 2311–2321.

(29) Pellegatti, L.; Sedelmeier, J. Synthesis of Vildagliptin Utilizing Continuous Flow and Batch Technologies. *Org. Process Res. Dev.* **2015**, *19* (4), 551–554.

(30) Kobayashi, M.; Shimizu, S. Nitrile Hydrolases. *Current Opinion in Chemical Biology*. Current Biology Ltd February 1, 2000, pp 95–102.

(31) Fleming, F. F. Nitrile-Containing Natural Products. *Nat. Prod. Rep.* **1999**, *16* (5), 597–606.

(32) Egelkamp, R.; Zimmermann, T.; Schneider, D.; Hertel, R.; Daniel, R. Impact of Nitriles on Bacterial Communities. *Front. Environ. Sci.* **2019**, *7*, 103.

(33) Yan, G.; Zhang, Y.; Wang, J. Recent Advances in the Synthesis of Aryl Nitrile Compounds. *Adv. Synth. Catal.* **2017**, *359* (23), 4068–4105.

(34) Shenvi, R. A.; O'Malley, D. P.; Baran, P. S. Chemoselectivity: The Mother of Invention in Total Synthesis. *Acc. Chem. Res.* **2009**, *42* (4), 530–541.

(35) Croatt, M. P.; Carreira, E. M. Probing the Role of the Mycosamine C2′-OH on the Activity of Amphotericin B. *Org. Lett.* **2011**, *13* (6), 1390–1393.

(36) Wender, P. A.; Clarke, M. O.; Horan, J. C. Role of the A-Ring of Bryostatin Analogues in PKC Binding: Synthesis and Initial Biological Evaluation of New A-Ring-Modified Bryologs. *Org. Lett.* **2005**, *7* (10), 1995–1998.

(37) Zhang, W.; Haskins, C. W.; Yang, Y.; Dai, M. Synthesis of Nitriles via Palladium-Catalyzed Water Shuffling from Amides to Acetonitrile. *Org. Biomol. Chem.* **2014**, *12* (45), 9109–9112.

(38) Enthaler, S.; Weidauer, M. Copper-Catalyzed Dehydration of Primary Amides to Nitriles. *Catal. Letters* **2011**, *141* (8), 1079–1085.

(39) Mineno, T.; Shinada, M.; Watanabe, K.; Yoshimitsu, H.; Miyashita, H.; Kansui, H. Highly-Efficient Conversion of Primary Amides to Nitriles Using Indium(III) Triflate as the Catalyst. *Int. J. Org. Chem.* **2014**, *04* (01), 1–6.

(40) Enthaler, S. Straightforward Iron-Catalyzed Synthesis of Nitriles by Dehydration of Primary Amides. *European J. Org. Chem.* **2011**, (25)

(41) Paguigan, N. D.; Al-Huniti, M. H.; Raja, H. A.; Czarnecki, A.; Burdette, J. E.; González-Medina, M.; Medina-Franco, J. L.; Polyak, S. J.; Pearce, C. J.; Croatt, M. P.; Oberlies, N.H. Chemoselective Fluorination and Chemoinformatic Analysis of Griseofulvin: Natural vs Fluorinated Fungal Metabolites. *Bioorganic Med. Chem.* **2017**, *25* (20), 5238–5246.

(42) Leitgeb, B.; Szekeres, A.; Manczinger, L.; Vágvölgyi, C.; Kredics, L. The History of Alamethicin: A Review of the Most Extensively Studied Peptaibol. *Chemistry and Biodiversity*. Chem Biodivers 2007, pp 1027–1051.

(43) Chen, C.; Wang, C.; Zhang, J.; Zhao, Y. Palladium-Catalyzed Ortho -Selective C-H Fluorination of Oxalyl Amide-Protected Benzylamines. *J. Org. Chem.* **2015**, *80* (2), 942–949.

(44) Furuya, T.; Ritter, T. Carbon-Fluorine Reductive Elimination from a High-Valent Palladium Fluoride. *J. Am. Chem. Soc.* **2008**, *130* (31), 10060–10061.

(45) Wadzinski, T. J.; Steinauer, A.; Hie, L.; Pelletier, G.; Schepartz, A.; Miller, S. J. Rapid Phenolic O-Glycosylation of Small Molecules and Complex Unprotected Peptides in Aqueous Solvent. *Nat. Chem.* **2018**, *10* (6), 644–652.

(46) Morrison, K. L.; Weiss, G. A. Combinatorial Alanine-Scanning. *Current Opinion in Chemical Biology*, **2001**, pp 302–307.

(47) Meyer, C. E.; Reusser, F. A Polypeptide Antibacterial Agent Isolated from Trichoderma Viride. *Experientia* **1967**, *23* (2), 85–86.

(48) Fakhouri, L.; El-Elimat, T.; Hurst, D. P.; Reggio, P. H.; Pearce, C. J.; Oberlies, N. H.; Croatt, M. P. Isolation, Semisynthesis, Covalent Docking and Transforming Growth Factor Beta-Activated Kinase 1 (TAK1)-Inhibitory Activities of (5Z)-7-Oxozeaenol Analogues. *Bioorganic Med. Chem.* **2015**, *23* (21), 6993–6999.

(49) Sy-Cordero, A. A.; Figueroa, M.; Raja, H. A.; Meza Aviña, M. E.; Croatt, M. P.; Adcock, A. F.; Kroll, D. J.; Wani, M. C.; Pearce, C. J.; Oberlies, N. H. Spiroscytalin, a New Tetramic Acid and Other Metabolites of Mixed Biogenesis from Scytalidium Cuboideum. *Tetrahedron* **2015**, *71* (47), 8899–8904.

(50) Fox, R. O.; Richards, F. M. A Voltage-Gated Ion Channel Model Inferred from the Crystal Structure of Alamethicin at 1.5-Å Resolution. *Nature* **1982**, *300* (5890), 325–330.

(51) Daniel, J. F. D. S.; Rodrigues Filho, E. Peptaibols of Trichoderma. *Natural Product Reports*. Royal Society of Chemistry September 26, 2007, pp 1128–1141.

(52) Banerjee, U.; Tsui, F. P.; Balasubramanian, T. N.; Marshall, G. R.; Chan, S. I. Structure of Alamethicin in Solution. One- and Two-Dimensional 1H Nuclear Magnetic Resonance Studies at 500 MHz. *J. Mol. Biol.* **1983**, *165* (4), 757–775.

(53) VOGEL, H. Comparison of the Conformation and Orientation of Alamethicin and Melittin in Lipid Membranes. *Biochem.* **1987**, *26* (14).

(54) Fraternali, F. Restrained and Unrestrained Molecular Dynamics Simulations in the NVT Ensemble of Alamethicin. *Biopolymers* **1990**, *30* (11–12), 1083–1099.

(55) Greenfield, N.; Fasman, G. D. Computed Circular Dichroism Spectra for the Evaluation of Protein Conformation. *Biochemistry* **1969**, *8* (10), 4108–4116.

(56) Peggion, C.; Jost, M.; De Borggraeve, W. M.; Crisma, M.; Formaggio, F.; Toniolo, C. Conformational Analysis of TOAC-Labelled Alamethicin F50/5 Analogues. *Chem. Biodivers.* **2007**, *4* (6), 1256–1268.

(57) Okabe, H.; Naraoka, A.; Isogawa, T.; Oishi, S.; Naka, H. Acceptor-Controlled Transfer Dehydration of Amides to Nitriles. *Org. Lett.* **2019**, *21* (12), 4767–4770.

(58) Pourbaix, M. *Atlas of Electrochemical Equilibria In-Aqueous Solutions*, Second Eng.; National Association of Corrosion Engineers, 1974.

.

APPENDIX A: SUPPORTING INFORMATION

Supporting information for Development and Utilization of a Palladium-Catalyzed Dehydration of Primary Amides to Form Nitriles, presented as published in the Journal of Organic Chemistry.

Mohammed H. Al-Huniti, José Rivera-Chávez, Katsuya L. Colón, Jarrod L. Stanley, Joanna E. Burdette, Cedric J. Pearce, Nicholas H. Oberlies, and Mitchell P. Croatt

General Synthetic Information

All anhydrous reactions were performed in oven dried glassware under a nitrogen atmosphere. Unless otherwise noted, all solvents and reagents were obtained from commercial sources and used without further purification. Chromatographic purification was performed using silica gel (60 Å, 32-63 μm). NMR spectra were recorded in $CDCl_3$, acetone-d_6, or DMSO-d_6 using a JEOL ECA 400 spectrometer (400 MHz for 1H, 100 MHz for ^{13}C, and 376.5 MHz for ^{19}F), and JEOL ECA spectrometer (500 MHz for ^{1}H, 125 MHz for ^{13}C, and 470 MHz for ^{19}F). Coupling constants, *J*, are reported in hertz (Hz) and multiplicities are listed as singlet (s), doublet (d), triplet (t), quartet (q), quintet (quint), doublet of doublets (dd), triplet of triplets (tt), multiplet (m), etc. High Resolution Mass Spectra were acquired on a Thermo Fisher Scientific LTQ Orbitrap XL MS system.

General Procedure for the Synthesis of Amides 9a-9v

To an oven dried round-bottom flask, benzoic acid (1000 mg, 8.18 mmol) was dissolved in dry THF (25.0 mL) and then thionyl chloride (0.89 mL, 12.3 mmol) was added. The reaction mixture was heated to 50 °C for 1 hr and then allowed to cool to room temperature. The THF solution was cooled to 0 °C and then carefully poured into an icecooled ammonium hydroxide solution (37%, 6.0 mL) while stirring. After 5 min, the mixture was extracted with $CHCl_3$ (3 x 75.0 mL). The organic extract was dried and evaporated. The resultant solid was then soaked with hexane and filtered to obtain the desired amide in a pure form.

^{1}H and ^{13}C NMR spectra for compounds **9a**–**9v** are consistent with literature reports.

General Procedure for the Synthesis of Nitriles 10a-10v

To an oven dried microwave vial containing 4-methoxybenzamide (151.1 mg, 1.0 mmol) in acetonitrile (0.1 M), palladium acetate (22.4 mg, 0.1 mmol) and Selectfluor (70.8 mg, 0.2 mmol) were added. The reaction mixture was stirred at room temperature for 18 hr and then purified by column chromatography (gradient elution from pure hexane to 10% EtOAc in hexane) without the removal of solvent. Product was isolated as a white solid (126 mg, 96% yield).

^{1}H and ^{13}C NMR spectra for compounds **10a** – **10v** are consistent with literature reports ^{1}H NMR and ^{13}C NMR.

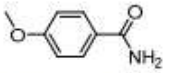

4-Methoxybenzamide 9a:[1] Following the General Procedure, product was isolated as a white solid (874 mg, 84% yield).
^{1}H NMR (400 MHz, acetone-d_6) δ 7.92 (d, J = 8.8 Hz, 2H), 7.36 (br. s, 1H), 6.97 (d, J = 8.8 Hz, 2H), 6.62 (br. s, 1H), 3.85 (s, 3H) ppm.
^{13}C NMR (100 MHz, acetone-d_6) δ 167.8, 162.3, 129.4 (2C), 126.8, 113.4 (2C), 54.9 ppm.
HRMS (APPI) calcd. for $C_8H_9NO_2$ $[M+H]^+$ calculated: 152.0706; observed: 152.0707.

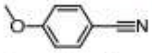

4-methoxybenzonitrile 10a:[1] Following the General Procedure, product was isolated as a white solid (126 mg, 96% yield) after column chromatography (gradient elution from pure hexane to 10% EtOAc in hexane).
^{1}H NMR (400 MHz, chloroform-d) δ 7.56 (d, J = 9.0 Hz, 2H), 6.92 (d, J = 9.0 Hz, 2H), 3.83 (s, 3H) ppm.

Figure A1: Spectroscopic Data for 4-Methoxybenzamide 9a and Corresponding Nitrile 10a (1 of 4)

^{13}C NMR (100 MHz, chloroform-d) δ 162.9, 134.1 (2C), 119.4, 114.8 (2C), 104.0, 55.6 ppm.
HRMS (APPI) calcd. for C_8H_7NO $[M+H]^+$ calculated: 134.0600; observed: 134.0601.

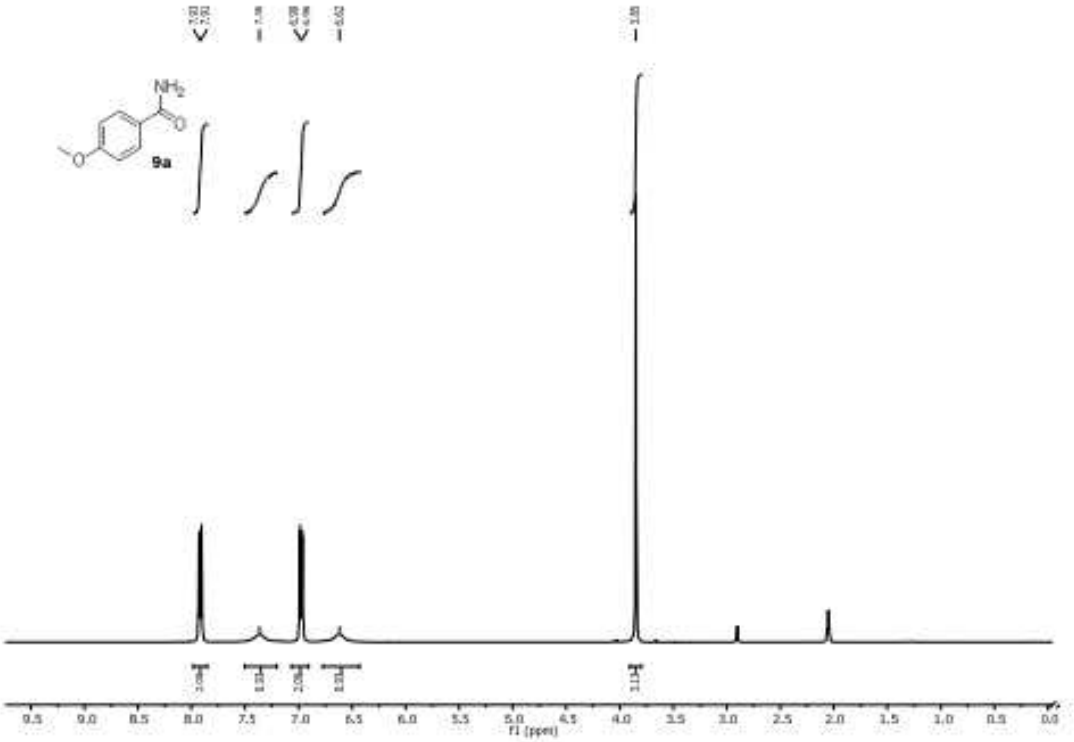

Figure A2: Spectroscopic Data for 4-Methoxybenzamide 9a and Corresponding Nitrile 10a (2 of 4)

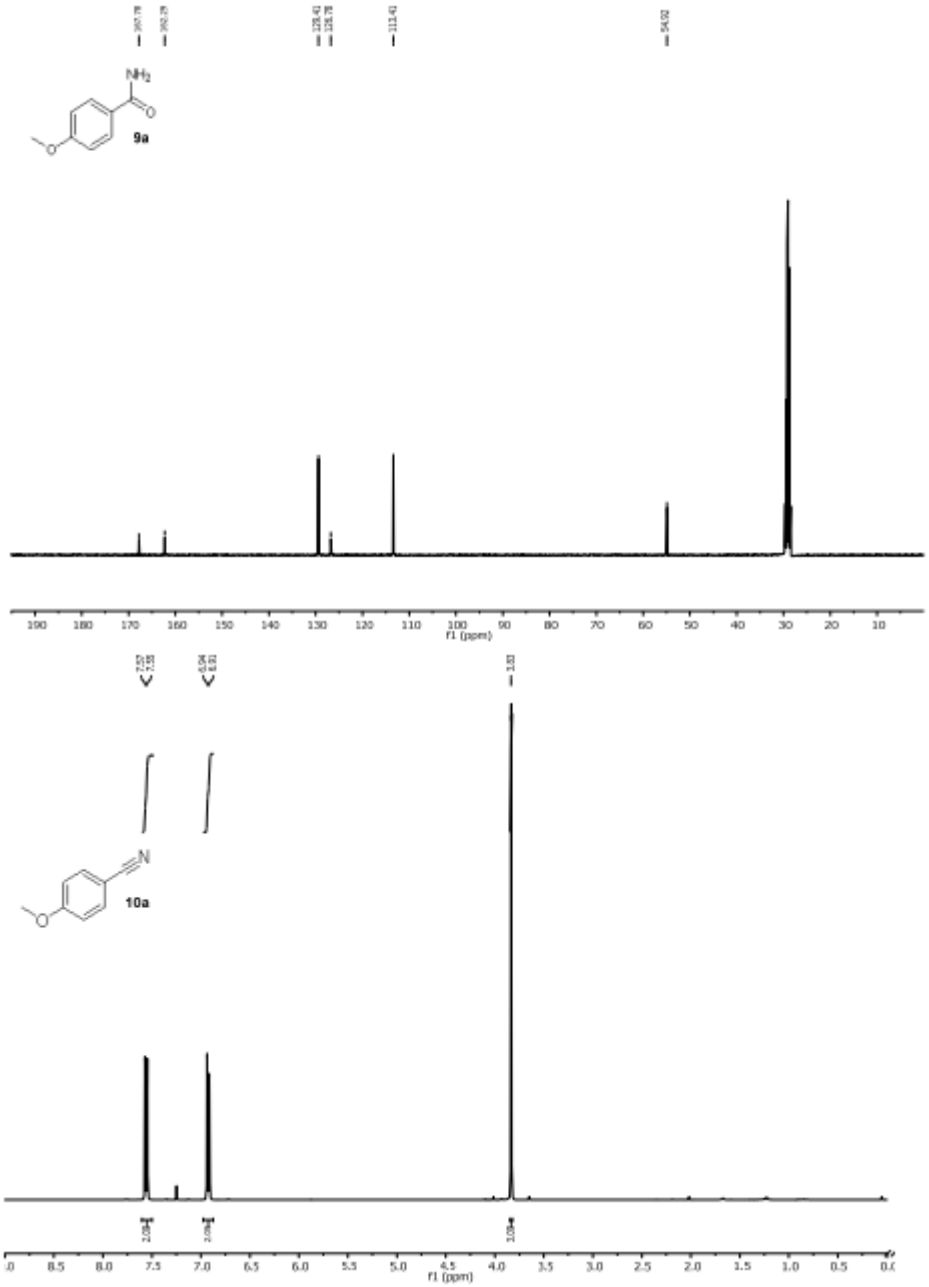

Figure A3: Spectroscopic Data for 4-Methoxybenzamide 9a and Corresponding Nitrile 10a (3 of 4)

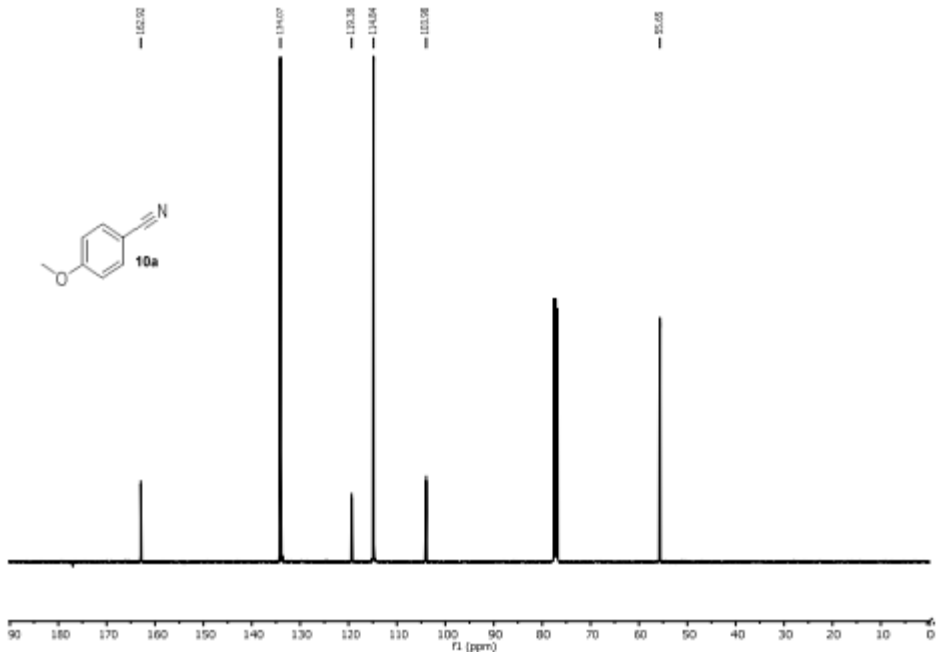

Figure A4: Spectroscopic Data for 4-Methoxybenzamide 9a and Corresponding Nitrile 10a (4 of 4)

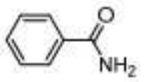

Benzamide 9b:[2] Following the General Procedure, product was isolated as a white solid (903 mg, 91% yield).
^{1}H NMR (500 MHz, chloroform-d) δ 7.85 – 7.76 (m, 2H), 7.54 – 7.50 (m, 1H), 7.44 (t, *J* = 7.6 Hz, 2H), 5.99 (br. s, 2H) ppm.
^{13}C NMR (125 MHz, chloroform-d) δ 169.4, 133.5, 132.1, 128.7 (2C), 127.4 (2C) ppm.
HRMS (APPI) calcd. for C_7H_7NO $[M+H]^+$ calculated: 122.0600; observed: 122.0593.
^{1}H and ^{13}C NMR are consistent with literature reports.[2]

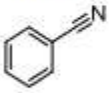

Benzonitrile 10b:[2] Following the General Procedure, product was isolated as a colorless oil (30 mg, 88% yield) after column chromatography (hexane).
^{1}H NMR (500 MHz, chloroform-d) δ 7.71 – 7.62 (m, 2H), 7.62 – 7.59 (m, 1H), 7.48 (t, *J* = 7.9 Hz, 2H) ppm.
^{13}C NMR (125 MHz, chloroform-d) δ 132.9, 132.3 (2C), 129.2 (2C), 119.0, 112.5 ppm.
^{1}H and ^{13}C NMR are consistent with literature reports.[2]

Figure A5: Spectroscopic Data for Benzamide 9b and Corresponding Nitrile 10b (1 of 3)

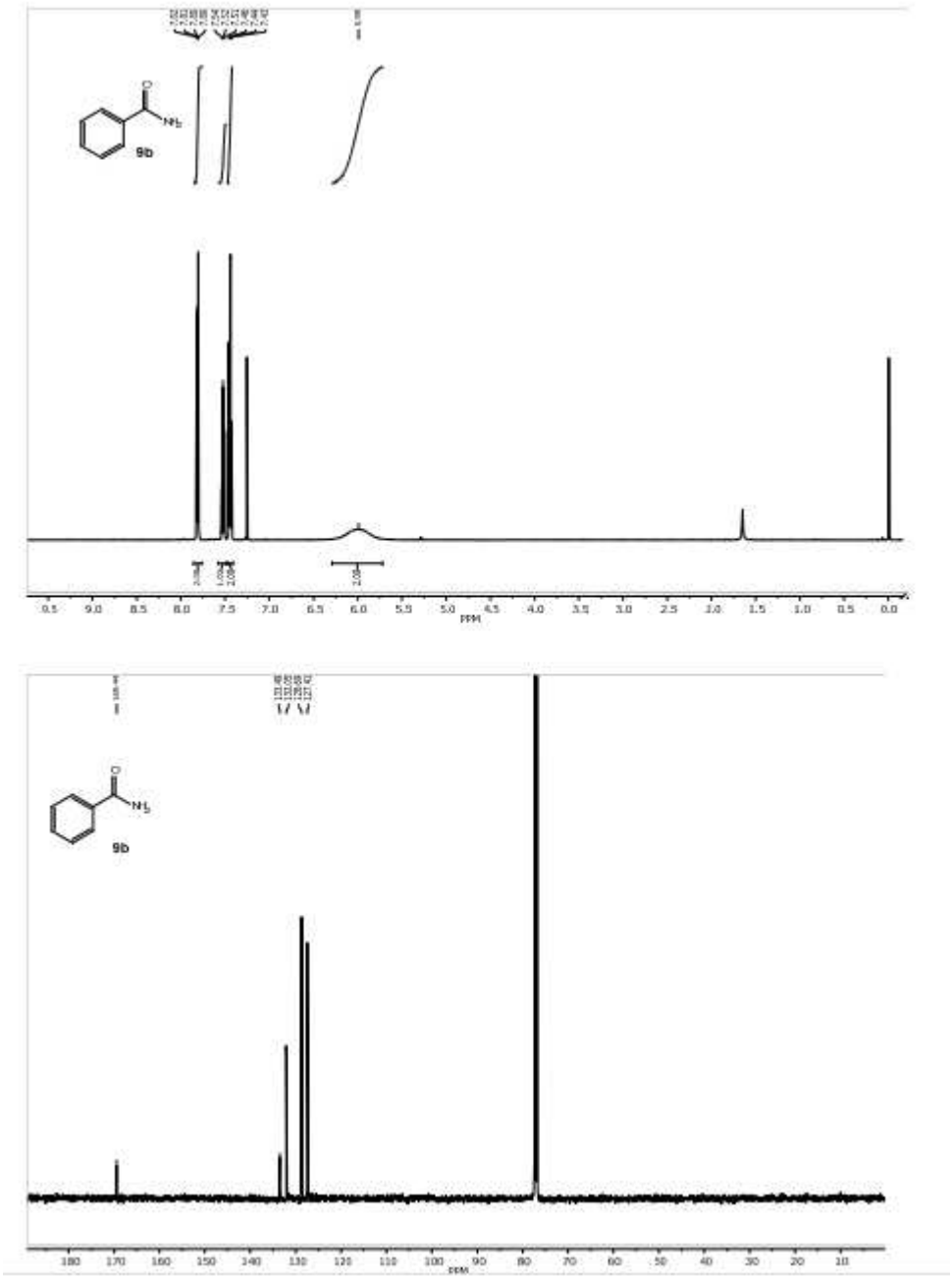

Figure A6: Spectroscopic Data for Benzamide 9b and Corresponding Nitrile 10b (2 of 3)

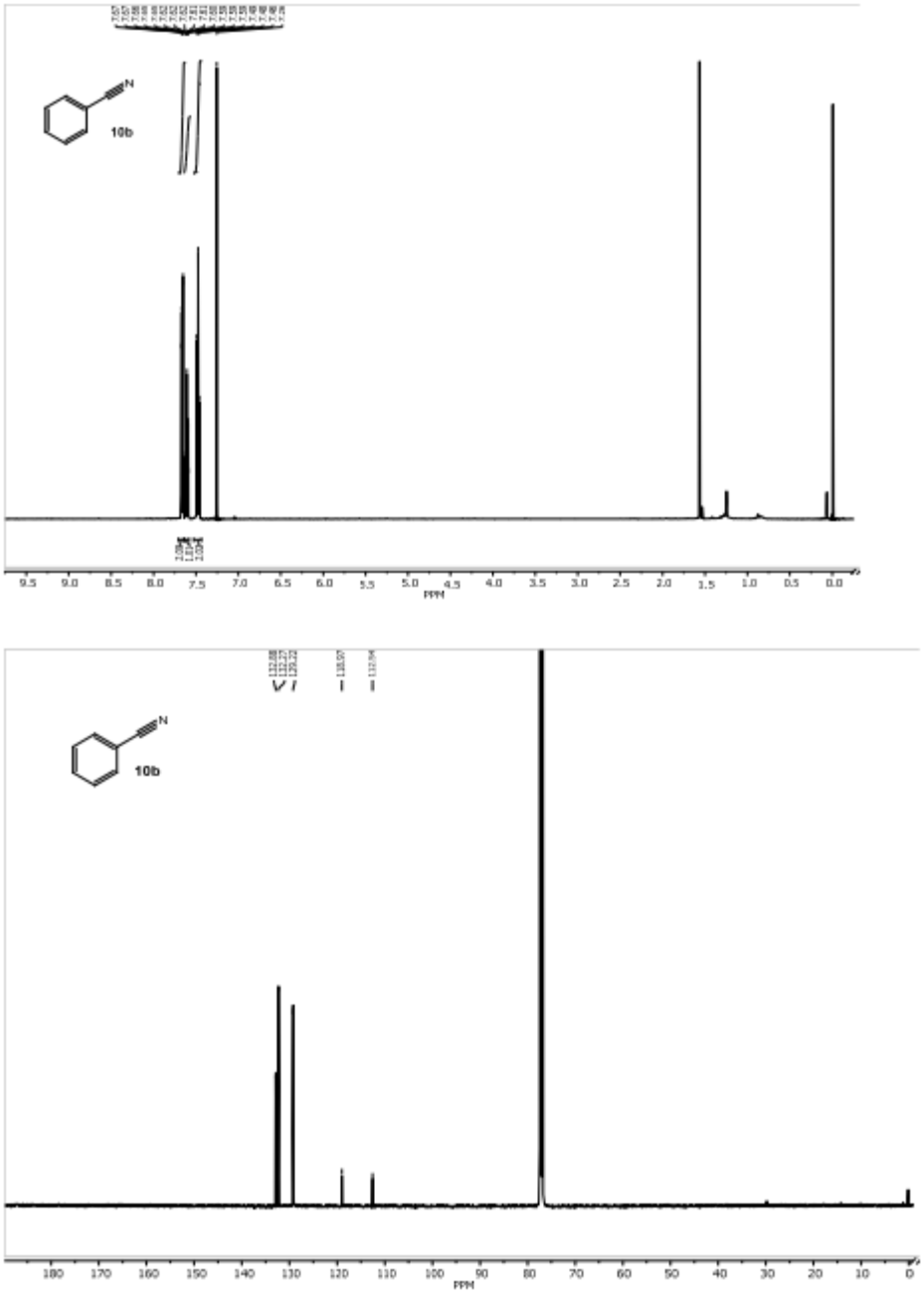

Figure A7: Spectroscopic Data for Benzamide 9b and Corresponding Nitrile 10b (3 of 3)

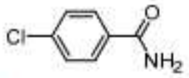

4-Chlorobenzamide 9c;[1] Following the General Procedure, product was isolated as a white solid (690 mg, 78% yield).
^{1}H NMR (400 MHz, acetone-d_6) δ 7.96 (d, J = 8.4 Hz, 2H), 7.62 (br. s, 1H), 7.49 (d, J = 8.6 Hz, 2H), 6.97 (br. s, 1H) ppm.
^{13}C NMR (100 MHz, acetone-d_6) δ 167.3, 136.9, 133.2, 129.4 (2C), 128.4 (2C) ppm.
HRMS (APPI) calcd. for C_7H_6ClNO $[M+H]^+$ calculated: 156.0216; observed: 156.0212.

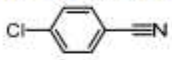

4-Chlorobenzonitrile 10c;[1] Following the General Procedure, product was isolated as a white solid (46 mg, 93% yield) after column chromatography (gradient elution from pure hexane to 10% EtOAc in hexane).
^{1}H NMR (400 MHz, chloroform-d) δ 7.60 (d, J = 8.6 Hz, 2H), 7.46 (d, J = 8.6 Hz, 2H) ppm.
^{13}C NMR (100 MHz, chloroform-d) δ 139.6, 133.5 (2C), 129.8 (2C), 118.1, 110.8 ppm.
HRMS (APPI) calcd. for C_7H_4ClNO $[M+H]^+$ calculated:138.0105; observed: 138.0108.

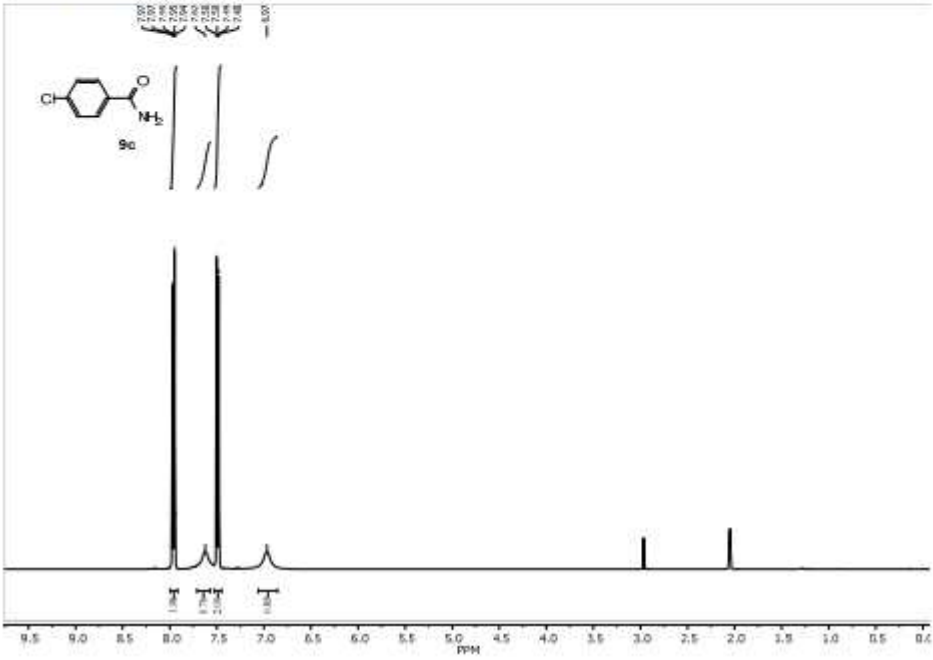

Figure A8: Spectroscopic Data for 4-Chlorobenzamide 9c and Corresponding Nitrile 10c (1 of 3)

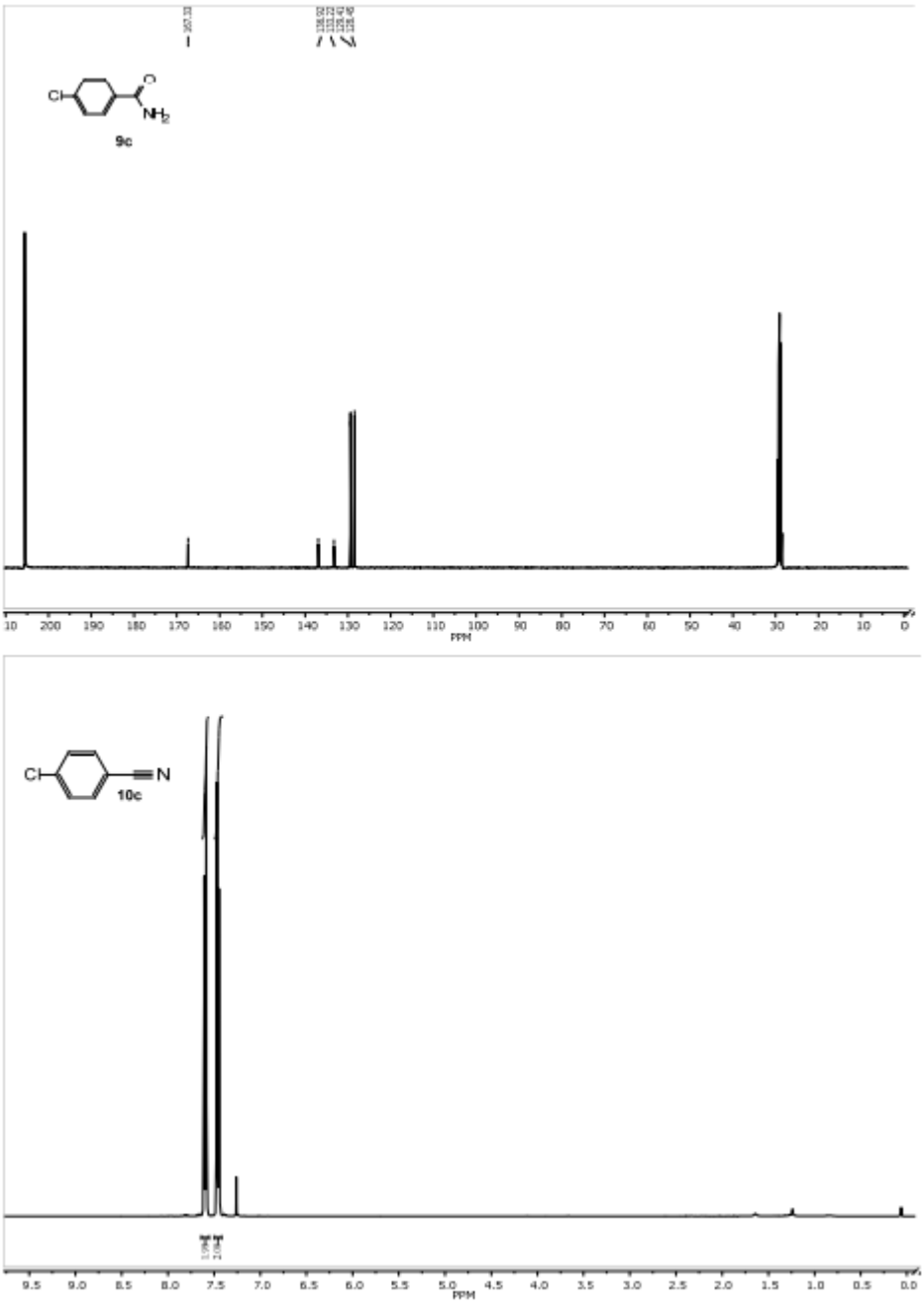

Figure A9: Spectroscopic Data for 4-Chlorobenzamide 9c and Corresponding Nitrile 10c (2 of 3)

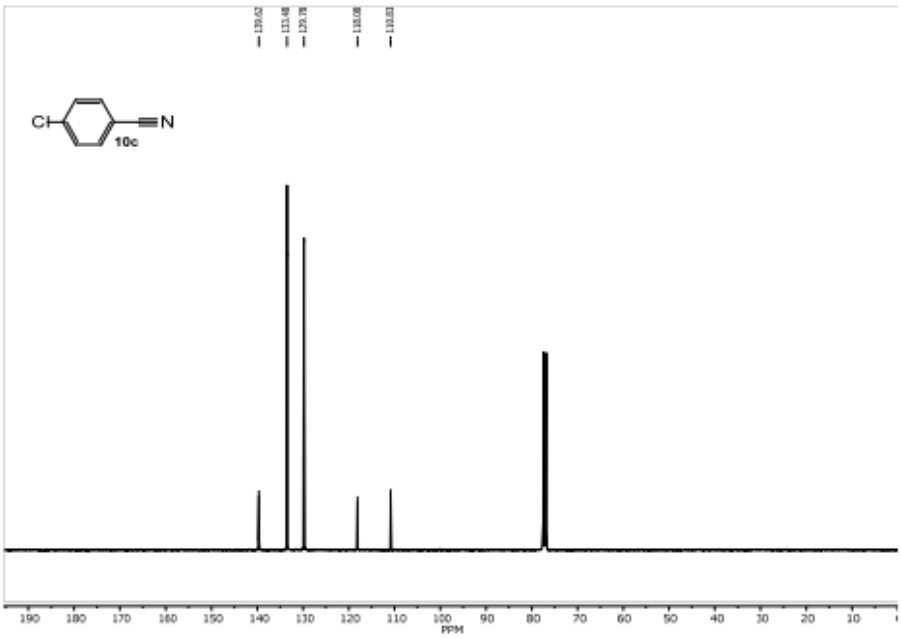

Figure A10: Spectroscopic Data for 4-Chlorobenzamide 9c and Corresponding Nitrile 10c (3 of 3)

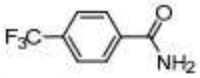

4-(trifluoromethyl)benzamide 9d:[1] Following the General Procedure, product was isolated as a white solid (874 mg, 74% yield).
^{1}H NMR (400 MHz, acetone-d_6) δ 8.15 (d, J = 8.1 Hz, 2H), 7.82 (d, J = 8.1 Hz, 2H), 7.76 (br. s, 1H), 7.09 (br. s, 1H) ppm.
^{13}C NMR (100 MHz, acetone-d_6) δ 167.1, 138.2, 132.3 (q, $J_{C\text{-}F}$ = 32.4 Hz), 128.4 (2C), 125.3 (q, $J_{C\text{-}F}$ = 3.6 Hz, 2C), 124.1 (q, $J_{C\text{-}F}$ = 271 Hz) ppm.
^{19}F NMR (376 MHz, acetone-d_6) δ -63.28 ppm.
HRMS (APPI) calcd. for $C_8H_6F_3NO$ $[M+H]^+$ calculated:190.0474; observed: 190.0476.

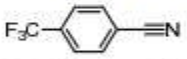

4-(trifluoromethyl)benzonitrile 10d:[1] Following the General Procedure, product was isolated as a colorless solid (21 mg, 42% yield) after column chromatography (gradient elution from pure hexane to 10% EtOAc in hexane).
^{1}H NMR (400 MHz, chloroform-d) δ 7.81 (d, J = 8.3 Hz, 2H), 7.76 (d, J = 8.3 Hz, 2H) ppm.
^{13}C NMR (100 MHz, chloroform-d) δ 134.6 (q, J = 33.3 Hz), 132.8 (2C), 126.3 (q, J = 3.8 Hz, 2C), 123.1 (q, J = 271 Hz), 117.5, 116.1 ppm.

Figure A11: Spectroscopic Data for 4-(trifluoromethyl)benzamide 9d and Corresponding Nitrile 10d (1 of 4)

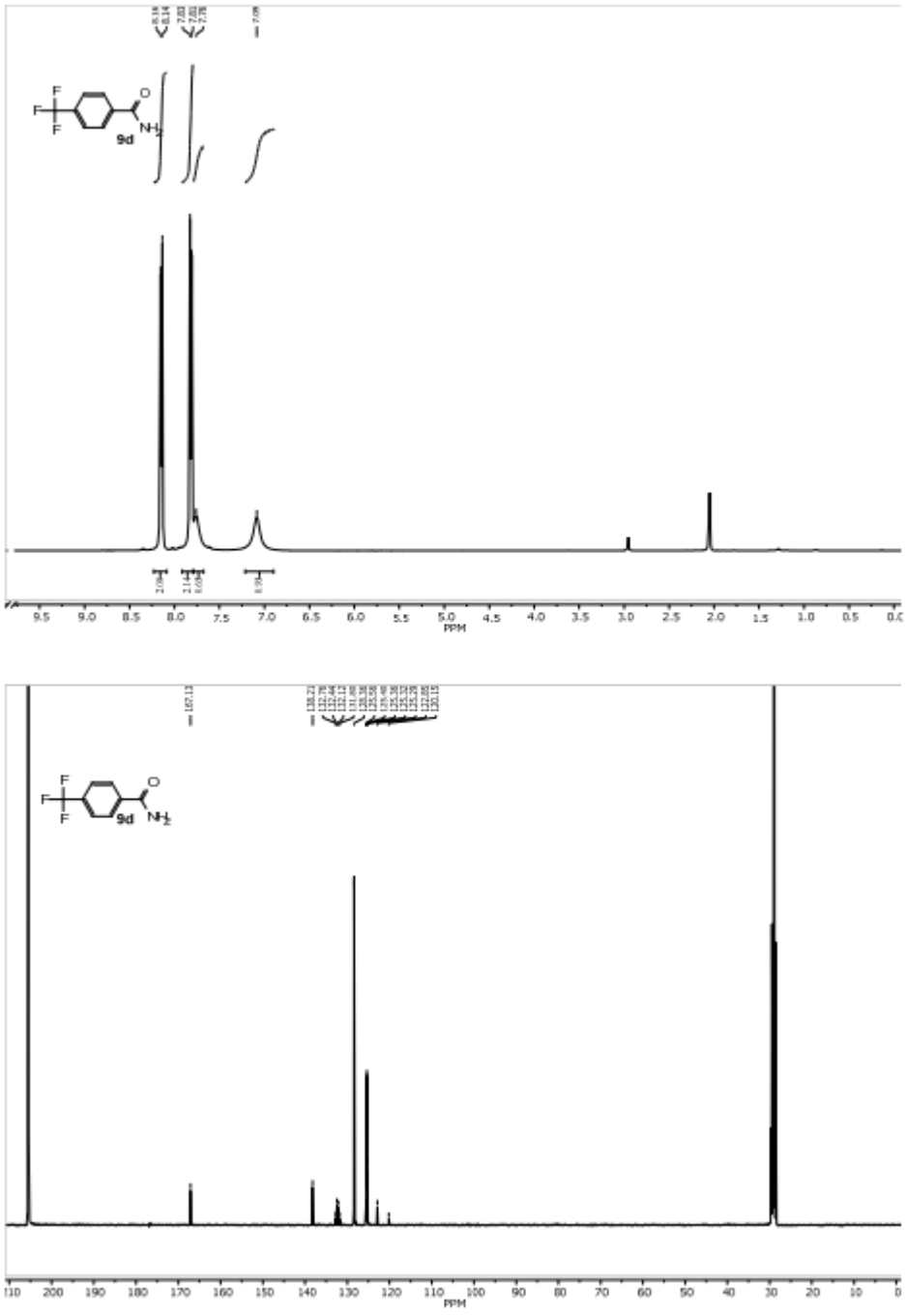

Figure A12: Spectroscopic Data for 4-(trifluoromethyl)benzamide 9d and Corresponding Nitrile 10d (2 of 4)

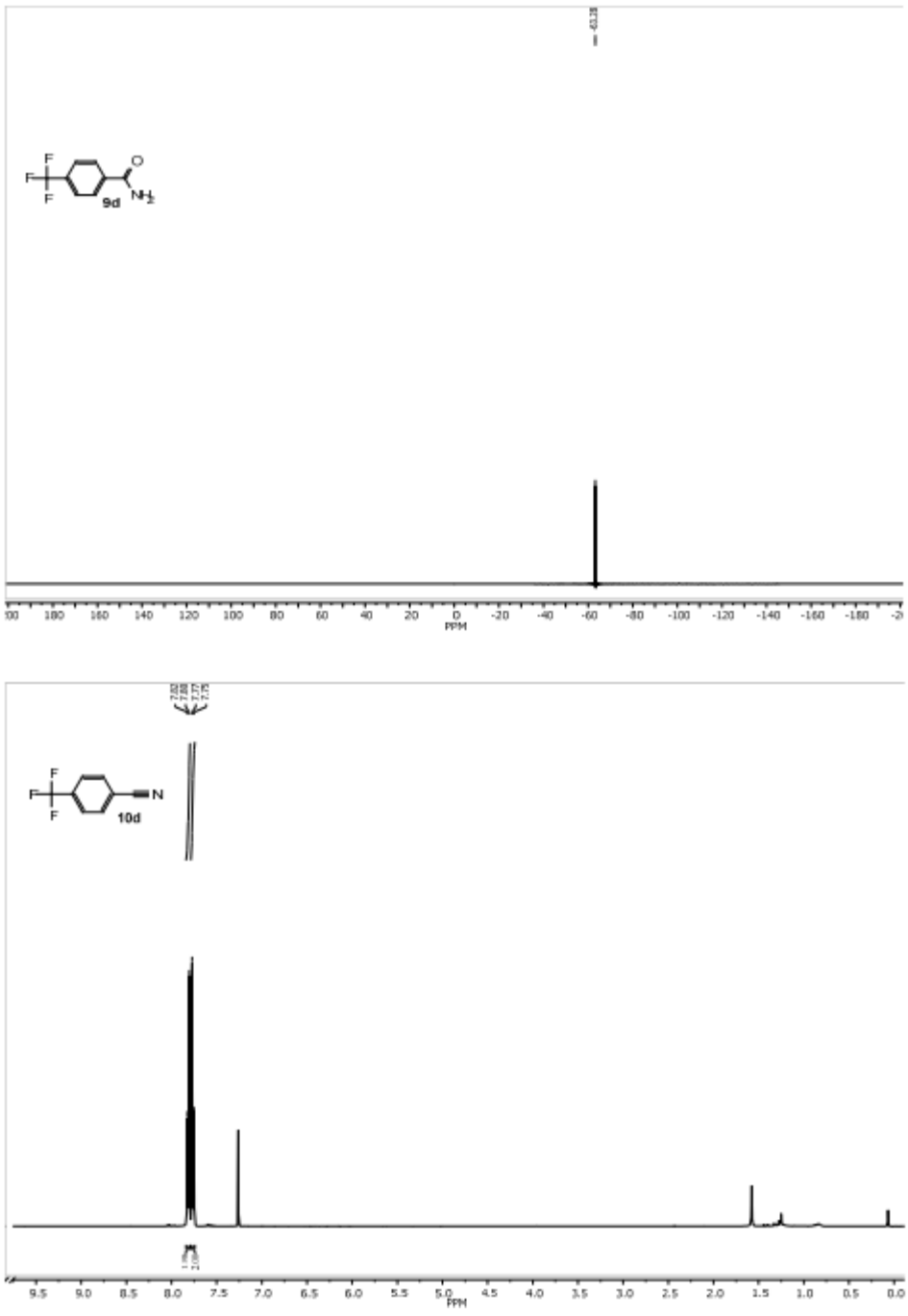

Figure A13: Spectroscopic Data for 4-(trifluoromethyl)benzamide 9d and Corresponding Nitrile 10d (3 of 4)

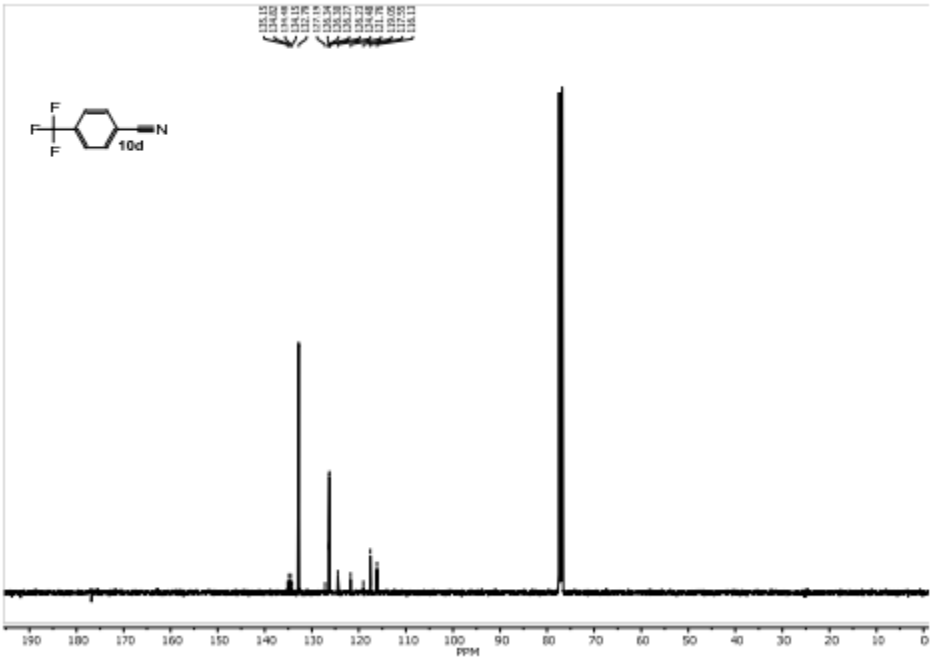

Figure A14: Spectroscopic Data for 4-(trifluoromethyl)benzamide 9d and Corresponding Nitrile 10d (4 of 4)

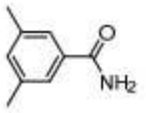

3,5-dimethylbenzamide 9e:[3] Following the General Procedure, product was isolated as a white solid (379 mg, 76% yield).

^{1}H NMR (400 MHz, DMSO-d_6) δ 7.82 (br. s, 1H), 7.44 (s, 2H), 7.22 (br. s, 1H), 7.10 (s, 1H), 2.26 (s, 6H) ppm.

^{13}C NMR (100 MHz, acetone-d_6) δ 169.4, 138.6 (2C), 135.4, 133.5, 126.2 (2C), 21.2 (2C) ppm.

HRMS (APPI) calcd. for $C_9H_{11}NO$ $[M+H]^+$ calculated: 150.0913; observed: 150.0914.

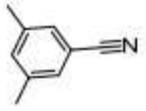

3,5-dimethylbenzonitrile 10e:[3] Following the General Procedure, product was isolated as a white solid (38 mg, 86% yield) after column chromatography (gradient elution from pure hexane to 10% EtOAc in hexane).

^{1}H NMR (400 MHz, chloroform-*d*) δ 7.23 (s, 2H), 7.19 (s, 1H), 2.32 (s, 6H) ppm.

^{13}C NMR (100 MHz, chloroform-*d*) δ 139.1 (2C), 134.7, 129.7 (2C), 119.3, 112.1, 21.1 (2C) ppm.

Figure A15: Spectroscopic Data for 3,5-dimethylbenzamide 9e and Corresponding Nitrile 10e (1 of 3)

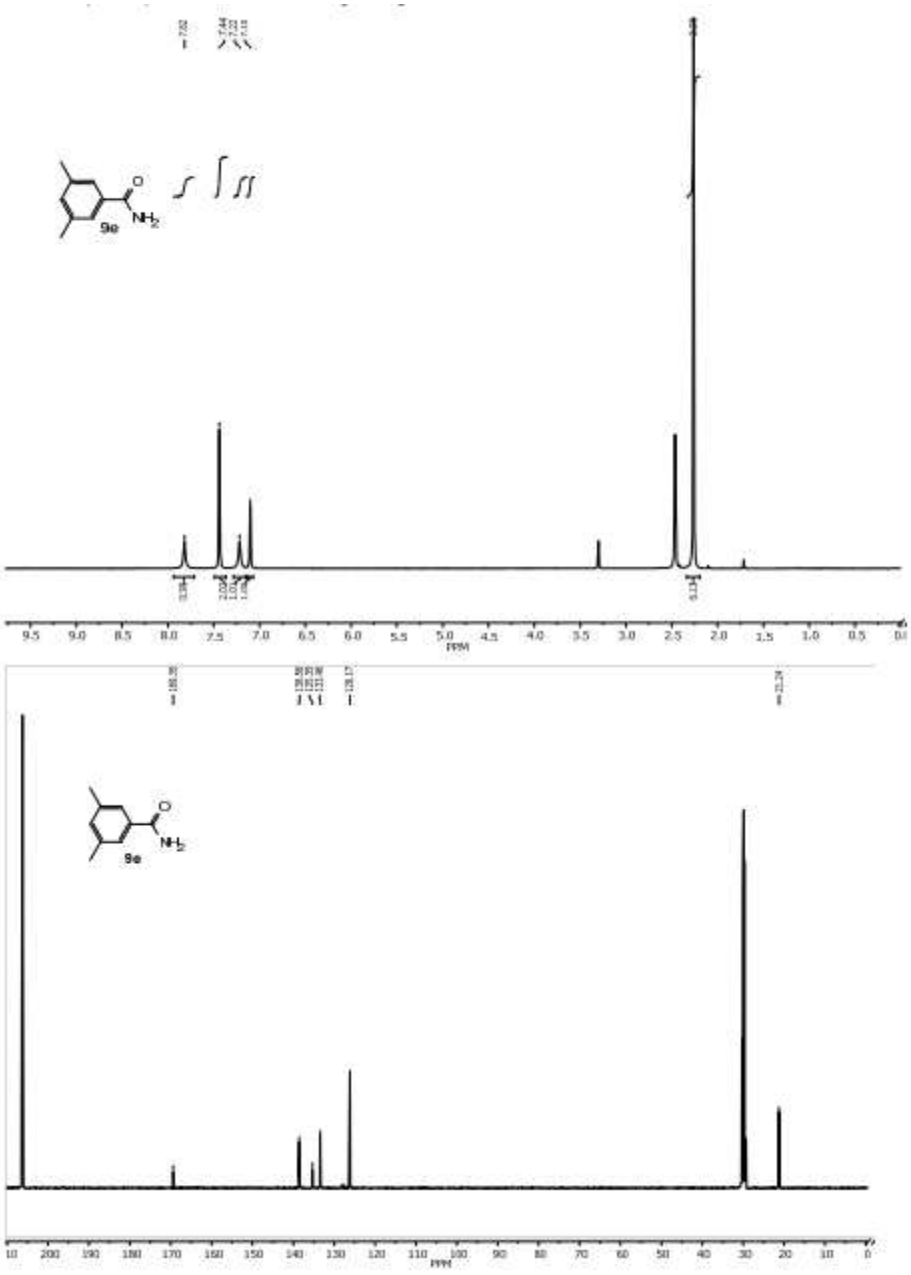

Figure A16: Spectroscopic Data for 3,5-dimethylbenzamide 9e and Corresponding Nitrile 10e (2 of 3)

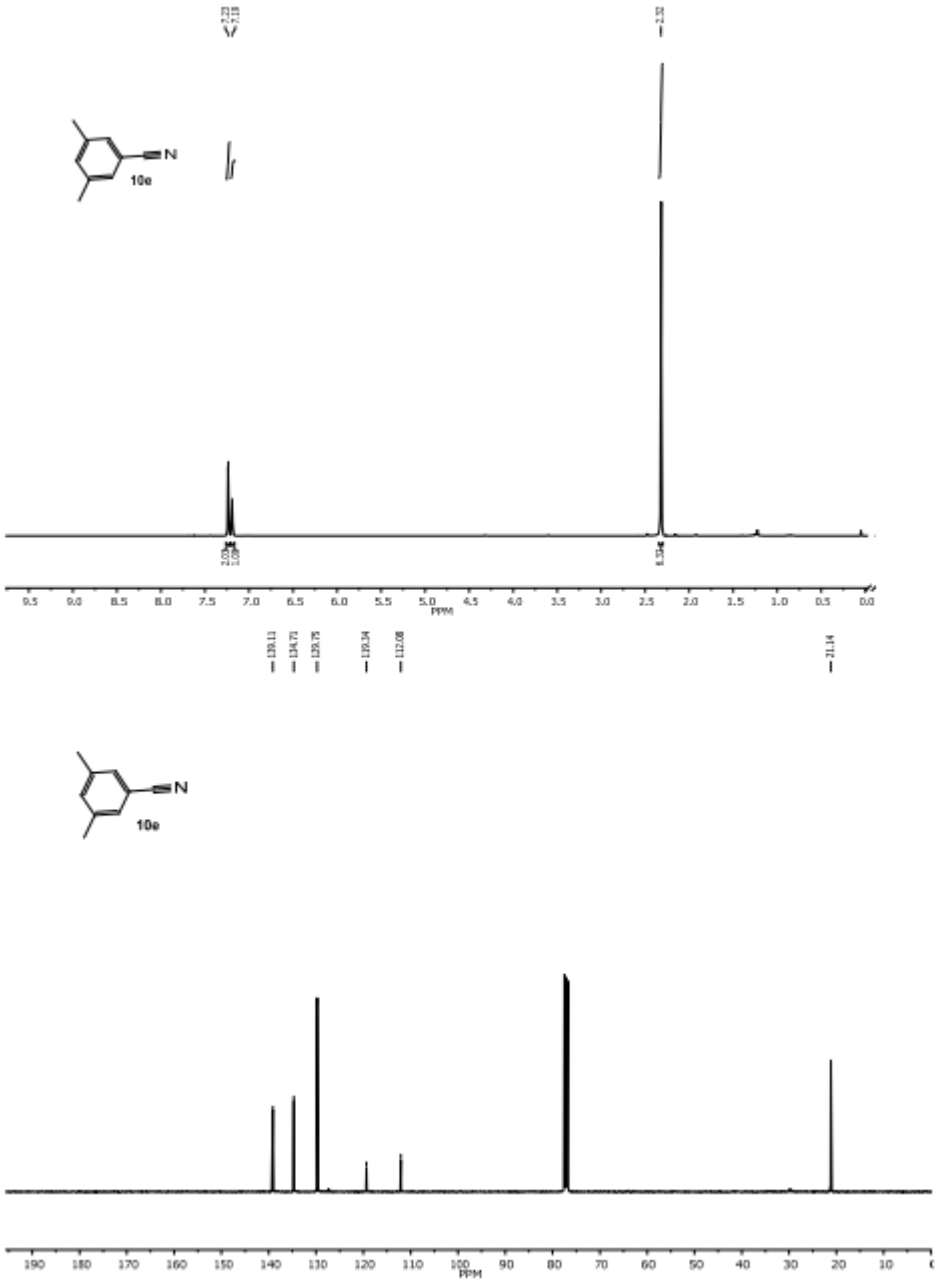

Figure A17: Spectroscopic Data for 3,5-dimethylbenzamide 9e and Corresponding Nitrile 10e (3 of 3)

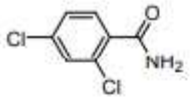

2,4-Dichlorobenzamide 9f:[4] Following the General Procedure, product was isolated as a white solid (420 mg, 83% yield).

^{1}H NMR (400 MHz, acetone-d_6) δ 7.60 – 7.52 (m, 2H), 7.43 (dd, J = 8.2, 1.9 Hz, 1H), 7.32 (br. s, 1H), 7.04 (br. s, 1H) ppm.

^{13}C NMR (100 MHz, acetone-d_6) δ 167.0, 135.7, 135.2, 131.6, 130.5, 129.5, 127.2 ppm.

HRMS (APPI) calcd. for $C_7H_5Cl_2NO$ $[M+H]^+$ calculated: 189.9826; observed: 189.9818.

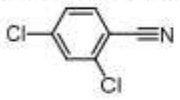

2,4-Dichlorobenzonitrile 10f:[5] Following the General Procedure, product was isolated as a white solid (36 mg, 80% yield) after column chromatography (gradient elution from pure hexane to 10% EtOAc in hexane).

^{1}H NMR (400 MHz, chloroform-d) δ 7.61 (d, J = 8.3 Hz, 1H), 7.54 (d, J = 1.9 Hz, 1H), 7.37 (dd, J = 8.3, 1.9 Hz, 1H) ppm.

^{13}C NMR (100 MHz, chloroform-d) δ 140.2, 137.9, 134.7, 130.4, 128.0, 115.4, 112.0 ppm.

GCMS calcd. for: $C_7H_3Cl_2N$:171; observed:171

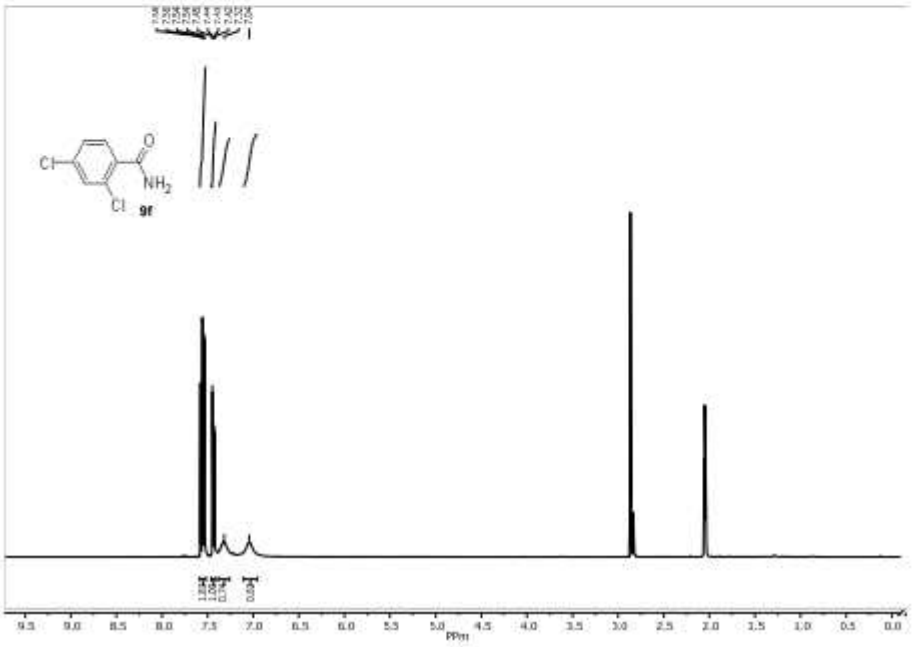

Figure A18: Spectroscopic Data for 2,4-Dichlorobenzamide 9f and Corresponding Nitrile 10f (1 of 3)

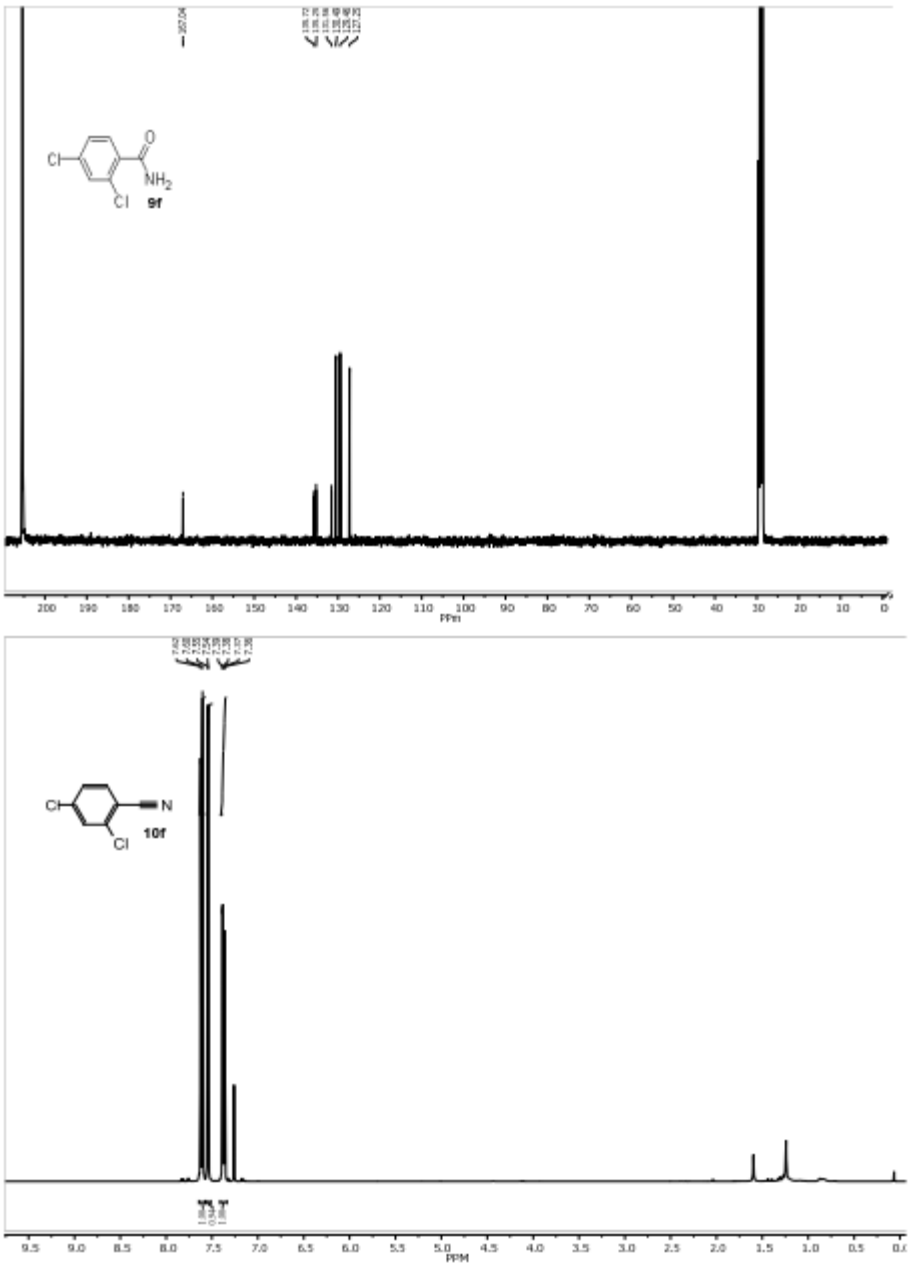

Figure A19: Spectroscopic Data for 2,4-Dichlorobenzamide 9f and Corresponding Nitrile 10f (2 of 3)

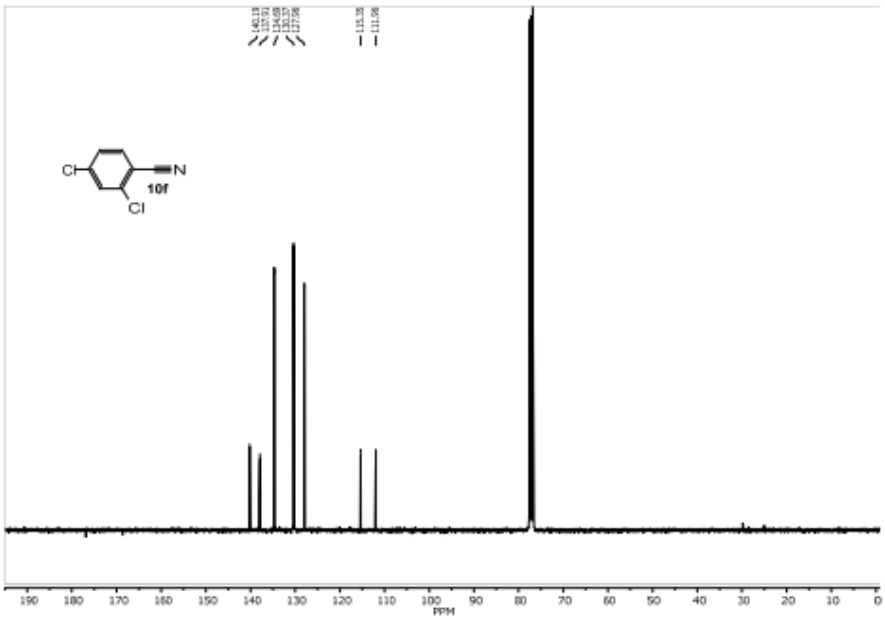

Figure A20: Spectroscopic Data for 2,4-Dichlorobenzamide 9f and Corresponding Nitrile 10f (3 of 3)

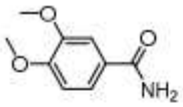

3,4-Dimethoxybenzamide 9g:[6] Following the General Procedure, product was isolated as a white solid (570 mg, 87% yield).

^{1}H NMR (400 MHz, DMSO-d_6) δ 7.87 (br. s, 1H), 7.49 (dd, J = 8.3, 1.9 Hz, 1H), 7.46 (d, J = 1.9 Hz, 1H), 7.22 (br. s, 1H), 6.99 (d, J = 8.3 Hz, 1H), 3.79 (s, 3H), 3.79 (s, 3H) ppm.

^{13}C NMR (100 MHz, DMSO-d_6) δ 167.5, 151.2, 148.1, 126.5, 120.7, 110.9, 110.8, 55.6, 55.5 ppm.

HRMS (APPI) calcd. for $C_9H_{11}NO_3$ $[M+H]^+$ calculated: 182.0817; observed: 182.0810.

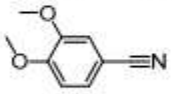

3,4-dimethoxybenzonitrile 10g:[7] Following the General Procedure, product was isolated as a solid (43 mg, 95% yield) after column chromatography (gradient elution from pure hexane to 10% EtOAc in hexane).

^{1}H NMR (400 MHz, chloroform-d) δ 7.28 (dd, J = 8.4, 2.0 Hz, 1H), 7.06 (d, J = 2.0 Hz, 1H), 6.89 (d, J = 8.4 Hz, 1H), 3.92 (s, 3H), 3.89 (s, 3H) ppm.

^{13}C NMR (100 MHz, chloroform-d) δ 152.9, 149.2, 126.6, 119.4, 114.0, 111.3, 104.0, 56.22, 56.2 ppm.

Figure A21: Spectroscopic Data for 3,4-Dimethoxybenzamide 9g and Corresponding Nitrile 10g (1 of 3)

HRMS (APPI) calcd. for $C_9H_9NO_2$ $[M+H]^+$ calculated: 164.0706; observed: 164.0707.

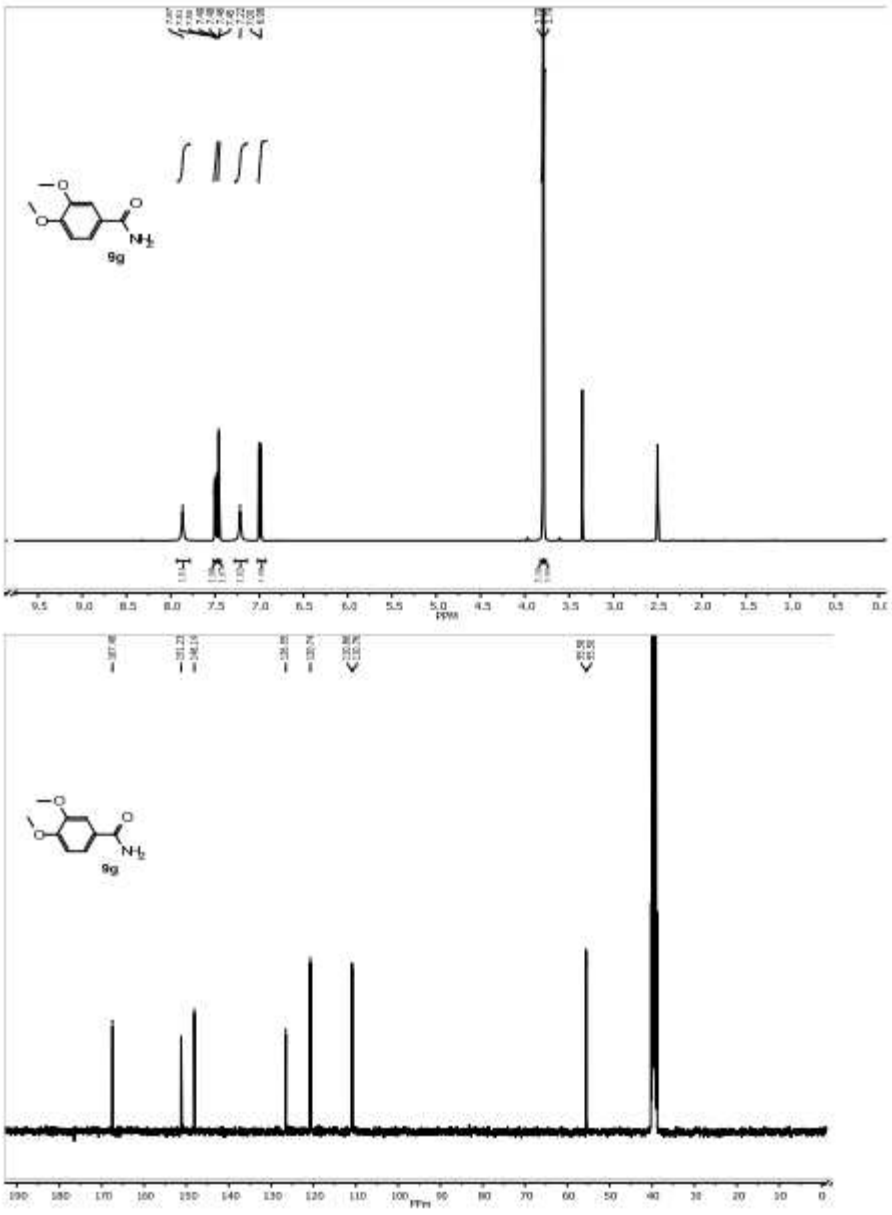

Figure A22: Spectroscopic Data for 3,4-Dimethoxybenzamide 9g and Corresponding Nitrile 10g (2 of 3)

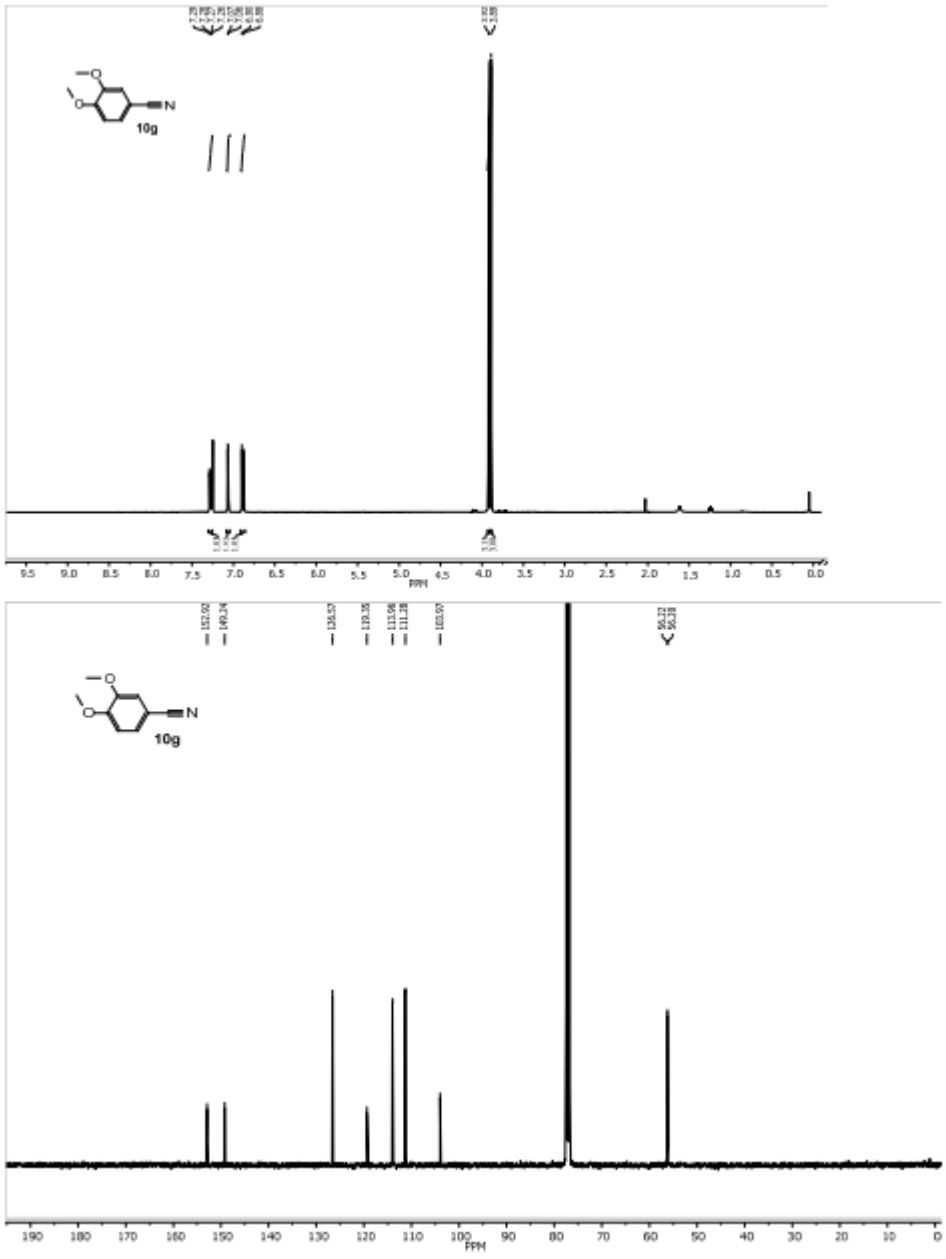

Figure A23: Spectroscopic Data for 3,4-Dimethoxybenzamide 9g and Corresponding Nitrile 10g (3 of 3)

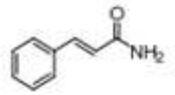

(*E*)-Cinnamamide 9h:[1] Following the General Procedure, product was isolated as a white solid (329 mg, 87% yield).

^{1}H NMR (400 MHz, DMSO-d_6) δ 7.56 – 7.46 (m, 3H), 7.42 – 7.29 (m, 4H), 7.10 (br. s, 1H), 6.57 (d, J = 15.9 Hz, 1H) ppm.

^{13}C NMR (100 MHz, DMSO-d_6) δ 167.2, 139.7, 135.4, 130.0, 129.5 (2C), 128.1 (2C), 122.8 ppm.

HRMS (APPI) calcd. for C_9H_9NO $[M+H]^+$ calculated: 148.0762; observed: 148.0755.

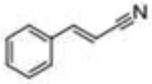

(*E*)-Cinnamonitrile 10h:[1] Following the General Procedure, product was isolated as a colorless oil (39 mg, 89% yield) after column chromatography (gradient elution from pure hexane to 10% EtOAc in hexane).

^{1}H NMR (400 MHz, chloroform-d) δ 7.49 – 7.34 (m, 6H), 5.87 (d, J = 16.8 Hz, 1H) ppm.

^{13}C NMR (100 MHz, chloroform-d) δ 150.7, 133.6, 131.3, 129.2 (2C), 127.5 (2C), 118.3, 96.4 ppm.

HRMS (APPI) calcd. for C_9H_7N $[M+H]^+$ calculated: 130.0651; observed: 130.0653.

Figure A24: Spectroscopic Data for (*E*)-Cinnamamide 9h and Corresponding Nitrile 10h (1 of 4)

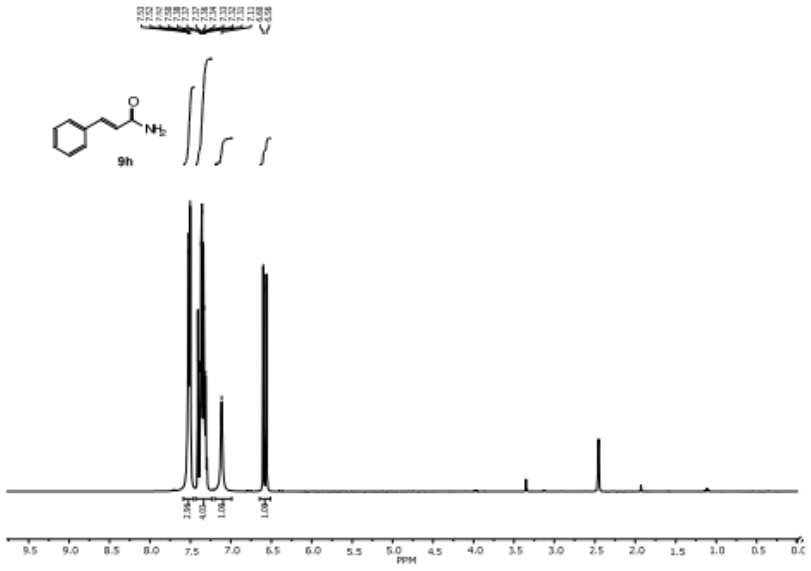

Figure A25: Spectroscopic Data for (*E*)-Cinnamamide 9h and Corresponding Nitrile 10h (2 of 4)

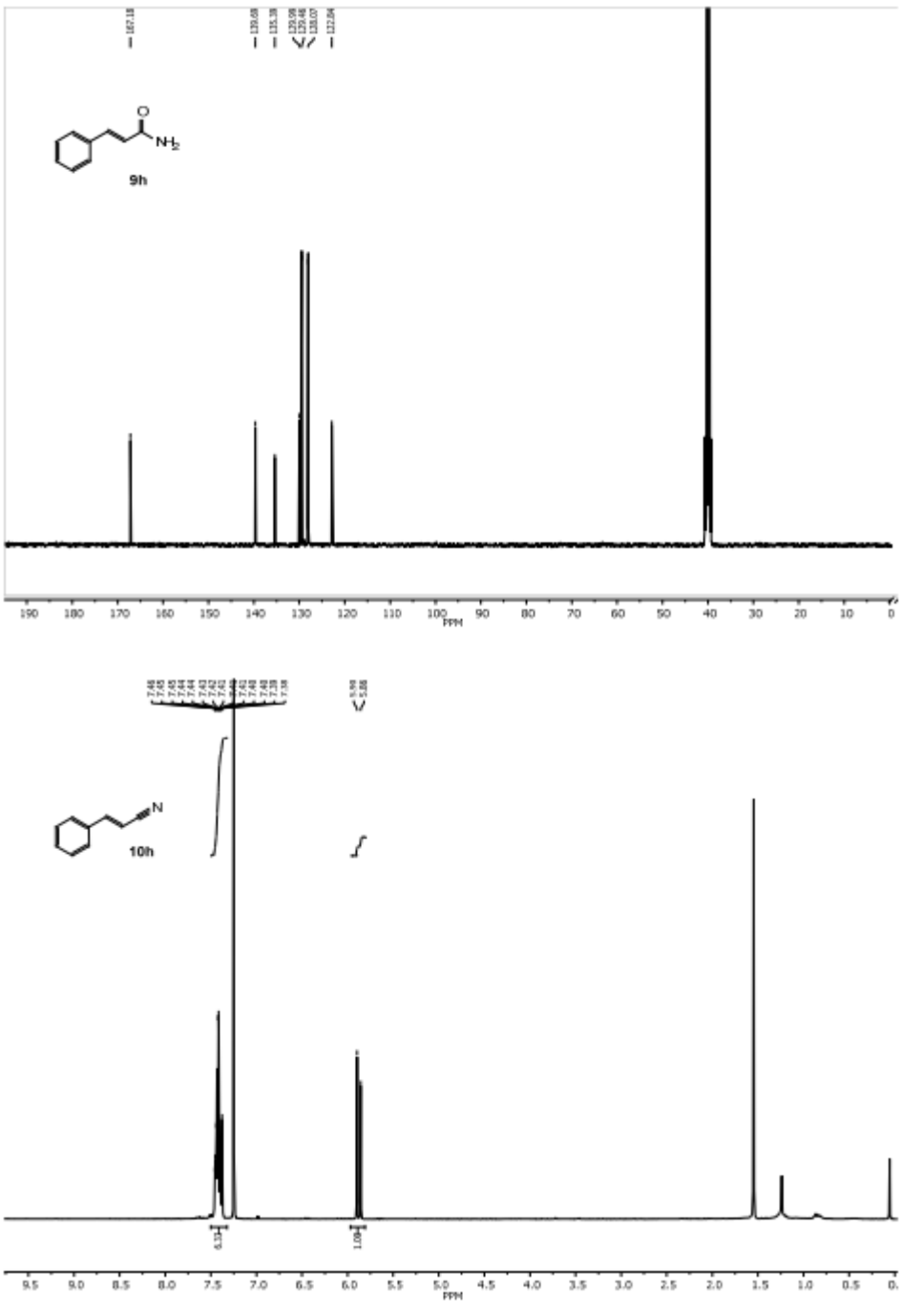

Figure A26: Spectroscopic Data for (*E*)-Cinnamamide 9h and Corresponding Nitrile 10h (3 of 4)

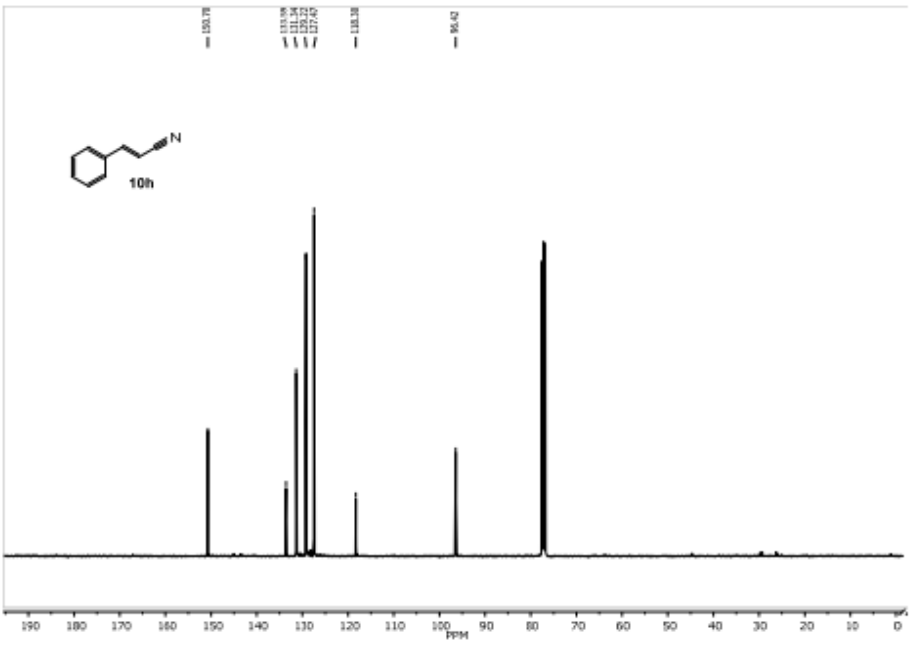

Figure A27: Spectroscopic Data for (*E*)-Cinnamamide 9h and Corresponding Nitrile 10h (4 of 4)

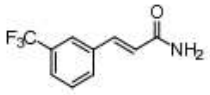

(*E*)-3-(3-(trifluoromethyl)phenyl)acrylamide 9i:[8] Following the General Procedure, product was isolated as a yellow solid (500 mg, 87% yield).

^{1}H NMR (400 MHz, DMSO-d_6) δ 7.87 (s, 1H), 7.85 (d, J = 7.8 Hz, 1H), 7.72 (d, J = 7.8 Hz, 1H), 7.65 (t, J = 7.7 Hz, 1H), 7.57 (br. s, 1H), 7.50 (d, J = 15.9 Hz, 1H), 7.23 (br. s, 1H), 6.76 (d, J = 15.9 Hz, 1H) ppm.

^{13}C NMR (100 MHz, DMSO-d_6) δ 166.7, 138.0, 136.6, 131.9, 130.6, 130.2 (q, $J_{C\text{-}F}$ = 31.7 Hz), 126.3 (q, $J_{C\text{-}F}$ = 3.7 Hz), 125.0, 124.6 (q, $J_{C\text{-}F}$ = 271 Hz) 124.4 (d, J = 3.9 Hz) ppm.

HRMS (APPI) calcd. for $C_{10}H_8F_3NO$ $[M+H]^+$ calculated: 216.0636; observed: 216.0628.

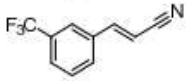

(*E*)-3-(3-(trifluoromethyl)phenyl)acrylonitrile 10i:[9] Following the General Procedure, product was isolated as a colorless oil (38 mg, 83% yield) after column chromatography (gradient elution from pure hexane to 10% EtOAc in hexane).

^{1}H NMR (400 MHz, chloroform-d) δ 7.72 – 7.66 (m, 2H), 7.63 (d, J = 7.9 Hz, 1H), 7.55 (t, J = 7.9 Hz, 1H), 7.42 (d, J = 16.6 Hz, 1H), 5.97 (d, J= 16.6 Hz, 1H) ppm.

^{13}C NMR (100 MHz, chloroform-d) δ 148.9, 134.3, 131.9 (q, $J_{C\text{-}F}$ = 32.8 Hz), 130.5, 129.9, 127.7 (q, $J_{C\text{-}F}$ = 3.8 Hz), 124.1 (t, $J_{C\text{-}F}$ = 3.9 Hz), 123.6 (q, $J_{C\text{-}F}$ = 271 Hz), 117.5, 98.7 ppm.

Figure A28: Spectroscopic Data for (*E*)-3-(3-trifluoromethyl)phenyl)acrylamide 9i and Corresponding Nitrile 10i (1 of 3)

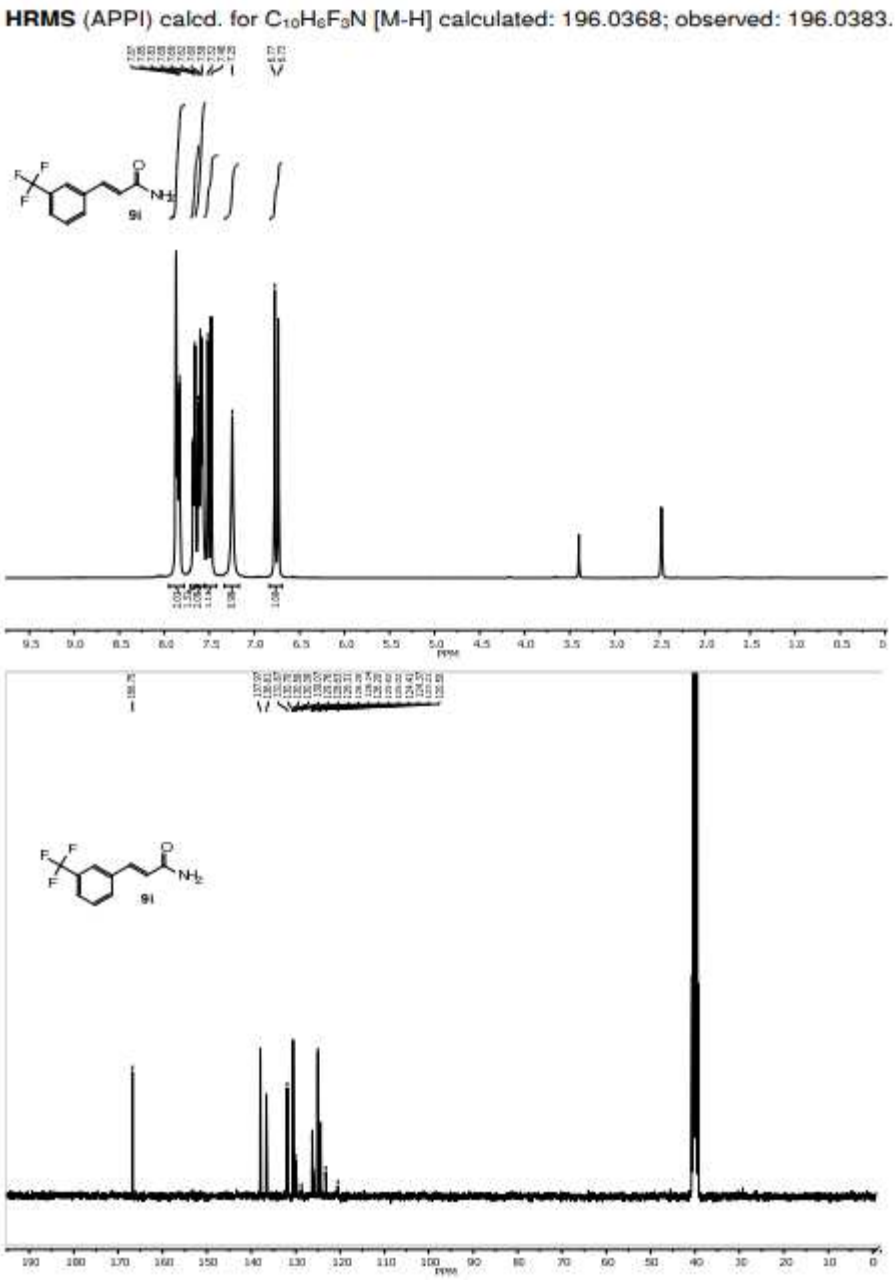

Figure A29: Spectroscopic Data for (*E*)-3-(3-trifluoromethyl)phenyl)acrylamide 9i and Corresponding Nitrile 10i (2 of 3)

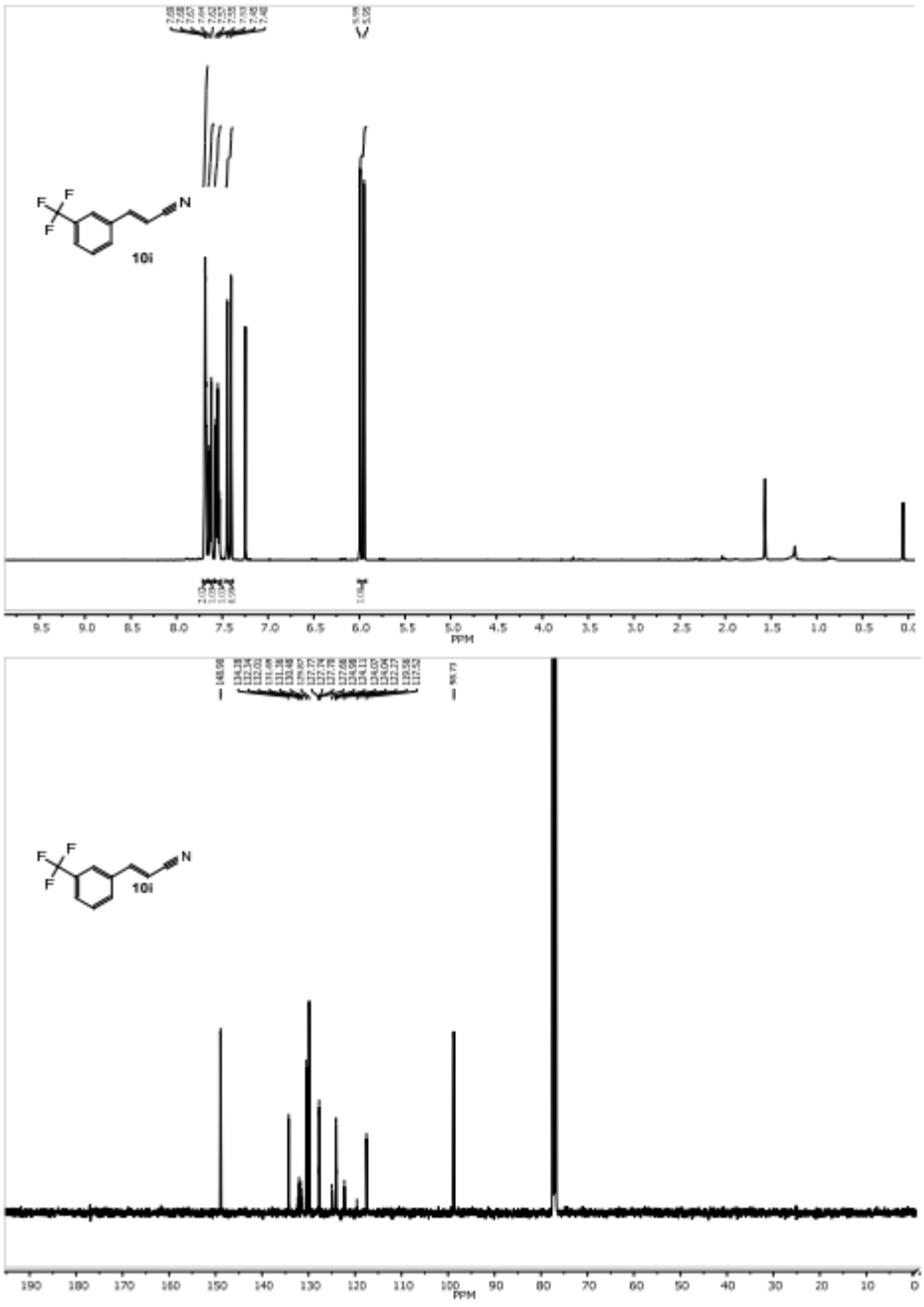

Figure A30: Spectroscopic Data for (*E*)-3-(3-trifluoromethyl)phenyl)acrylamide 9i and Corresponding Nitrile 10i (3 of 3)

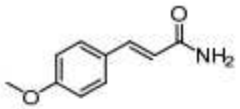

(*E*)-3-(4-methoxyphenyl)acrylamide 9j:[10] Following the General Procedure, product was isolated as a white solid (410 mg, 87% yield).

^{1}H NMR (500 MHz, chloroform-d) δ 7.60 (d, *J* = 15.6 Hz, 1H), 7.47 (d, *J* = 8.8 Hz, 2H), 6.90 (d, *J* = 8.8 Hz, 2H), 6.32 (d, *J* = 15.6 Hz, 1H), 5.46 (br. s, 2H), 3.83 (s, 3H) ppm.

^{13}C NMR (125 MHz, chloroform-d) δ 168.0, 161.2, 142.4, 129.7 (2C), 127.3, 116.9, 114.4 (2C), 55.5 ppm.

HRMS (APPI) calcd. for $C_{10}H_{11}NO_2$ [M+H] calculated:178.0863; observed: 178.0855.

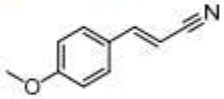

(*E*)-3-(4-methoxyphenyl)acrylonitrile 10j:[11] Following the General Procedure, product was isolated as a yellow solid (38 mg, 85% yield) after column chromatography (gradient elution from pure hexane to 10% EtOAc in hexane).

^{1}H NMR (500 MHz, chloroform-d) δ 7.39 (d, *J* = 8.7 Hz, 2H), 7.33 (d, *J* = 16.6 Hz, 1H), 6.91 (d, *J* = 8.8 Hz, 2H), 5.71 (d, *J* = 16.6 Hz, 1H), 3.84 (s, 3H) ppm.

^{13}C NMR (125 MHz, chloroform-d) δ 162.1, 150.2, 129.2 (2C), 126.4, 118.8, 114.6 (2C), 93.4, 55.6 ppm.

HRMS(APPI) calcd. for $C_{10}H_9NO$ [M+H] calculated: 160.0762 observed: 160.0759.

Figure A31: Spectroscopic Data for (*E*)-3-(4-methoxyphenyl)acrylamide 9j and Corresponding Nitrile 10j (1 of 3)

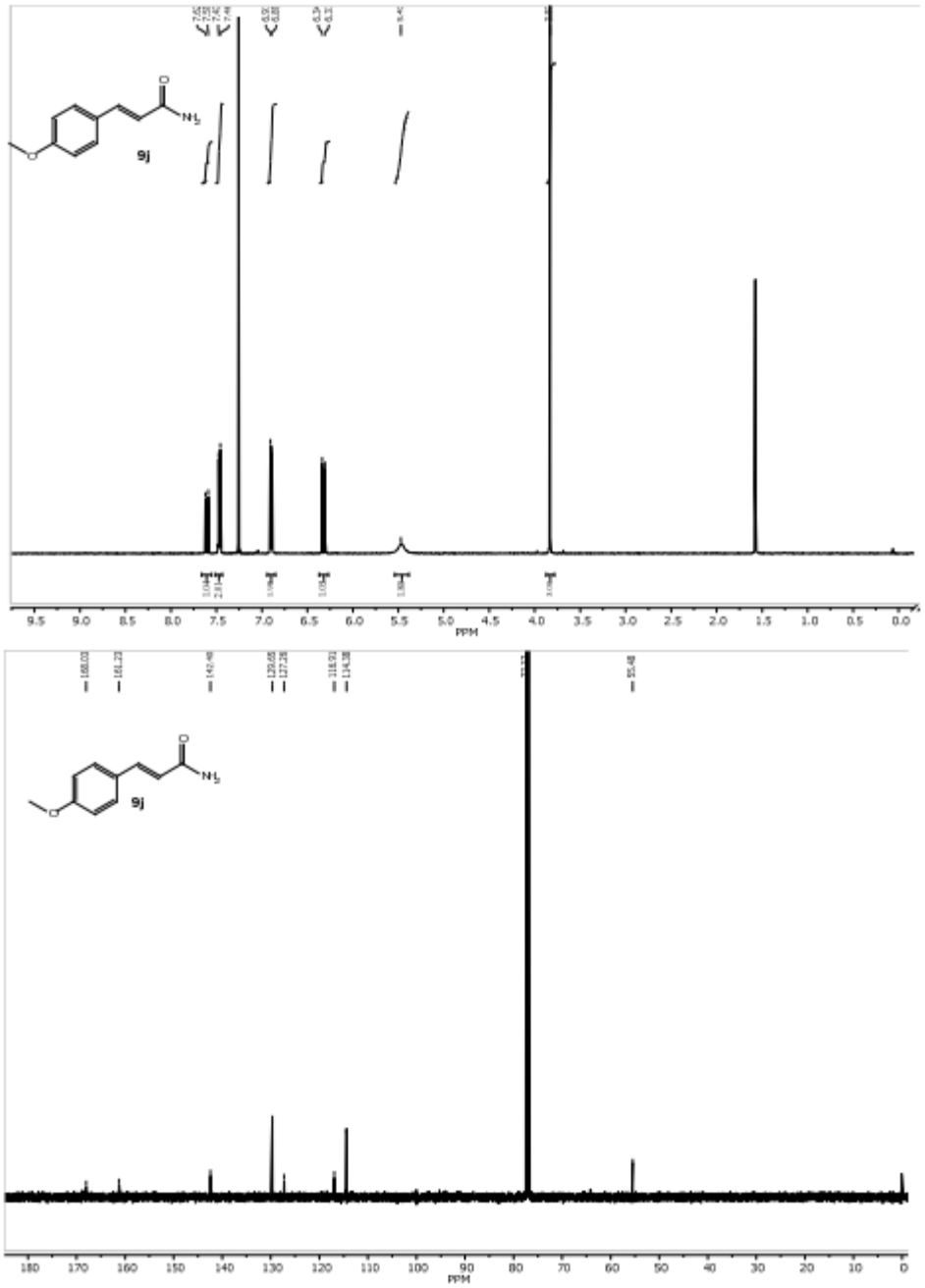

Figure A32: Spectroscopic Data for (*E*)-3-(4-methoxyphenyl)acrylamide 9j and Corresponding Nitrile 10j (2 of 3)

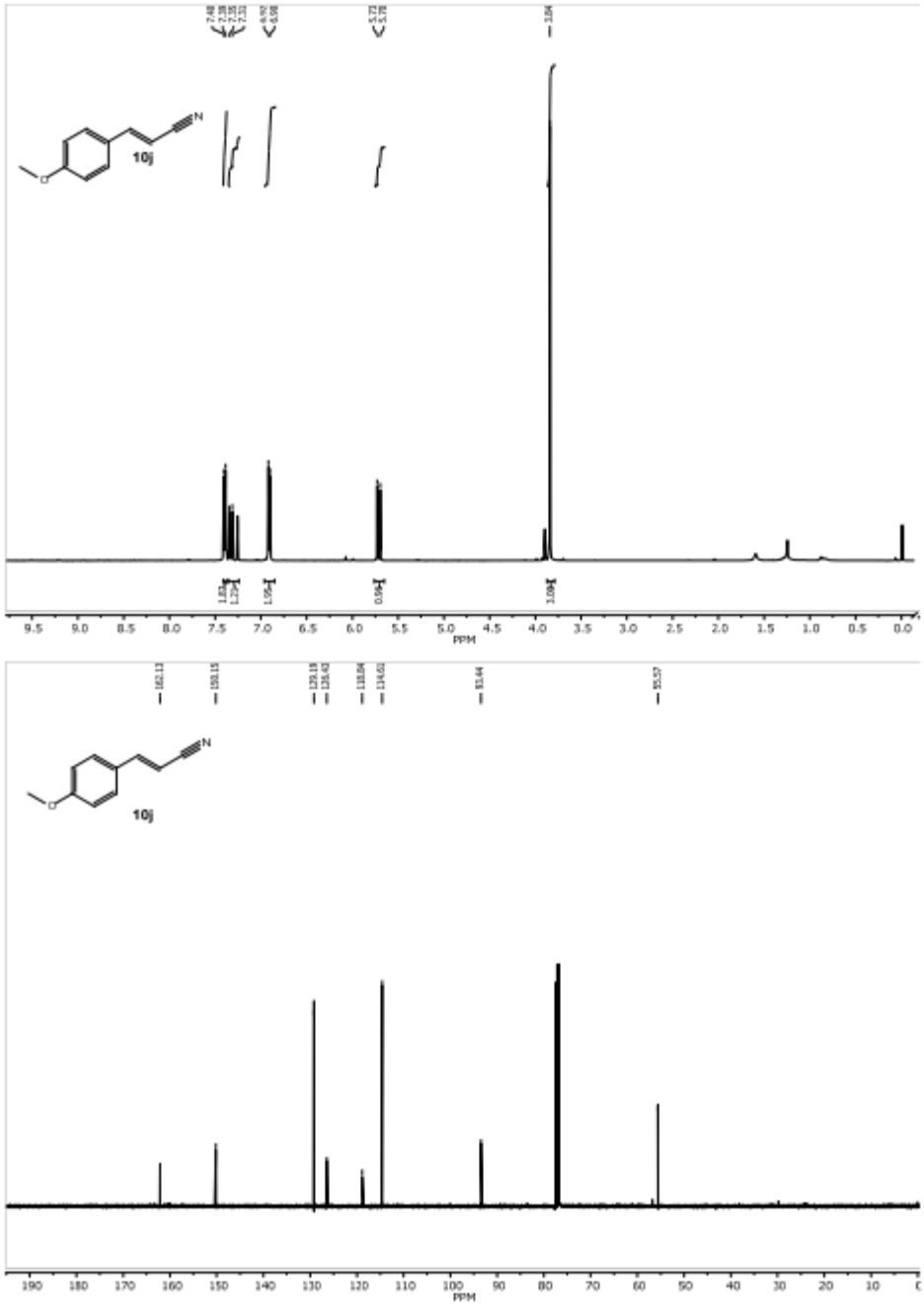

Figure A33: Spectroscopic Data for (*E*)-3-(4-methoxyphenyl)acrylamide 9j and Corresponding Nitrile 10j (3 of 3)

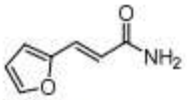

(*E*)-3-(furan-2-yl)acrylamide 9k:[12] Following the General Procedure, product was isolated as a yellow solid (472 mg, quantitative).

^{1}H NMR (400 MHz, DMSO-d_6) δ 7.76 (d, J = 1.8 Hz, 1H), 7.58 (br. s, 1H), 7.21 (d, J = 15.6 Hz, 1H), 7.10 (br. s, 1H), 6.75 (d, J = 3.3 Hz, 1H), 6.58 (dd, J = 3.3, 1.8 Hz, 1H), 6.40 (d, J = 15.6 Hz, 1H) ppm.

^{13}C NMR (100 MHz, DMSO-d_6) δ 166.5, 151.0, 144.8, 126.6, 119.6, 113.8, 112.4 ppm.

HRMS (APPI) calcd. for $C_7H_7NO_2$ $[M+H]^+$ calculated: 138.0555; observed: 138.0547.

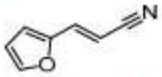

(*E*)-3-(furan-2-yl)acrylonitrile 10k:[13] Following the General Procedure, product was isolated as a colorless oil (36 mg, 83% yield) after column chromatography (gradient elution from pure hexane to 10% EtOAc in hexane).

^{1}H NMR (400 MHz, chloroform-d) δ 7.48 (d, J = 1.8 Hz, 1H), 7.10 (d, J = 16.1 Hz, 1H), 6.61 (d, J = 3.4 Hz, 1H), 6.49 (dd, J = 3.4, 1.8 Hz, 1H), 5.75 (d, J = 16.1 Hz, 1H) ppm.

^{13}C NMR (100 MHz, chloroform-d) δ 149.9, 145.6, 136.2, 118.4, 115.6, 112.7, 93.5 ppm.

HRMS (APPI) calcd. for C_7H_5N $[M+H]^+$ calculated: 120.0444; observed: 120.0445.

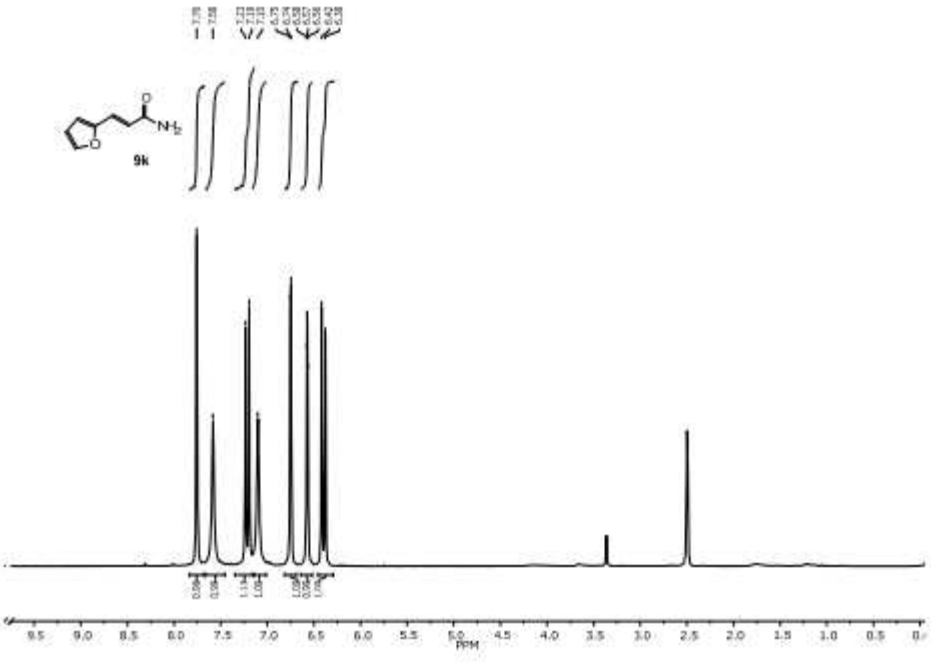

Figure A34: Spectroscopic Data for (*E*)-3-(furan-2-yl)acrylamide 9k and Corresponding Nitrile 10k (1 of 3)

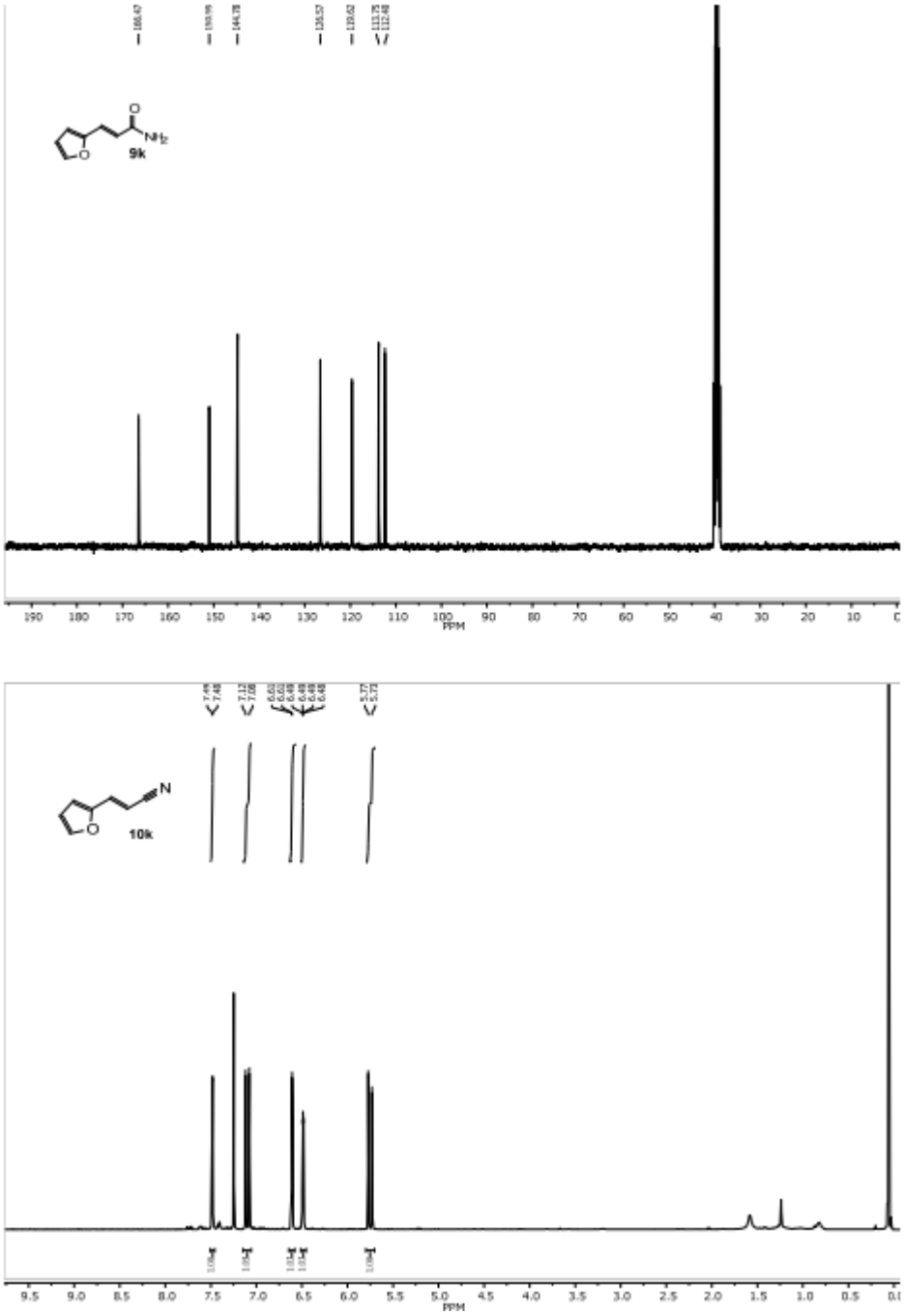

Figure A35: Spectroscopic Data for (*E*)-3-(furan-2-yl)acrylamide 9k and Corresponding Nitrile 10k (2 of 3)

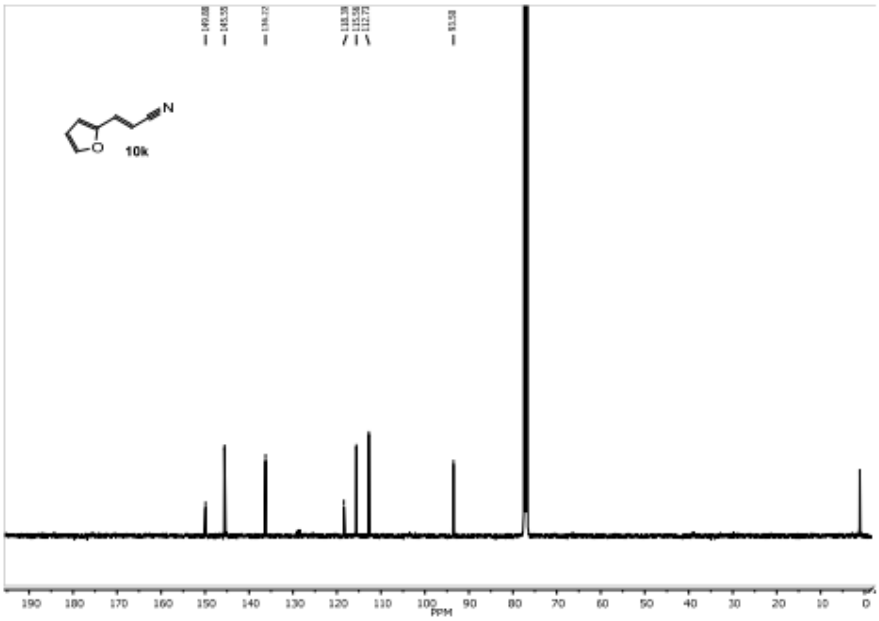

Figure A36: Spectroscopic Data for (*E*)-3-(furan-2-yl)acrylamide 9k and Corresponding Nitrile 10k (3 of 3)

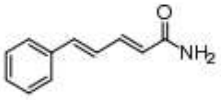

(2*E*,4*E*)-5-phenylpenta-2,4-dienamide 9l:[14] Following the General Procedure, product was isolated as a yellow solid (297 mg, 60% yield).

^{1}H NMR (400 MHz, DMSO-d_6) δ 7.56 (d, J = 7.3 Hz, 2H), 7.53 (br. s, 1H), 7.37 (t, J = 7.4 Hz, 2H), 7.30 (t, J = 7.3 Hz, 1H), 7.19 (dd, J = 14.9, 10.8 Hz, 1H), 7.05 (dd, J = 15.4, 10.8 Hz, 1H), 7.03 (br. s, 1H), 6.93 (d, J = 15.5 Hz, 1H), 6.13 (d, J = 14.9 Hz, 1H) ppm.

^{13}C NMR (100 MHz, DMSO-d_6) δ 166.8, 139.7, 138.0, 136.3, 128.8 (2C), 128.6, 127.0 (3C), 125.7 ppm.

HRMS (APPI) calcd. for $C_{11}H_{11}NO$ $[M+H]^+$ calculated: 174.0919; observed: 174.0912.

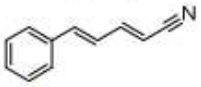

(2*E*,4*E*)-5-phenylpenta-2,4-dienenitrile 10l:[14] Following the General Procedure, product was isolated as a colorless oil (38 mg, 86% yield) after column chromatography (gradient elution from pure hexane to 10% EtOAc in hexane).

^{1}H NMR (400 MHz, chloroform-d) δ 7.46 (d, J = 6.6 Hz, 2H), 7.37 (m, 3H), 7.16 (dd, J = 15.7, 10.0 Hz, 1H), 6.84 (m, 2H), 5.43 (d, J = 15.9 Hz, 1H) ppm.

^{13}C NMR (100 MHz, chloroform-d) δ 150.4, 141.5, 135.3, 129.8, 129.0 (2C), 127.5 (2C), 125.5, 118.5, 98.4 ppm.

Figure A37: Spectroscopic Data for (2*E*,4*E*)-5-phenylpenta-2,4-dienamide 9l and Corresponding Nitrile 10l (1 of 4)

HRMS (APPI) calcd. for $C_{11}H_9N$ $[M+H]^+$ calculated: 156.0808; observed: 156.0809.

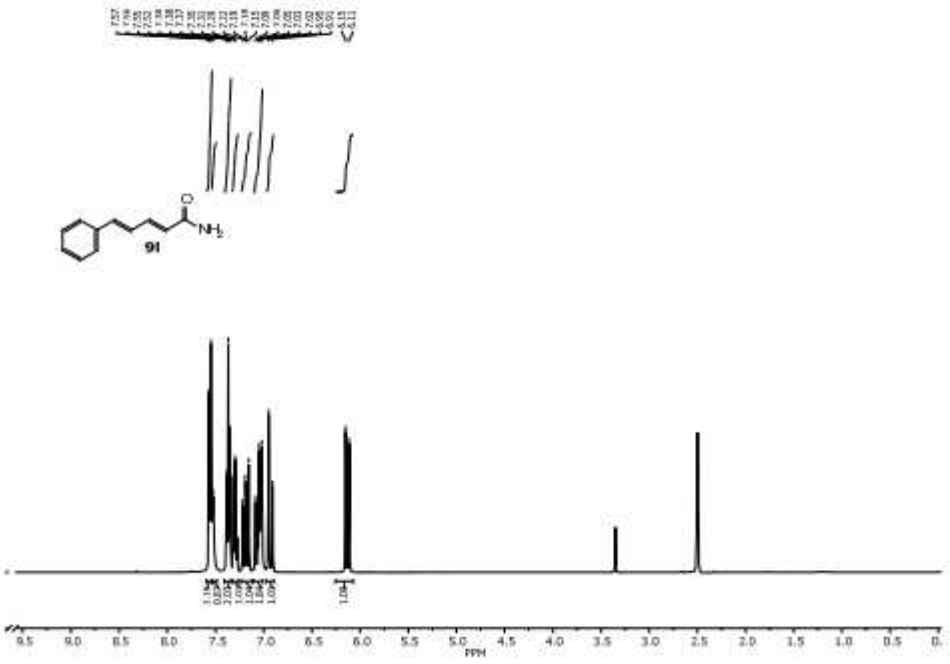

Figure A38: Spectroscopic Data for (2*E*,4*E*)-5-phenylpenta-2,4-dienamide 9l and Corresponding Nitrile 10l (2 of 4)

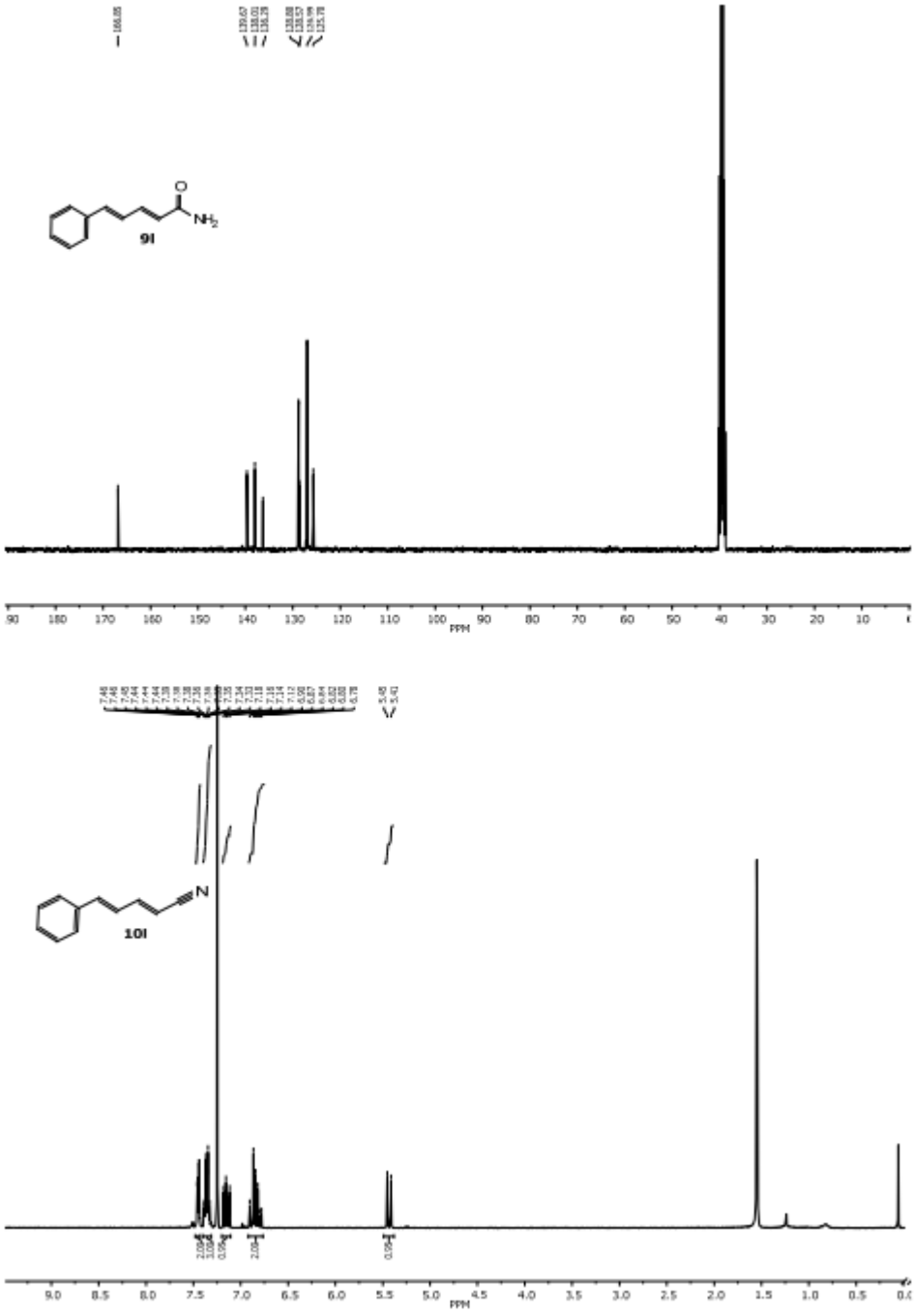

Figure A39: Spectroscopic Data for (2*E*,4*E*)-5-phenylpenta-2,4-dienamide 9l and Corresponding Nitrile 10l (3 of 4)

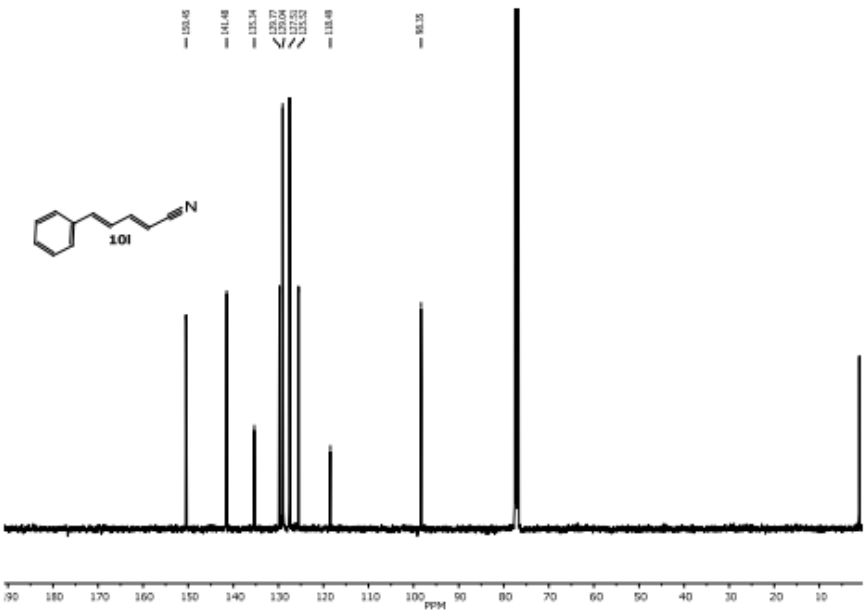

Figure A40: Spectroscopic Data for (2*E*,4*E*)-5-phenylpenta-2,4-dienamide 9l and Corresponding Nitrile 10l (4 of 4)

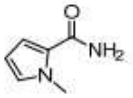

1-methyl-1H-pyrrole-2-carboxamide 9m:[15] Following the General Procedure, product was isolated as brown solid (481 mg, 97% yield).

^{1}H NMR (400 MHz, DMSO-d_6) δ 7.45 (br. s, 1H), 6.87 (t, J = 2.2 Hz, 1H), 6.84 (br. s, 1H), 6.78 (dd, J = 3.8, 1.8 Hz, 1H), 5.98 (dd, J = 3.8, 2.2 Hz, 1H), 3.82 (s, 3H) ppm.

^{13}C NMR (100 MHz, DMSO-d_6) δ 163.1, 127.9, 125.3, 113.0, 106.5, 36.3 ppm.

HRMS (APPI) calcd. for $C_6H_8N_2O$ $[M+H]^+$ calculated: 125.0715; observed: 125.0708.

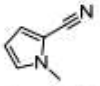

1-methyl-1H-pyrrole-2-carbonitrile 10m:[16] Following the General Procedure, product was isolated as a colorless oil (22 mg, 51% yield) after column chromatography (gradient elution from pure hexane to 10% EtOAc in hexane).

^{1}H NMR (400 MHz, chloroform-d) δ 6.90 – 6.58 (m, 2H), 6.15 (dd, J = 4.1, 2.7 Hz, 1H), 3.77 (s, 3H) ppm.

^{13}C NMR (100 MHz, chloroform-d) δ 127.6, 120.0, 113.9, 109.5, 104.5, 35.4 ppm.

HRMS (APPI) calcd. for $C_6H_6N_2$ $[M+H]^+$ calculated:107.0609; observed: 107.0605.

Figure A41: Spectroscopic Data for 1-methyl-1H-pyrrole-2-carboxamide 9m and Corresponding Nitrile 10m (1 of 3)

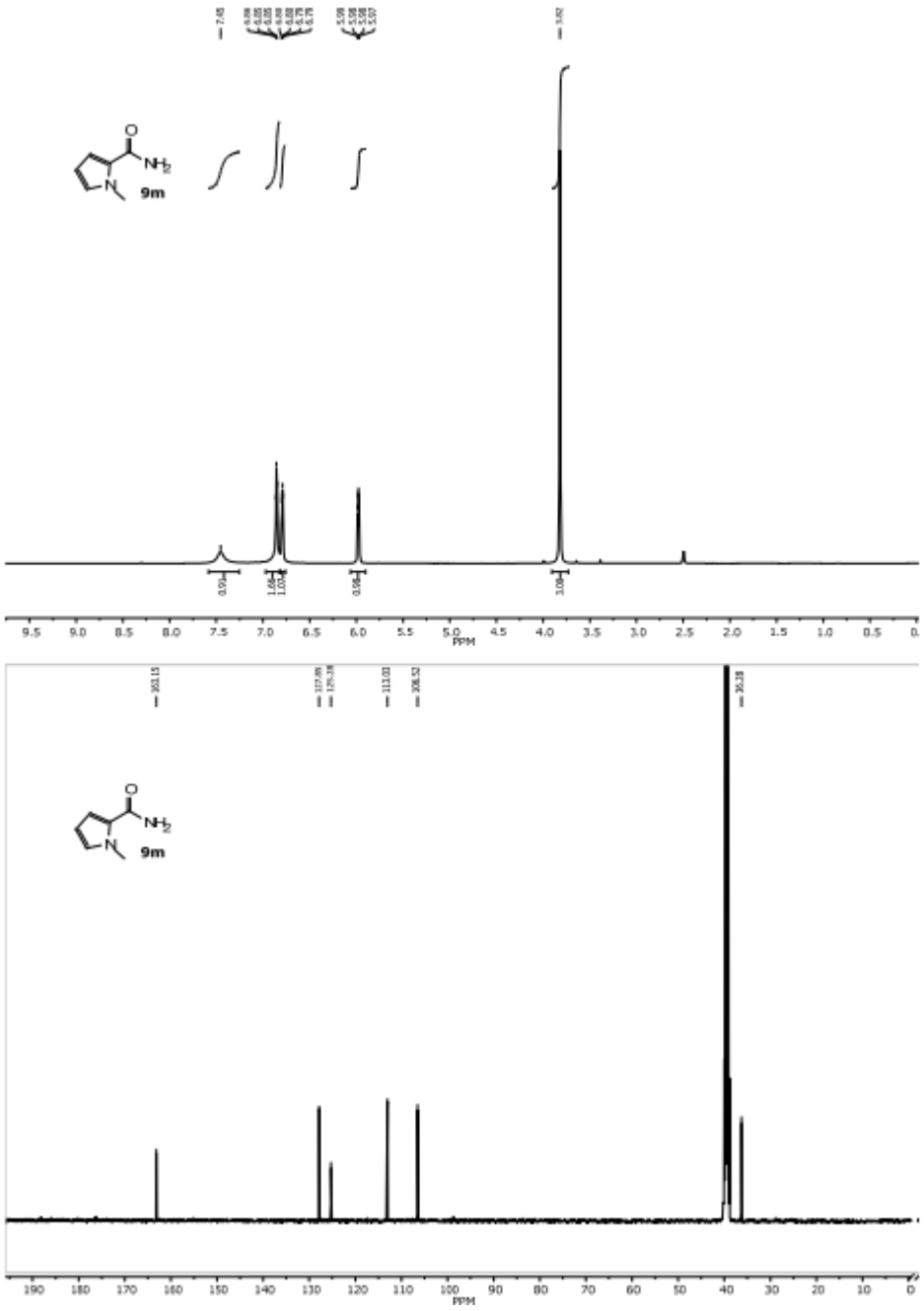

Figure A42: Spectroscopic Data for 1-methyl-1H-pyrrole-2-carboxamide 9m and Corresponding Nitrile 10m (2 of 3)

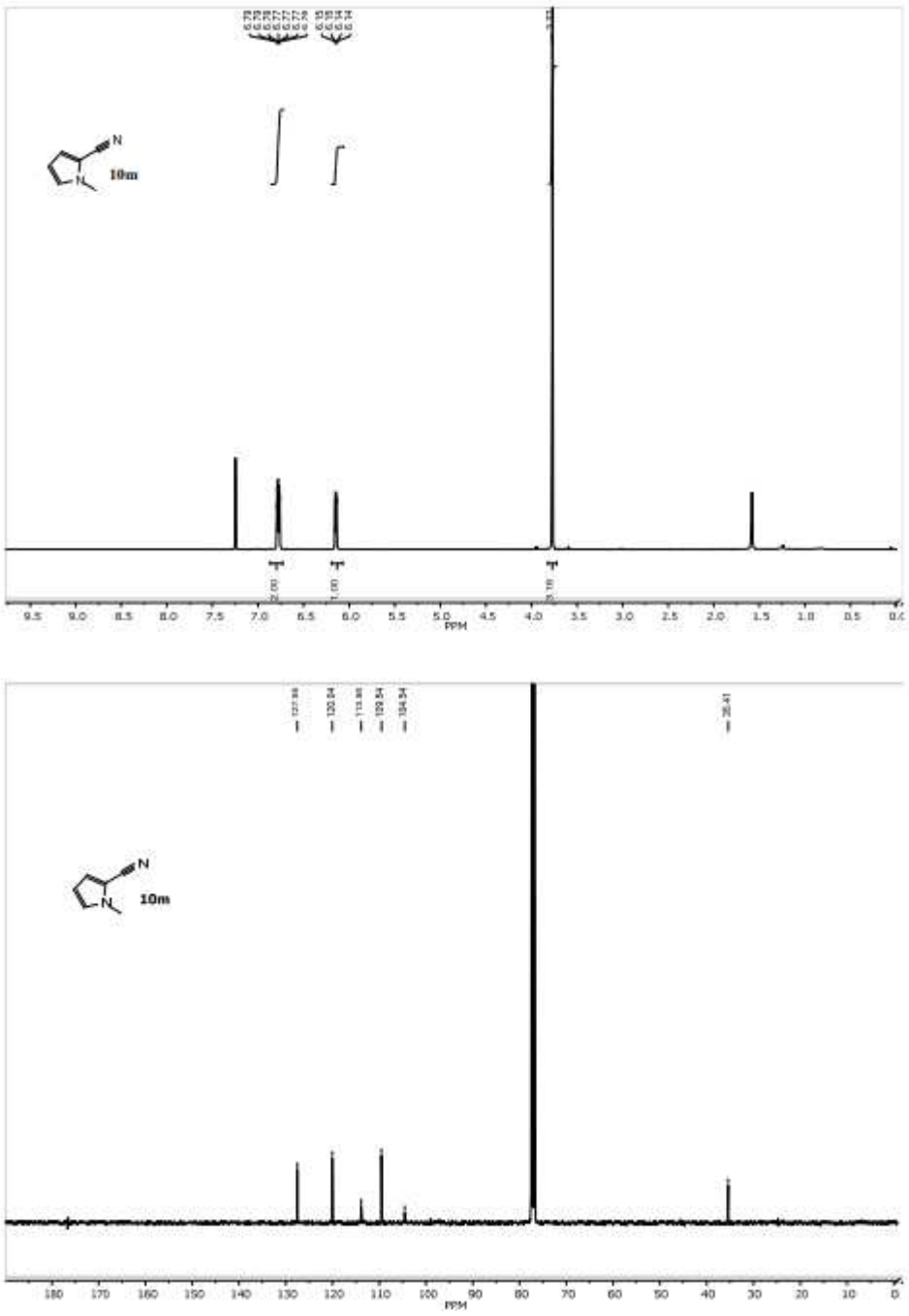

Figure A43: Spectroscopic Data for 1-methyl-1H-pyrrole-2-carboxamide 9m and Corresponding Nitrile 10m (3 of 3)

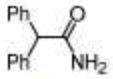

2,2-diphenylacetamide 9n: Following the General Procedure, product was isolated as a white solid (429 mg, 86% yield).

^{1}H NMR (400 MHz, DMSO-d_6) δ 7.69 (br. s, 1H), 7.33 – 7.27 (m, 8H), 7.29 – 7.16 (m, 2H), 7.10 (br. s, 1H), 4.92 (s, 1H) ppm.

^{13}C NMR (100 MHz, DMSO-d_6) δ 173.0, 140.5 (2C), 128.5 (4C), 128.2 (4C), 126.6 (2C), 56.3 ppm.

HRMS (APPI) calcd. for $C_{14}H_{13}NO$ $[M+H]^+$ calculated: 212.1075; observed: 212.1068.

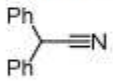

2,2-diphenylacetonitrile 10n: Following the General Procedure, product was isolated as a white solid (39 mg, 84% yield) after column chromatography (gradient elution from pure hexane to 10% EtOAc in hexane).

^{1}H NMR (400 MHz, chloroform-d) δ 7.62 – 7.06 (m, 10H), 5.14 (s, 1H) ppm.

^{13}C NMR (100 MHz, chloroform-d) δ 136.0 (2C), 129.3 (4C), 128.4 (2C), 127.8 (4C), 119.8, 42.7 ppm.

HRMS (APPI) calcd. for $C_{14}H_{11}N$ $[M+H]^+$ calculated: 194.0964; observed: 194.0971.

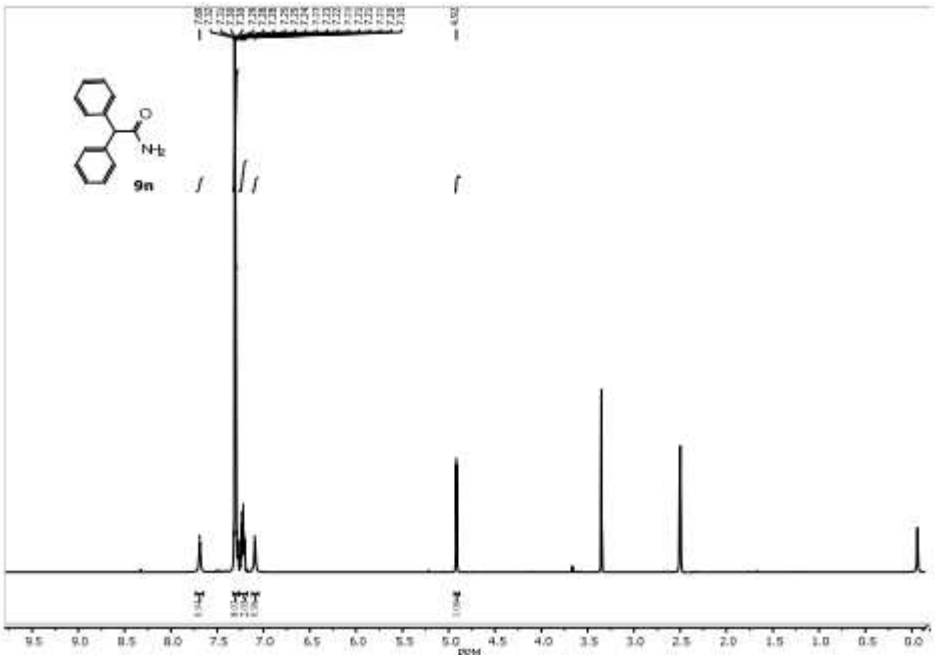

Figure A44: Spectroscopic Data for 2,2-diphenylacetamide 9n and Corresponding Nitrile 10n (1 of 3)

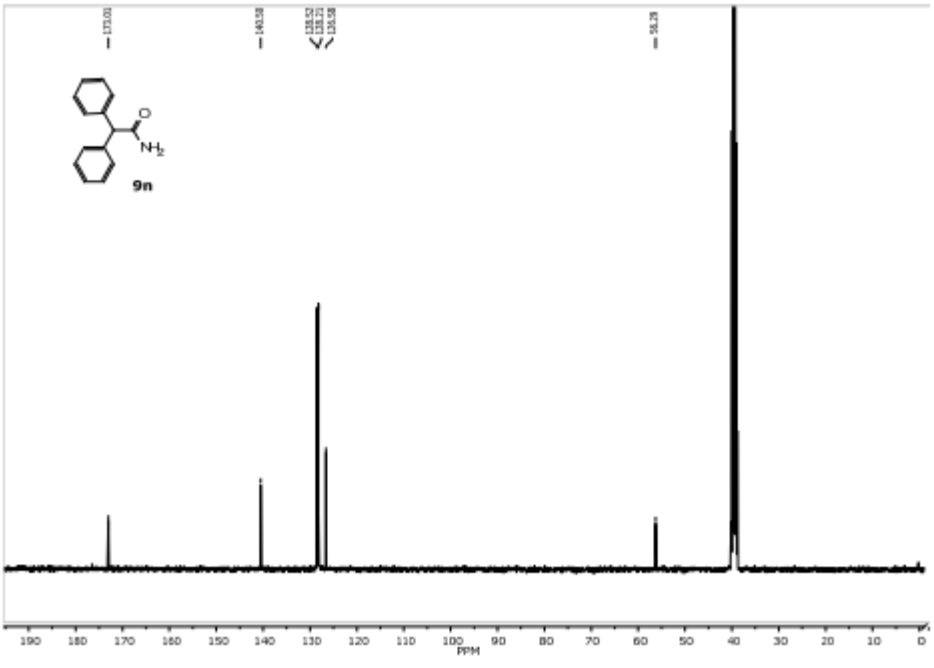

Figure A45: Spectroscopic Data for 2,2-diphenylacetamide 9n and Corresponding Nitrile 10n (2 of 3)

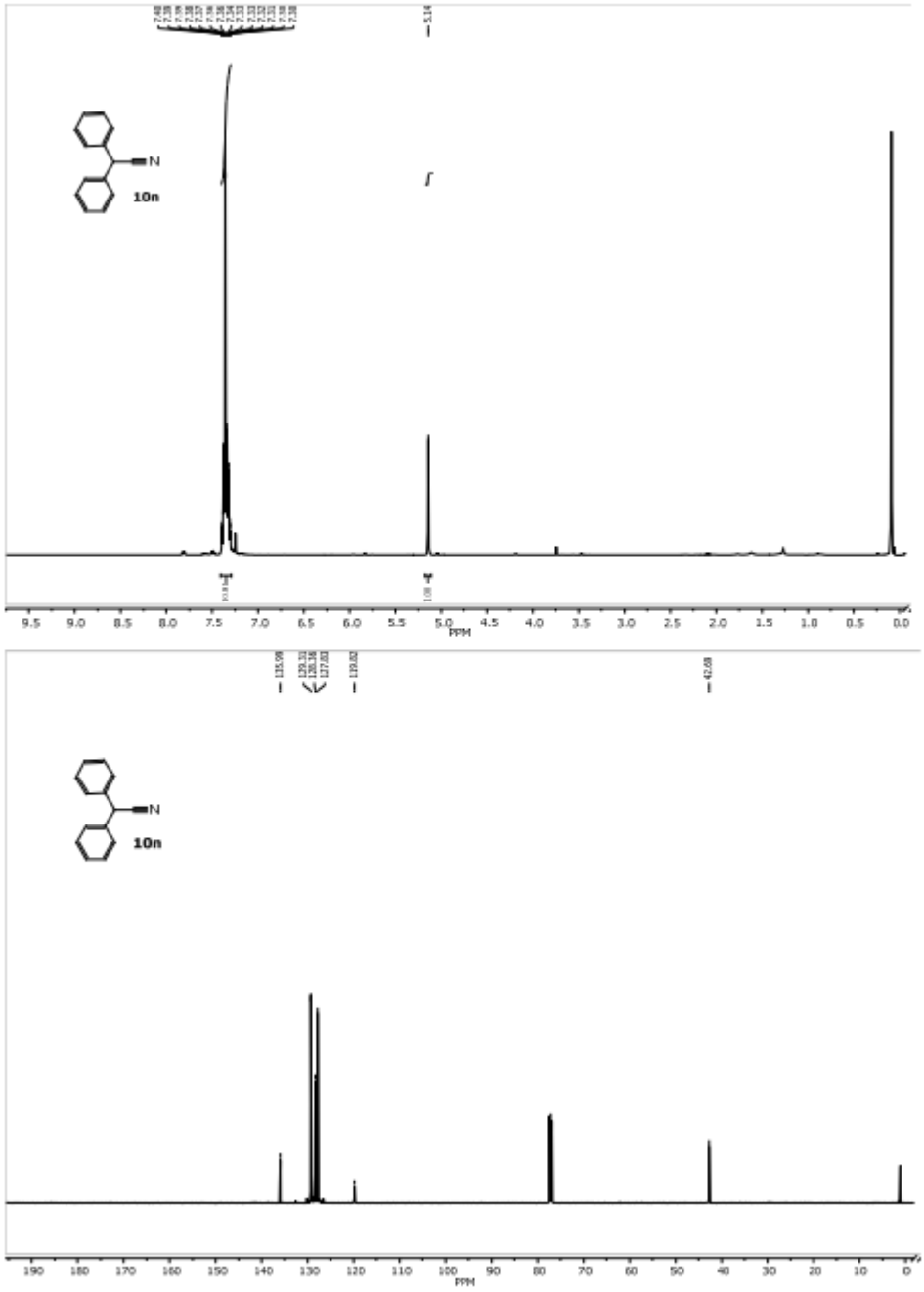

Figure A46: Spectroscopic Data for 2,2-diphenylacetamide 9n and Corresponding Nitrile 10n (3 of 3)

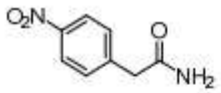

2-(4-nitrophenyl)acetamide 9o:[2] Following the General Procedure, product was isolated as a white solid (379 mg, 87% yield).

^{1}H NMR (400 MHz, DMSO-d_6) δ 8.17 (d, J = 8.7 Hz, 2H), 7.61 (br. s, 1H), 7.53 (d, J = 8.7 Hz, 2H), 7.04 (br. s, 1H), 3.55 (s, 2H) ppm.

^{13}C NMR (100 MHz, DMSO-d_6) δ 171.1, 146.2, 144.7, 130.5 (2C), 123.3 (2C), 41.8 ppm.

HRMS (APPI) calcd. for $C_8H_8N_2O_3$ [M-H]$^-$ calculated: 179.0457; observed: 179.0461.

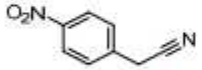

2-(4-nitrophenyl)acetonitrile 10o:[2] Following the General Procedure, product was isolated as a pale-yellow solid (40 mg, 88% yield) after column chromatography (gradient elution from pure hexane to 10% EtOAc in hexane).

^{1}H NMR (400 MHz, chloroform-d) δ 8.25 (d, J = 8.7 Hz, 2H), 7.53 (d, J = 8.6 Hz, 2H), 3.88 (s, 2H) ppm.

^{13}C NMR (100 MHz, chloroform-d) δ 147.9, 137.1, 129.1 (2C), 124.5 (2C), 116.6, 23.7 ppm.

HRMS (APPI) calcd. for $C_8H_6N_2O_2$ [M-H]$^-$ calculated: 161.0345; observed: 161.0358.

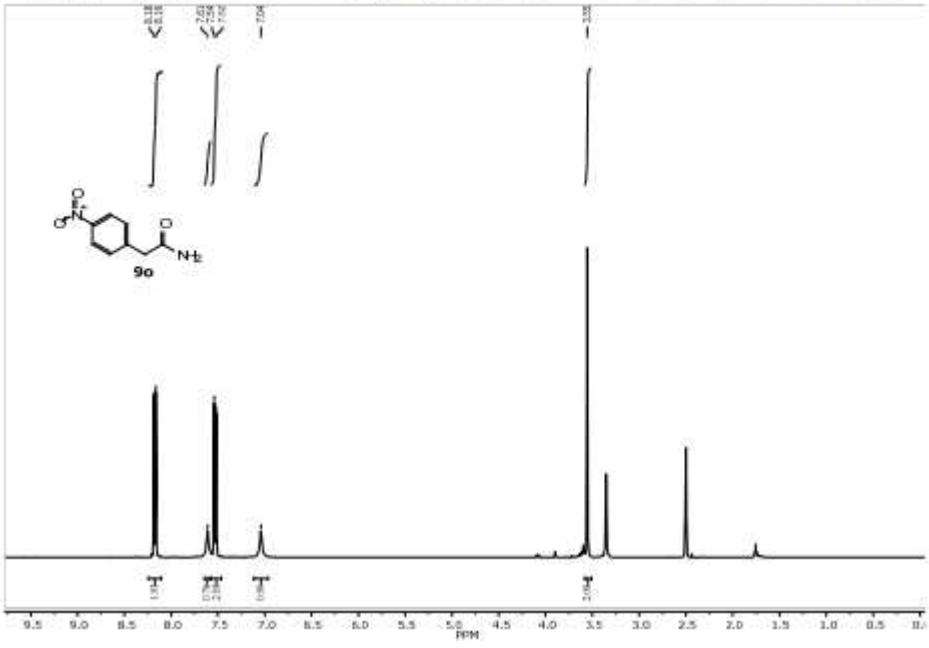

Figure A47: Spectroscopic Data for 2-(4-nitrophenyl)acetamide 9o and Corresponding Nitrile 10o (1 of 3)

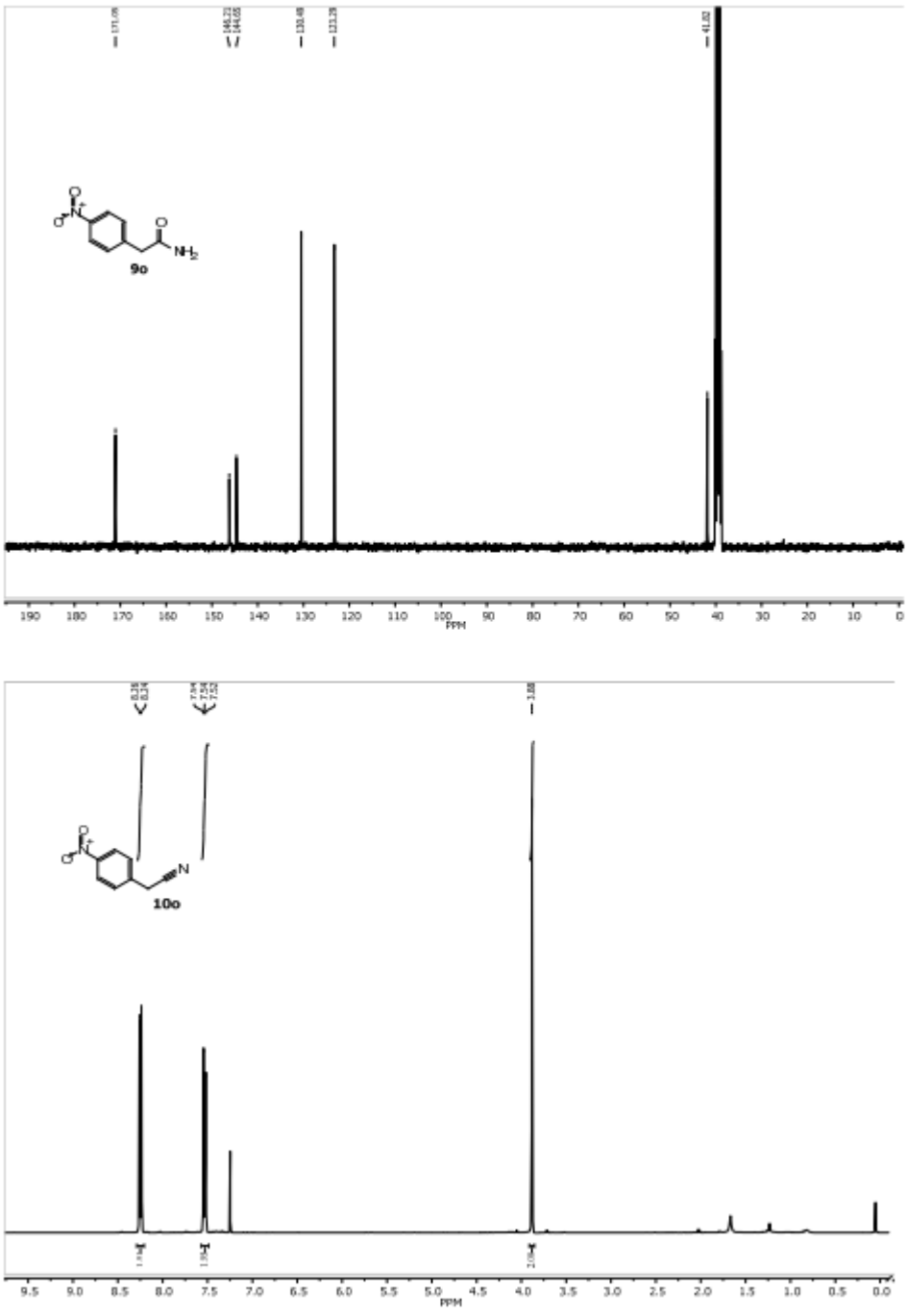

Figure A48: Spectroscopic Data for 2-(4-nitrophenyl)acetamide 9o and Corresponding Nitrile 10o (2 of 3)

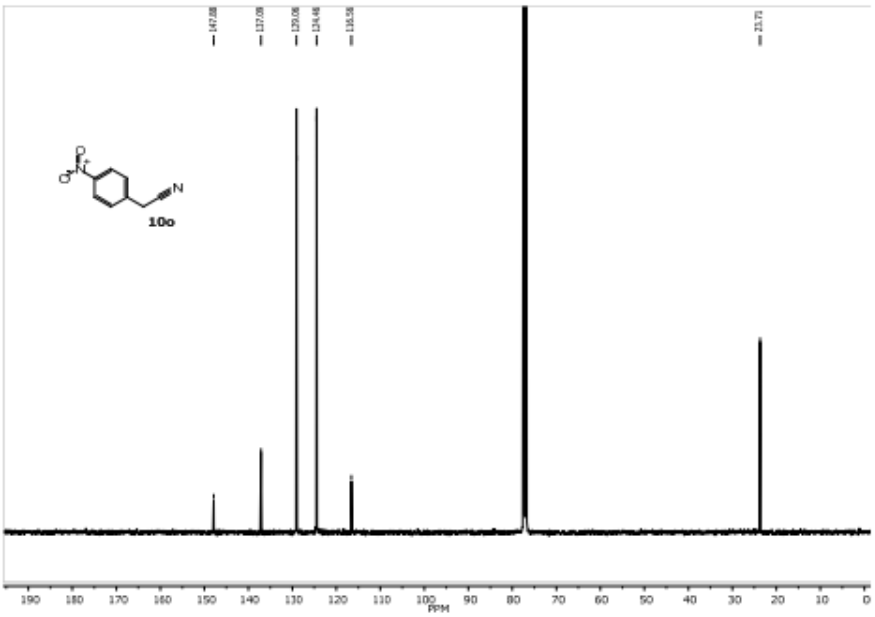

Figure A49: Spectroscopic Data for 2-(4-nitrophenyl)acetamide 9o and Corresponding Nitrile 10o (3 of 3)

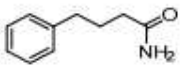

4-phenylbutanamide 9p:[14] Following the General Procedure, product was isolated as a white solid (311 mg, 31% yield).

^{1}H NMR (400 MHz, chloroform-d) δ 7.27 (t, J = 7.4 Hz, 2H), 7.21 – 7.12 (m, 3H), 5.51 (br. s, 1H), 5.39 (br. s, 1H), 2.66 (t, J = 7.5 Hz, 2H), 2.21 (t, J = 7.2 Hz, 2H), 1.97 (quint, J = 7.5 Hz, 2H) ppm.

^{13}C NMR (100 MHz, chloroform-d) δ 175.2, 141.5, 128.6 (2C), 128.5 (2C), 126.1, 35.2, 35.0, 26.9 ppm.

HRMS (APPI) calcd. for $C_{10}H_{13}NO$ [M+H] calculated: 164.1070 observed: 164.1062.

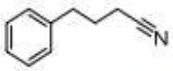

4-phenylbutanenitrile 10p:[14] Following the General Procedure, product was isolated as a colorless oil (36 mg, 81% yield) after column chromatography (gradient elution from pure hexane to 10% EtOAc in hexane).

^{1}H NMR (400 MHz, chloroform-d) δ 7.34 – 7.27 (m, 2H), 7.26 – 7.22 (m, 1H), 7.22 – 7.16 (m, 2H), 2.78 (t, J = 7.4 Hz, 2H), 2.31 (t, J = 7.1 Hz, 2H), 1.98 (q, J = 7.2 Hz, 2H) ppm.

^{13}C NMR (100 MHz, chloroform-d) δ 139.8, 128.8 (2C), 128.6 (2C), 126.6, 119.7, 34.5, 27.0, 16.5 ppm.

HRMS(APPI) calcd. for $C_{10}H_{11}N$ [M+H] calculated: 146.0964; observed: 146.0967.

Figure A50: Spectroscopic Data for 4-phenylbutanamide 9p and Corresponding Nitrile 10p (1 of 3)

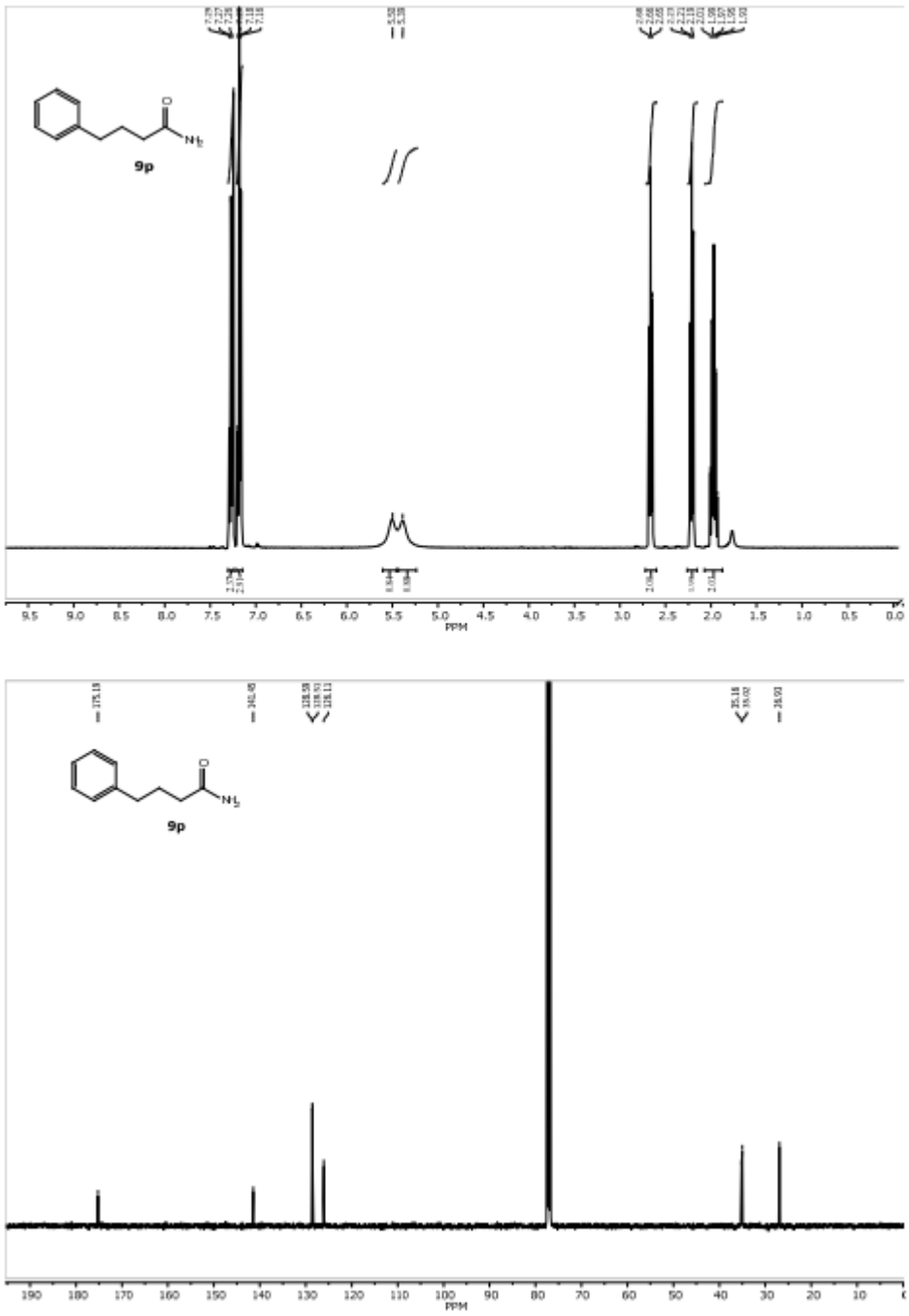

Figure A51: Spectroscopic Data for 4-phenylbutanamide 9p and Corresponding Nitrile 10p (2 of 3)

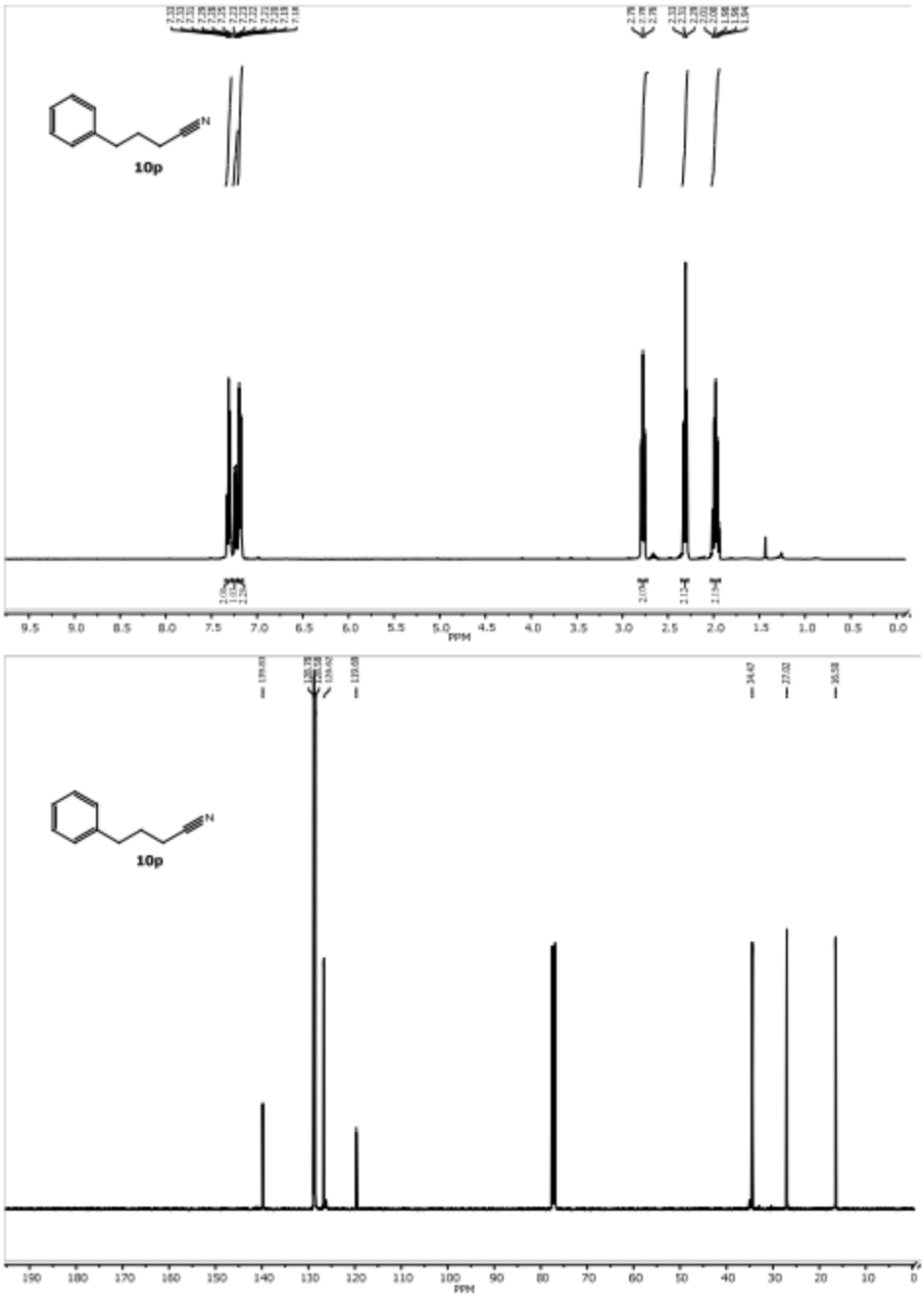

Figure A52: Spectroscopic Data for 4-phenylbutanamide 9p and Corresponding Nitrile 10p (3 of 3)

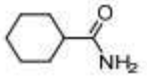

Cyclohexanecarboxamide 9q:[2] Following the General Procedure, product was isolated as a white solid (385 mg, 72% yield).

^{1}H NMR (400 MHz, DMSO-d_6) δ 7.15 (br. s, 1H), 6.64 (br. s, 1H), 2.04 (tt, J = 11.5, 3.3 Hz, 1H), 1.79 – 1.53 (m, 5H), 1.53 – 0.88 (m, 5H) ppm.

^{13}C NMR (100 MHz, DMSO-d_6) δ 177.4, 43.7, 29.2 (2C), 25.6, 25.4 (2C) ppm.

HRMS (APPI) calcd. for $C_7H_{13}NO$ $[M+H]^+$ calculated: 128.1069; observed:128.1070.

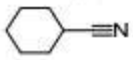

Cyclohexanecarbonitrile 10q:[2] Following the General Procedure, product was isolated as a colorless oil (36 mg, 84% yield) after column chromatography (gradient elution from pure hexane to 10% EtOAc in hexane).

^{1}H NMR (400 MHz, chloroform-d) δ 2.63 – 2.57 (m, 1H), 1.90 – 1.78 (m, 2H), 1.75 – 1.64 (m, 4H), 1.52 – 1.33 (m, 4H) ppm.

^{13}C NMR (100 MHz, chloroform-d) δ 122.8, 29.6 (2C), 28.1, 25.3 (2C), 24.1 ppm.

HRMS (APPI) calcd. for $C_7H_{11}N$ $[M+H]^+$ calculated: 110.0970; observed: 110.0965.

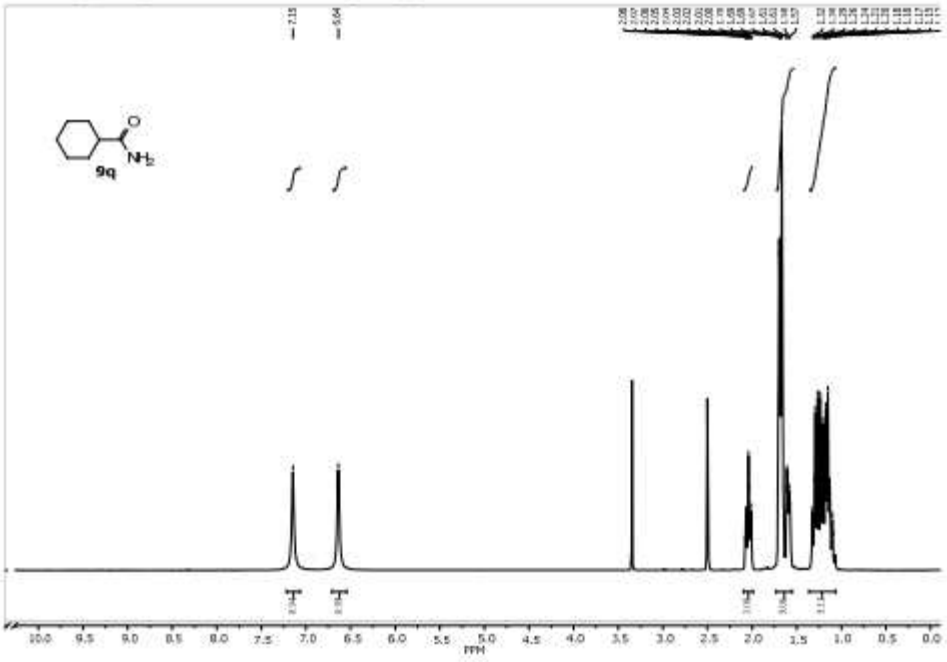

Figure A53: Spectroscopic Data for Cyclohexanecarboxamide 9q and Corresponding Nitrile 10q (1 of 3)

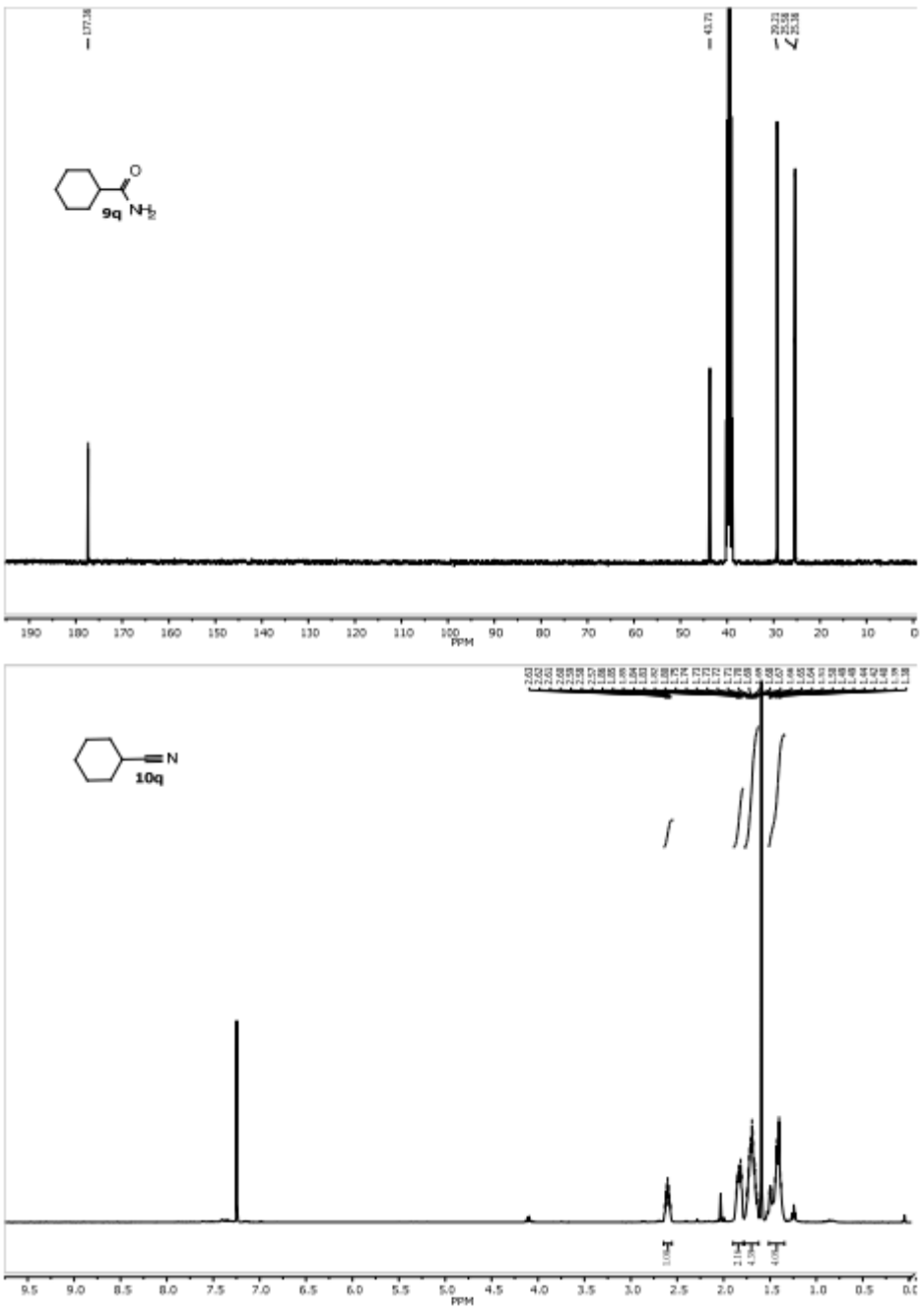

Figure A54: Spectroscopic Data for Cyclohexanecarboxamide 9q and Corresponding Nitrile 10q (2 of 3)

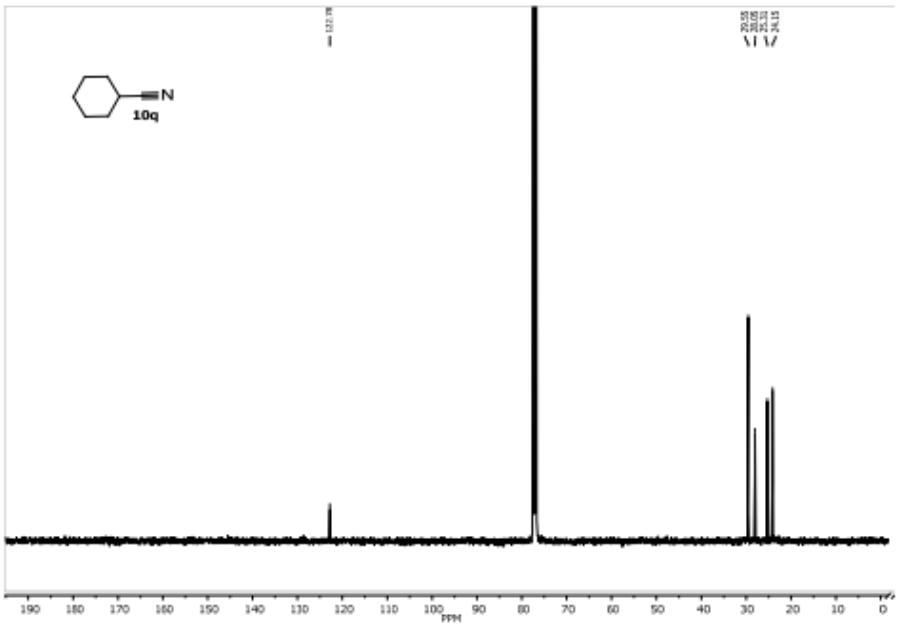

Figure A55: Spectroscopic Data for Cyclohexanecarboxamide 9q and Corresponding Nitrile 10q (3 of 3)

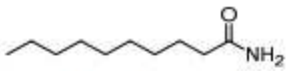

Decanamide 9r:[2] Following the General Procedure, product was isolated as a white solid (496 mg, 81% yield).

^{1}H NMR (400 MHz, chloroform-d) δ 5.33 (br. s, 2H), 2.21 (t, J = 7.5 Hz, 2H), 1.62 (quint, J = 7.6 Hz, 2H), 1.35 – 1.20 (m, 12H), 0.86 (t, J = 6.8 Hz, 3H) ppm.

^{13}C NMR (125 MHz, chloroform-d) δ 175.6, 36.0, 32.0, 29.5, 29.4, 29.4, 29.3, 25.6, 22.8, 14.2 ppm.

HRMS (APPI) calcd. for $C_{10}H_{21}NO$ [M+H] calculated: 172.1696; observed: 172.1689.

Decanenitrile 10r:[2] Following the General Procedure, product was isolated as a colorless oil (40 mg, 88% yield) after column chromatography (gradient elution from pure hexane to 5% EtOAc in hexane).

^{1}H NMR (400 MHz, chloroform-d) δ 2.32 (t, J = 7.1 Hz, 2H), 1.64 (quint, J = 7.4 Hz, 2H), 1.46 – 1.38 (m, 2H), 1.32 – 1.21 (m, 10H), 0.86 (t, J = 6.8 Hz, 3H) ppm.

^{13}C NMR (100 MHz, chloroform-d) δ 120.0, 31.9, 29.4, 29.3, 28.9, 28.8, 25.5, 22.7, 17.2, 14.2 ppm.

HRMS: $C_{10}H_{19}N^+$ [M+H] calculated: 154.1590; observed: 154.1585.

Figure A56: Spectroscopic Data for Decanamide 9r and Corresponding Nitrile 10r (1 of 3)

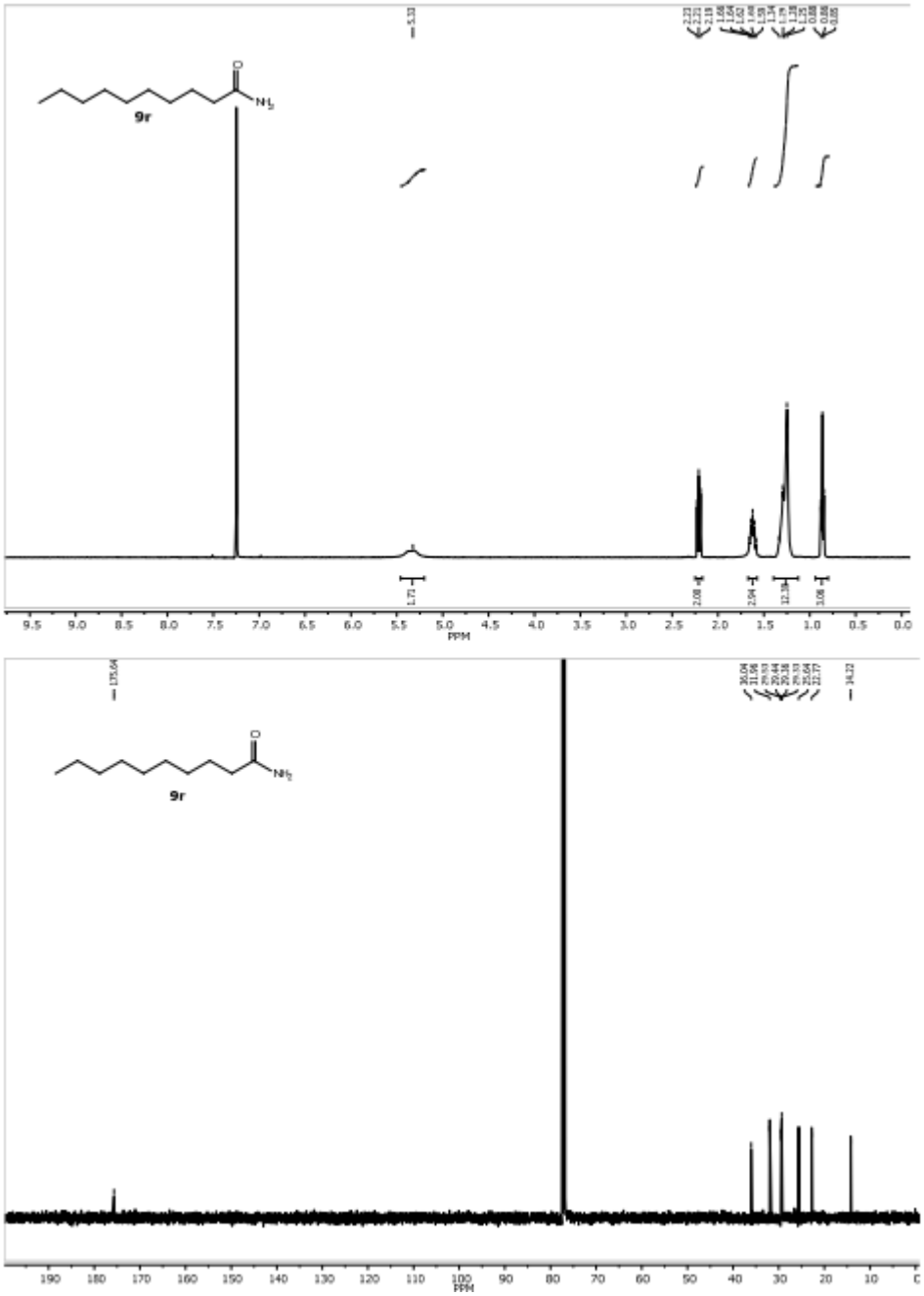

Figure A57: Spectroscopic Data for Decanamide 9r and Corresponding Nitrile 10r (2 of 3)

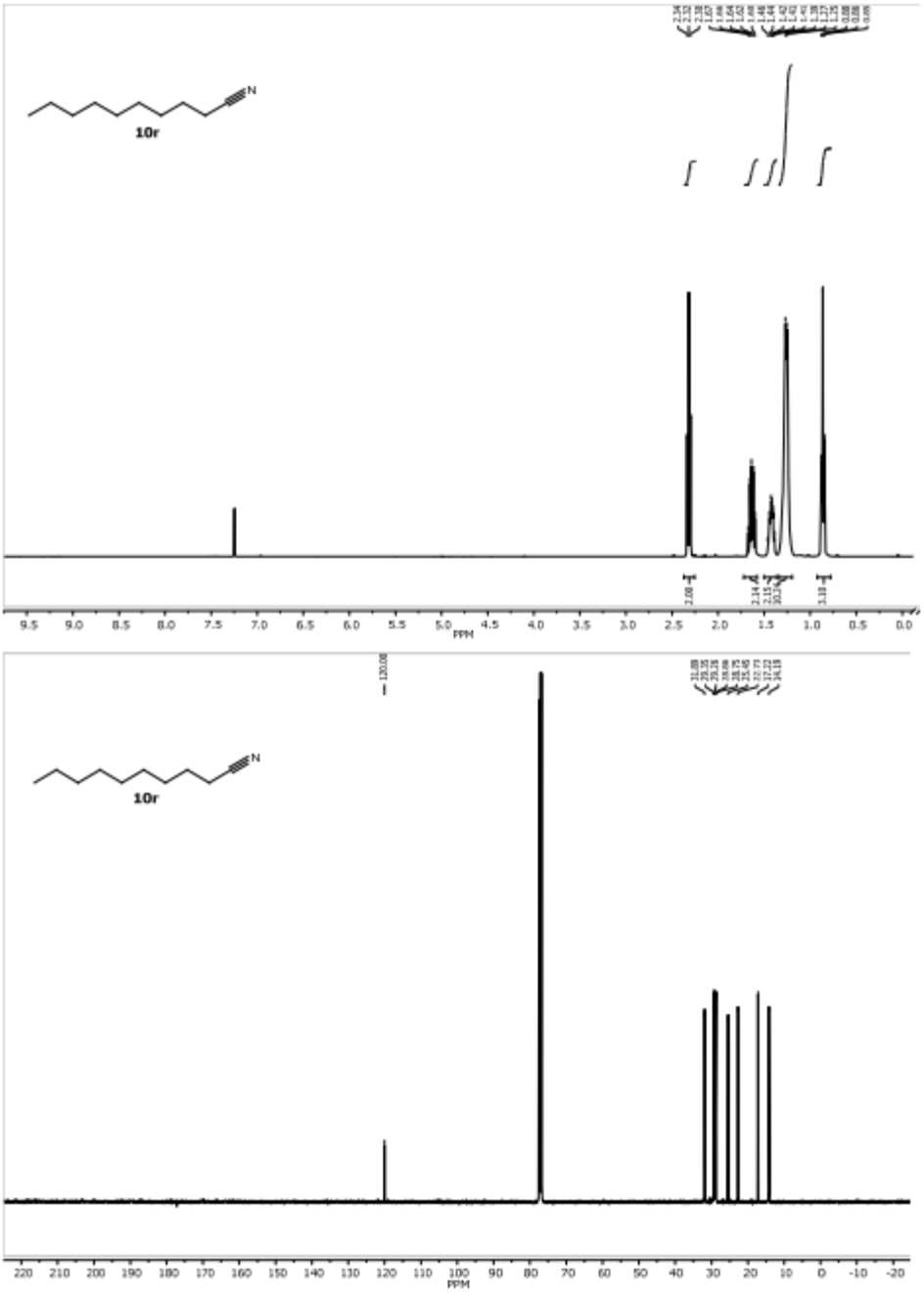

Figure A58: Spectroscopic Data for Decanamide 9r and Corresponding Nitrile 10r (3 of 3)

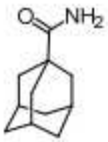

Adamantane-1-carboxamide 9s:[2] Following the General Procedure, product was isolated as a white solid (490 mg, 75% yield).

^{1}H NMR (400 MHz, DMSO-d_6) δ 6.94 (br. s, 1H), 6.68 (br. s, 1H), 1.99 – 1.89 (m, 3H), 1.74 (d, J = 2.9 Hz, 6H), 1.70 – 1.57 (m, 6H) ppm.

^{13}C NMR (100 MHz, DMSO-d_6) δ 179.3, 39.7, 38.8 (3C), 36.2 (3C), 27.7 (3C) ppm.

HRMS (APPI) calcd. for $C_{11}H_{17}NO$ $[M+H]^+$ calculated: 180.1388; observed: 180.1382.

Adamantane-1-carbonitrile 10s:[2] Following the General Procedure, product was isolated as a white solid (42 mg, 93% yield) after column chromatography (gradient elution from pure hexane to 10% EtOAc in hexane).

^{1}H NMR (400 MHz, chloroform-d) δ 2.02 (s, 9H), 1.71 (s, 6H) ppm.

^{13}C NMR (100 MHz, chloroform-d) δ 125.4, 40.0 (3C), 35.8 (3C), 30.2, 27.1 (3C) ppm.

HRMS (APPI) calcd. for $C_{11}H_{15}N$ $[M+H]^+$ calculated: 162.1277; observed: 162.1278.

Figure A59: Spectroscopic Data for Adamantane-1-carboxamide 9s and Corresponding Nitrile 10s (1 of 3)

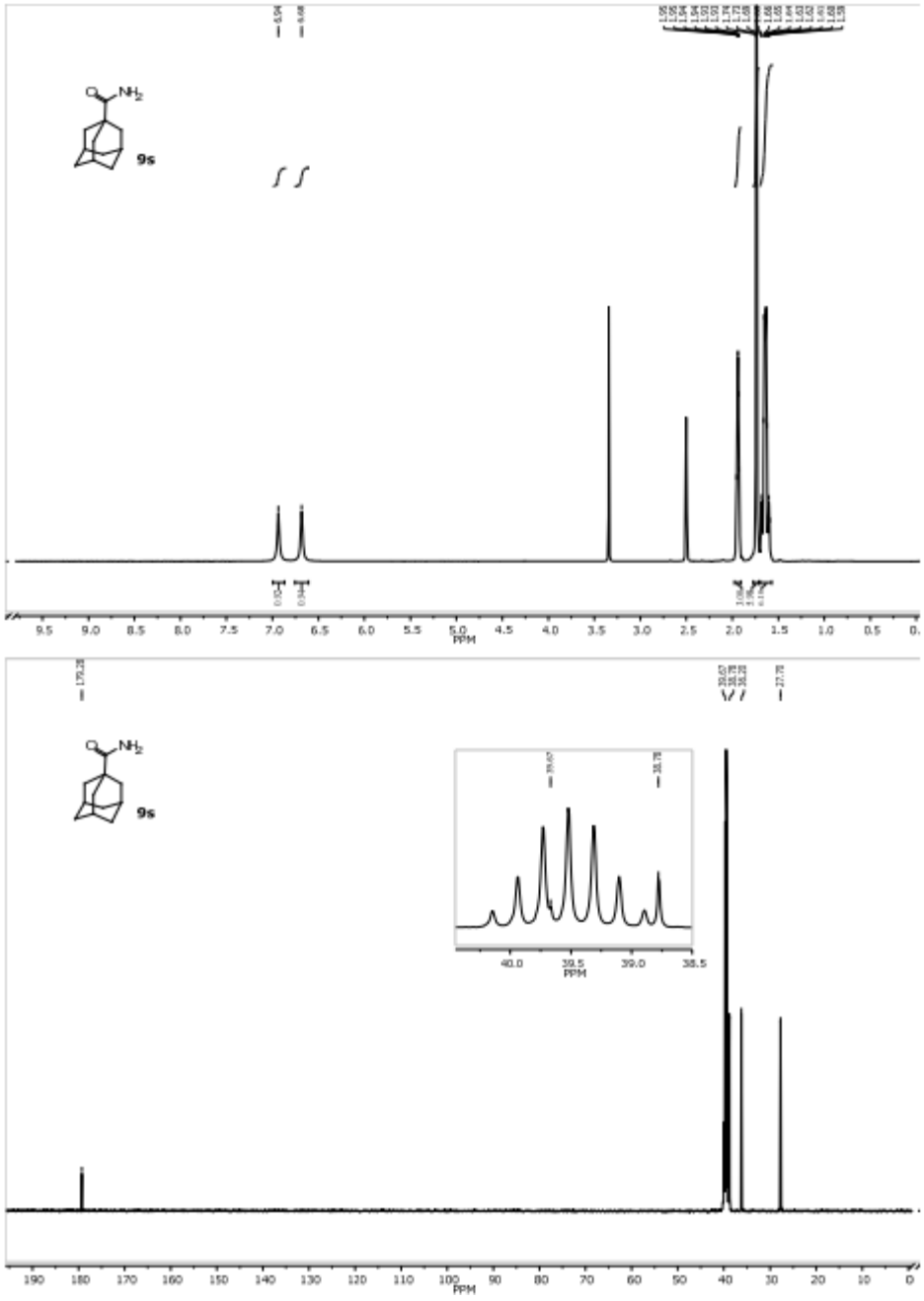

Figure A60: Spectroscopic Data for Adamantane-1-carboxamide 9s and Corresponding Nitrile 10s (2 of 3)

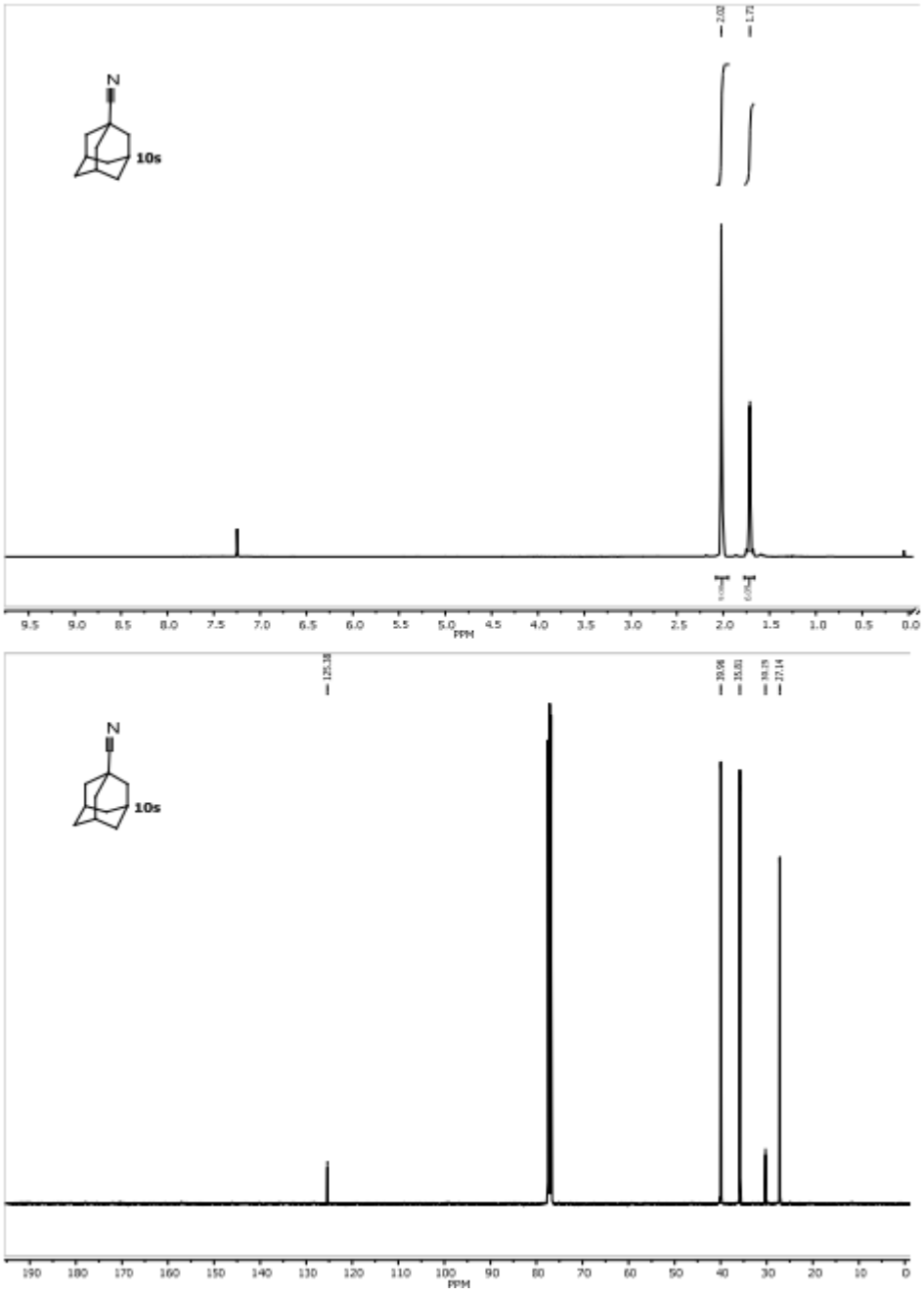

Figure A61: Spectroscopic Data for Adamantane-1-carboxamide 9s and Corresponding Nitrile 10s (3 of 3)

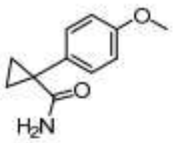

1-(4-methoxyphenyl)cyclopropane-1-carboxamide 9t: Following the General Procedure, product was isolated as a white solid (325 mg, 65% yield).

^{1}H NMR (400 MHz, DMSO-d_6) δ 7.26 (d, J = 8.7 Hz, 2H), 7.02 (br. s, 1H), 6.89 (d, J = 8.7 Hz, 2H), 6.02 (br. s, 1H), 3.74 (s, 3H), 1.29 (q, J = 3.6 Hz, 2H), 0.89 (q, J = 3.6 Hz, 2H) ppm.

^{13}C NMR (100 MHz, DMSO-d_6) δ 175.5, 158.8, 132.9, 132.0 (2C), 114.4 (2C), 55.6, 29.7, 15.2 (2C) ppm.

HRMS (APPI) calcd. for $C_{11}H_{13}NO_2$ $[M+H]^+$ calculated: 192.1025; observed: 192.1017.

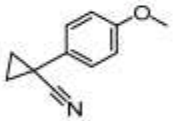

1-(4-methoxyphenyl)cyclopropane-1-carbonitrile 10t: Following the General Procedure, product was isolated as a colorless oil (39 mg, 86% yield) after column chromatography (gradient elution from pure hexane to 10% EtOAc in hexane).

^{1}H NMR (400 MHz, chloroform-d) δ 7.22 (d, J = 8.8 Hz, 2H), 6.86 (d, J = 8.8 Hz, 2H), 3.78 (s, 3H), 1.69 – 1.59 (m, 2H), 1.33 – 1.29 (m, 2H) ppm.

^{13}C NMR (100 MHz, chloroform-d) δ 159.2, 128.0, 127.7 (2C), 123.1, 114.4 (2C), 55.5, 17.5 (2C), 13.2 ppm.

HRMS (APPI) calcd. for $C_{11}H_{11}NO$ $[M+H]^+$ calculated: 174.0913; observed: 174.0915.

Figure A62: Spectroscopic Data for 1-(4-methoxyphenyl)cyclopropane-1-carboxamide 9t and Corresponding Nitrile 10t (1 of 3)

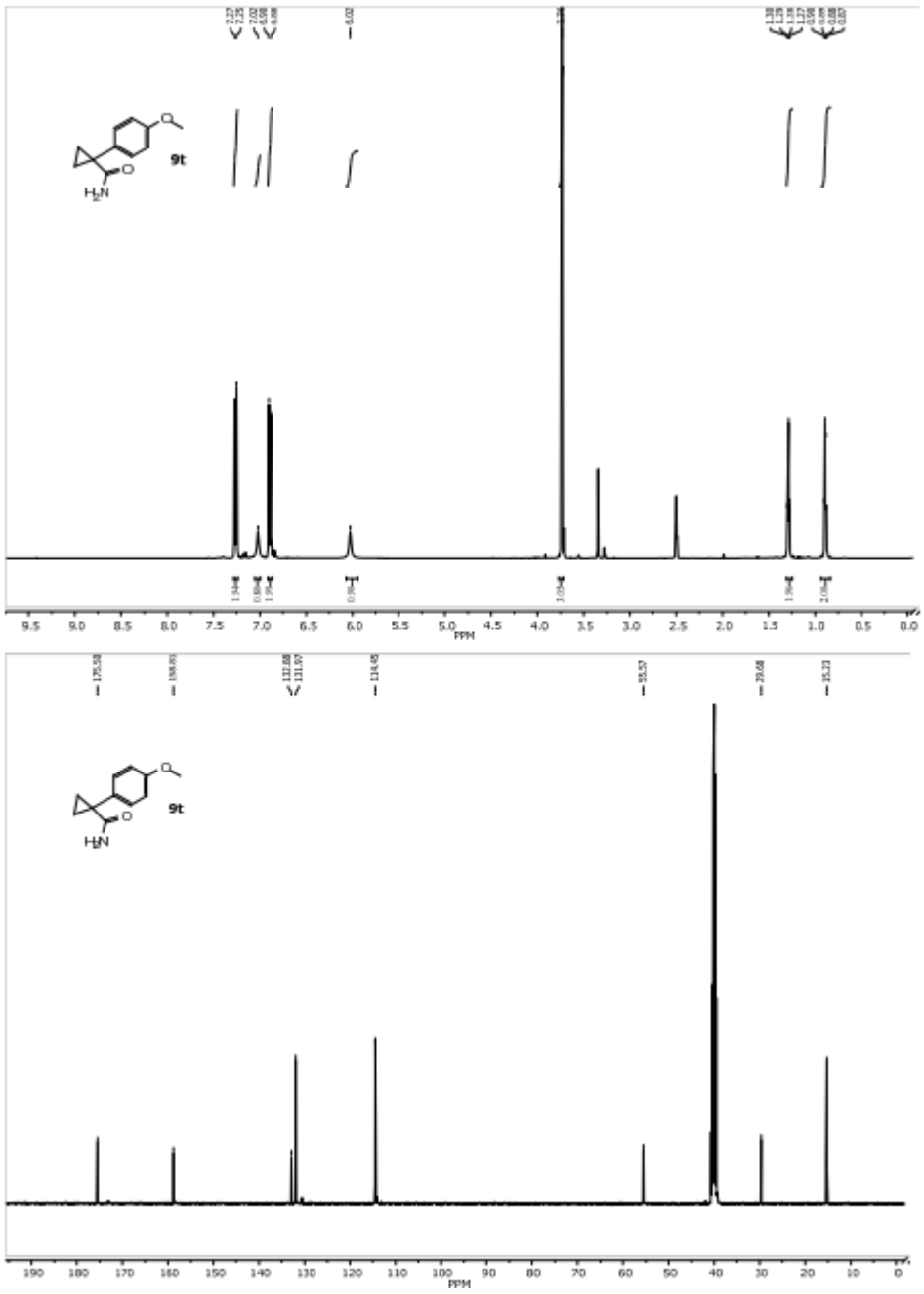

Figure A63: Spectroscopic Data for 1-(4-methoxyphenyl)cyclopropane-1-carboxamide 9t and Corresponding Nitrile 10t (2 of 3)

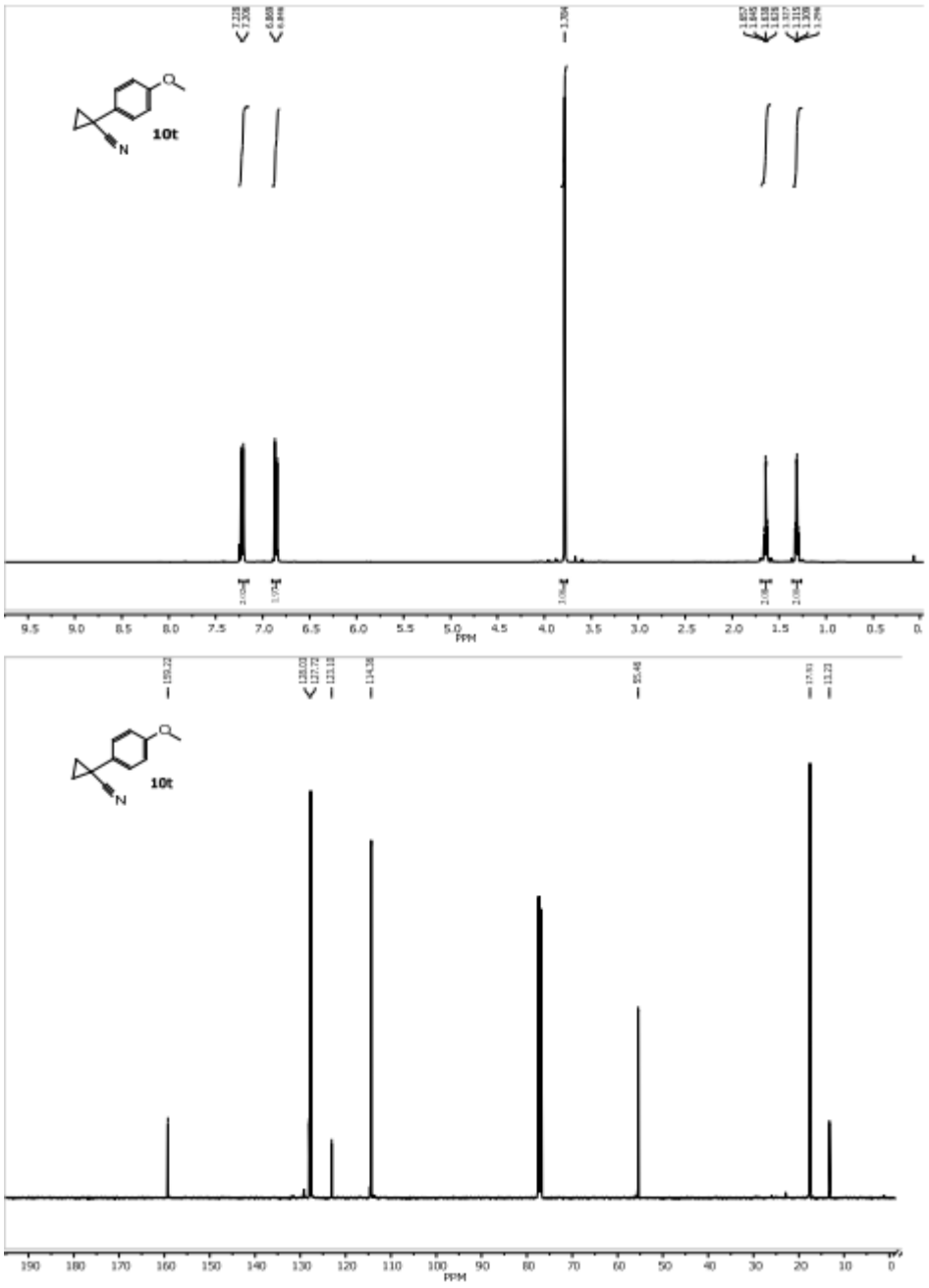

Figure A64: Spectroscopic Data for 1-(4-methoxyphenyl)cyclopropane-1-carboxamide 9t and Corresponding Nitrile 10t (3 of 3)

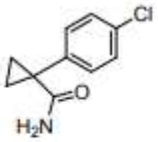

1-(4-chlorophenyl)cyclopropane-1-carboxamide 9u: Following the General Procedure, product was isolated as a white solid (246 mg, 48% yield).

^{1}H NMR (400 MHz, DMSO-d_6) δ 7.46 – 7.24 (m, 4H), 7.04 (br. s, 1H), 6.33 (br. s, 1H), 1.32 (q, J = 3.8 Hz, 2H), 0.94 (q, J = 3.8 Hz, 2H) ppm.

^{13}C NMR (100 MHz, DMSO-d_6) δ 174.7, 140.0, 132.7 (2C), 132.2, 128.9 (2C), 30.0, 15.2 (2C) ppm.

HRMS (APPI) calcd. for $C_{10}H_{10}ClNO$ $[M+H]^+$ calculated: 196.0529; observed: 196.0525.

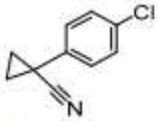

1-(4-chlorophenyl)cyclopropane-1-carbonitrile 10u:[17] Following the General Procedure, product was isolated as a colorless oil (37 mg, 82% yield) after column chromatography (gradient elution from pure hexane to 10% EtOAc in hexane).

^{1}H NMR (400 MHz, chloroform-d) δ 7.30 (d, J = 8.6 Hz, 2H), 7.21 (d, J = 8.6 Hz, 2H), 1.77 – 1.67 (m, 2H), 1.41 – 1.31 (m, 2H) ppm.

^{13}C NMR (100 MHz, chloroform-d) δ 134.7, 133.7, 129.2 (2C), 127.3 (2C), 122.3, 18.4 (2C), 13.5 ppm.

HRMS (APPI) calcd. for $C_{10}H_8ClN$ $[M+H]^+$ calculated: 178.0418; observed: 178.0419.

Figure A65: Spectroscopic Data for 1-(4-chlorophenyl)cyclopropane-1-carboxamide 9u and Corresponding Nitrile 10u (1 of 3)

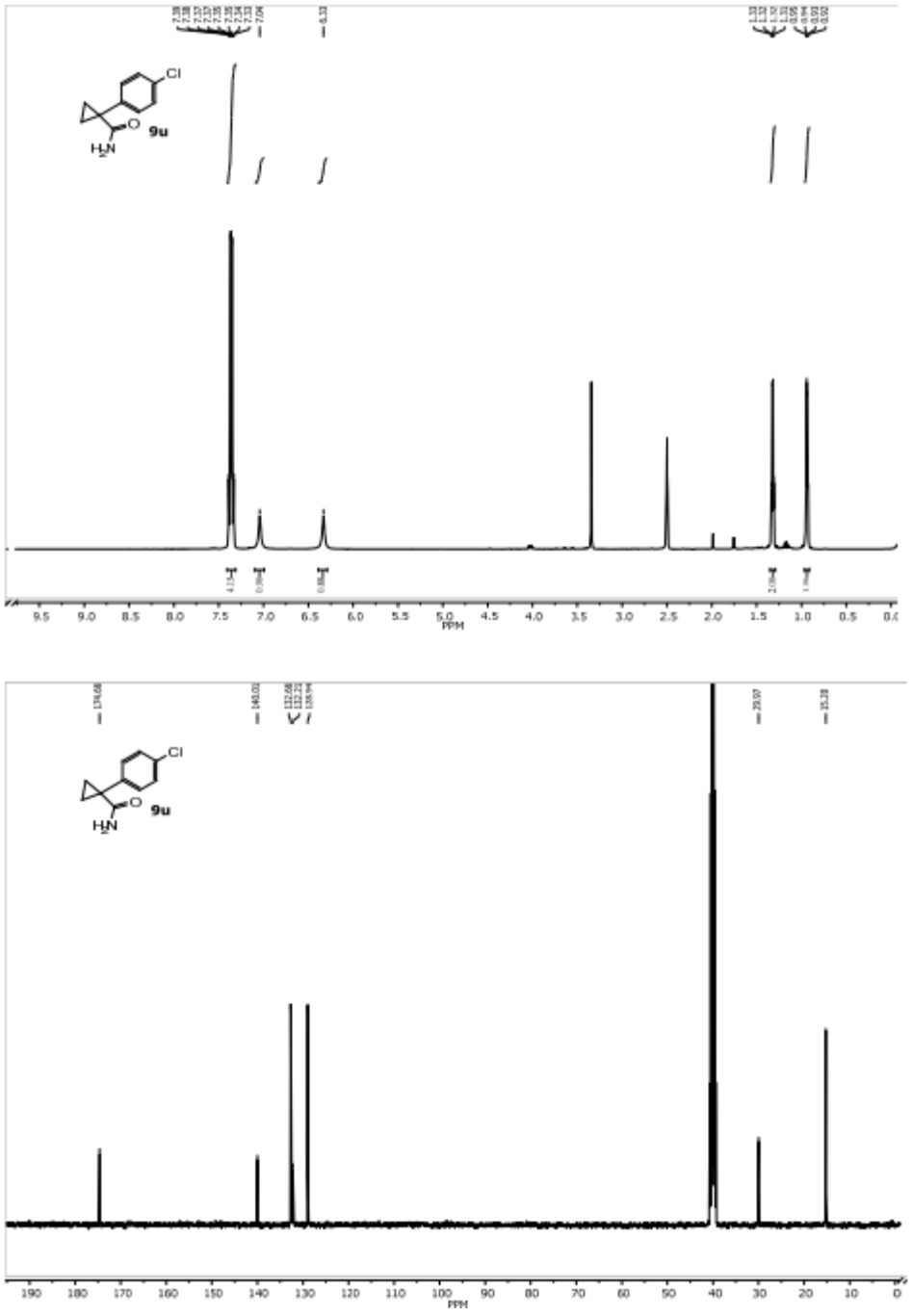

Figure A66: Spectroscopic Data for 1-(4-chlorophenyl)cyclopropane-1-carboxamide 9u and Corresponding Nitrile 10u (2 of 3)

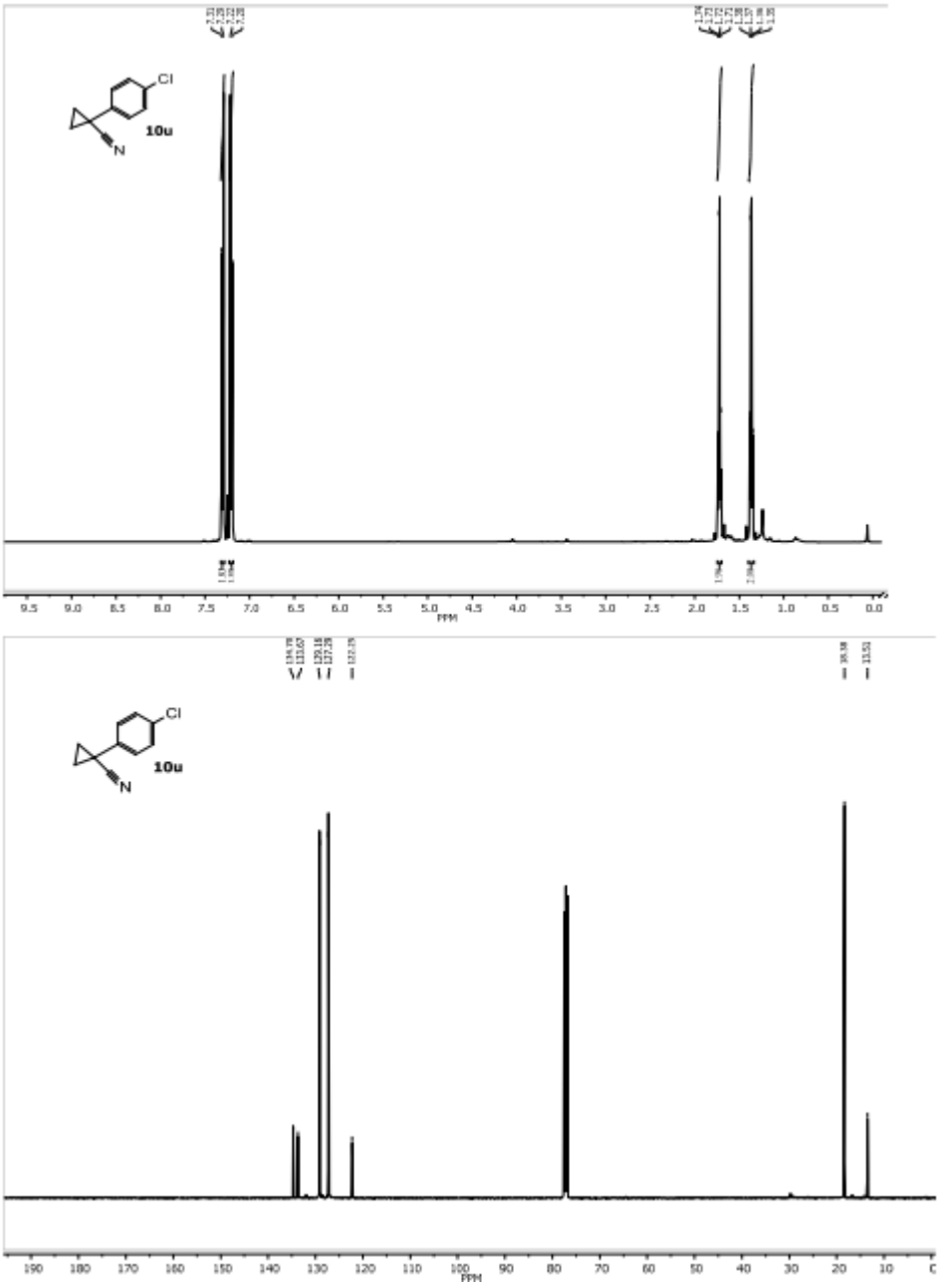

Figure A67: Spectroscopic Data for 1-(4-chlorophenyl)cyclopropane-1-carboxamide 9u and Corresponding Nitrile 10u (3 of 3)

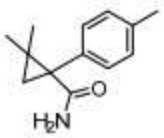

2,2-dimethyl-1-(p-tolyl)cyclopropane-1-carboxamide 9v: Following the General Procedure, product was isolated as a light brown solid (24 mg, 95% yield).

^{1}H NMR (500 MHz, chloroform-*d*) δ 7.21 (d, *J* = 7.9 Hz, 2H), 7.15 (d, *J* = 7.9 Hz, 2H), 5.76 (br. s, 1H), 5.61 (br. s, 1H), 2.34 (s, 3H), 1.77 (d, *J* = 4.1 Hz, 1H), 1.37 (s, 3H), 0.99 (d, *J* = 4.1 Hz, 1H), 0.90 (s, 3H) ppm.
^{13}C NMR (125 MHz, chloroform-d) δ 174.9, 137.3, 136.5, 130.8 (2C), 129.7 (2C), 29.8, 27.1, 26.9, 25.5, 21.2, 20.2 ppm.
HRMS (APPI) calcd. for $C_{13}H_{17}NO$ $[M+H]^+$ calculated: 204.1388; observed: 204.1381.

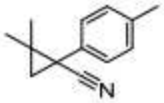

2,2-dimethyl-1-(p-tolyl)cyclopropane-1-carbonitrile 10v: Following the General Procedure, product was isolated as a light brown solid (7.6 mg, 93% yield) after column chromatography (gradient elution from pure hexane to 10% EtOAc in hexane).

1H NMR (500 MHz, chloroform-d) δ 7.19 – 7.14 (m, 4H), 2.34 (s, 3H), 1.52 (s, 3H), 1.46 (d, *J* = 5.4 Hz, 1H), 1.39 (d, *J* = 5.1 Hz, 1H), 0.81 (s, 3H) ppm.
^{13}C NMR (125 MHz, chloroform-d) δ 137.9, 131.2, 129.5 (2C), 129.2 (2C), 122.8, 26.8, 26.4, 24.4, 24.2, 21.3, 21.2 ppm.
HRMS (APPI) calcd. for $C_{13}H_{15}N$ $[M+H]^+$ calculated: 186.1277; observed: 186.1271.

Figure A68: Spectroscopic Data for 2,2-dimethyl-1-(p-tolyl)cyclopropane-1-carboxamide 9v and Corresponding Nitrile 10v (1 of 3)

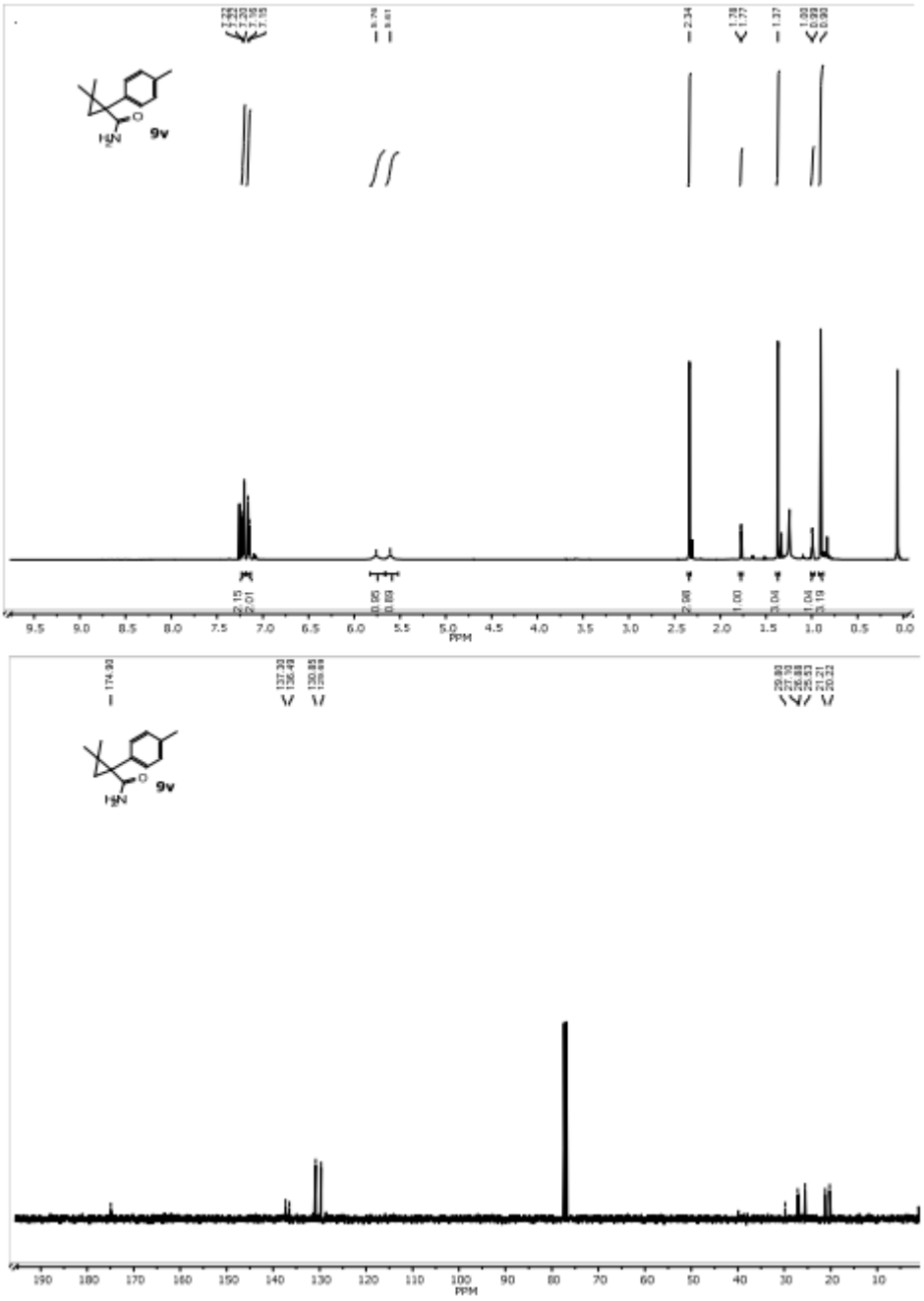

Figure A69: Spectroscopic Data for 2,2-dimethyl-1-(p-tolyl)cyclopropane-1-carboxamide 9v and Corresponding Nitrile 10v (2 of 3)

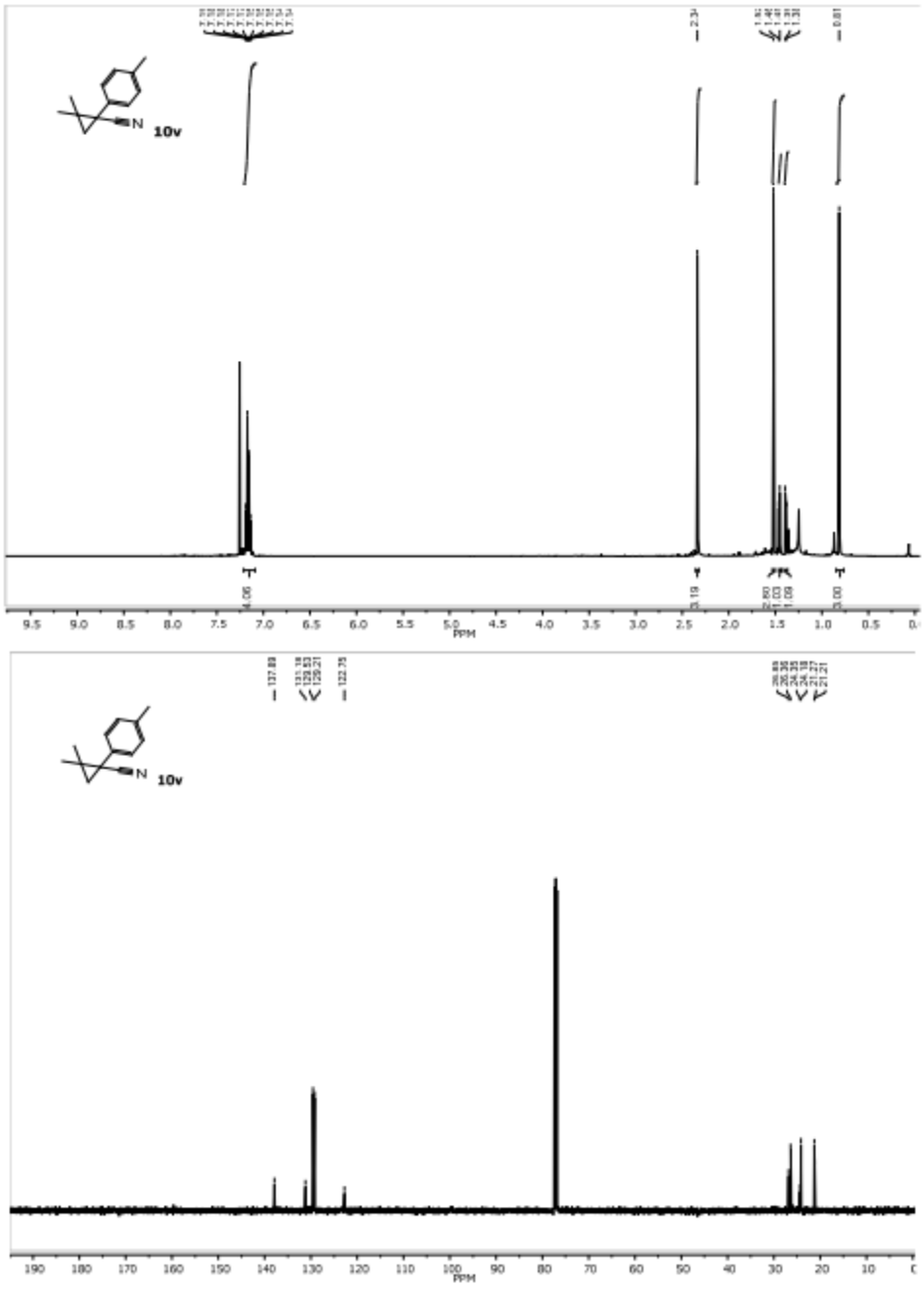

Figure A70: Spectroscopic Data for 2,2-dimethyl-1-(p-tolyl)cyclopropane-1-carboxamide 9v and Corresponding Nitrile 10v (3 of 3)

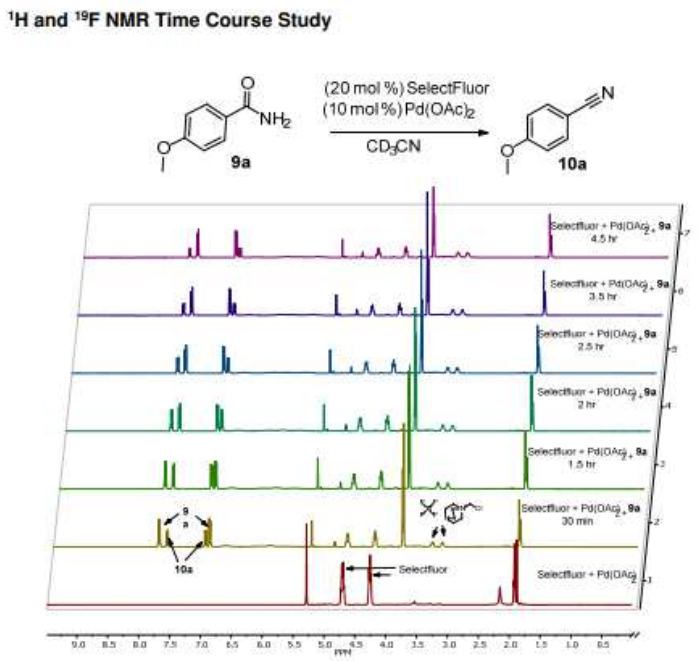

Figure A71: Stacked ^{1}H NMR Spectra for Reaction of 9a

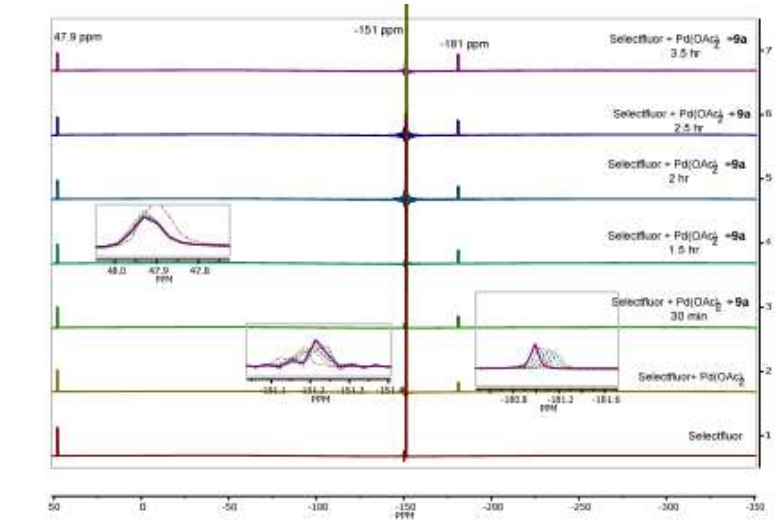

Figure A72: Stacked ^{19}F Spectra for Reaction of 9a

General Experimental Procedures with Alamethicin F50

The circular dichroism experiments were conducted in an Olis, DSM 17 CD spectrometer (Olis, Inc.) at a concentration of 100 ppm in MeCN at 25 °C. NMR experiments were conducted in DMSO-d6. NMR instrumentation was a JEOL ECA-500 NMR spectrometer operating at 500 MHz for ^{1}H, and 125 MHz for ^{13}C, or an Agilent 700 MHz NMR spectrometer equipped with a cryoprobe, operating at 700 MHz for -^{1}H and 175 MHz for ^{13}C. HRESIMS data was obtained using a Thermo QExactive Plus mass spectrometer (ThermoFisher Scientific) paired with an electrospray ionization source. The higher energy collisional dissociation (HCD) used a normalized energy of 35 for all the compounds to obtain MS/MS data. The UPLC separations were performed using a Waters Acquity system (Waters Corp.) using a BEH C18 column (50 mm × 2.1 mm, internal diameter, 1.7 µm) equilibrated at 40 °C and a flow rate set at 0.3 mL/min. The mobile phase consisted of a linear MeCN-H2O (acidified with 0.1% formic acid) gradient starting at 15% MeCN to 100% MeCN over 8 min. The mobile phase was held for another 1.5 min at 100% MeCN before returning to the starting conditions. The HPLC separations were performed using a Varian ProStar HPLC system connected to a ProStar 335 photodiode array detector (PDA) with UV detection set at 195 and 210 nm. Preparative HPLC purifications of isolated compounds were performed on an Atlantis T3 5 µm particle size C_{18} column (19 x 250 mm) at a flow rate of 17.0 mL/min, or a Phenomenex Synergi 4 µm particle size C_{12} column (21 x 250 mm) at a flow rate of 20.0 mL/min. Flash column chromatography was carried out with a Teledyne ISCO Combiflash Rf connected to ELSD S64 and PDA detectors, with the latter having UV detection set at 200-400 nm, all according to established protocols. All solvents were obtained from Fisher Scientific and used without further purification.

Fermentation, Extraction, and Isolation of Alamethicin F50

Fungal strain MSX70741 (Trichoderma arundinaceum) was isolated, identified, and grown as detailed previously. Approximately 130 mg of alamethacin F50 (**1**) was isolated from four scale-up cultures of MSX70741 as explained in detail recently.

Analysis of Alamethicin F50 Dehydration

The reaction analysis was carried out using UPLC/HRESIMS. The higher energy collisional dissociation (HCD) used a normalized energy of 35 for all the compounds to obtain MS/MS data. The UPLC separations were performed using an Acquity BEH C18 column (50 mm × 2.1 mm, internal diameter, 1.7 µm) equilibrated at 40 °C and a flow rate set at 0.3 mL/min. The mobile phase consisted of a linear MeCN-H2O (acidified with 0.1% formic acid) gradient starting at 40% MeCN to 100% MeCN over 3.7 min. The mobile phase was held for another 0.7 min at 100% MeCN before returning to the starting conditions. The area under the curve for each product was extracted from the base peak chromatogram using Thermo Xcalibur Qual Browser program. Figures 83 and 84 show the UPLC/MS data with color coding for the different analogues formed.

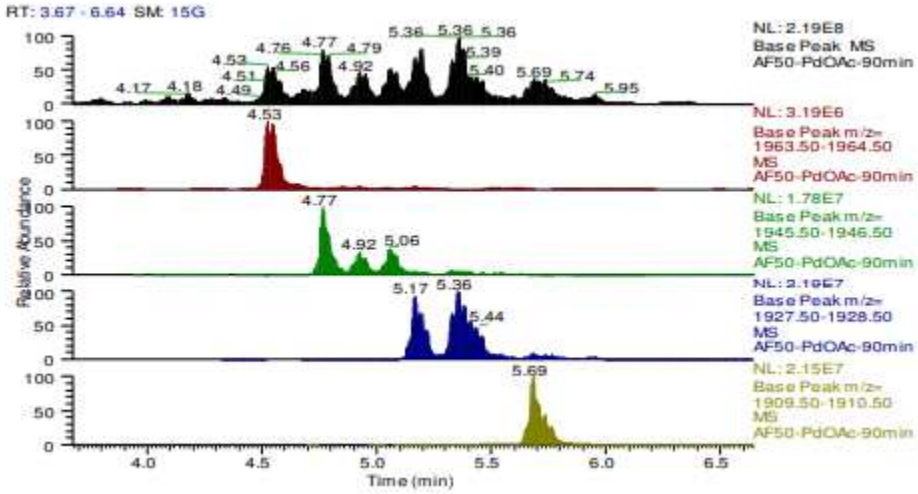

Figure A73: UPLC-HRESIMS analysis of the crude reaction of alamethicin F50 (1), $Pd(OAc)_2$ (5 mol %) and SelectFluor (1.0 equiv.) at room temperature, after 90 min. In Black the base peak chromatogram. In red the extracted ion chromatogram for alamethicin F50 (1), in green the extracted ion chromatogram for mononitrilealamethicin F50 derivatives (6-8), in blue the extracted ion chromatogram for dinitrilealamethicin F50 derivatives (3-5) and in yellow the extracted ion chromatogram for trinitrilealamethicin F50 derivative (2).

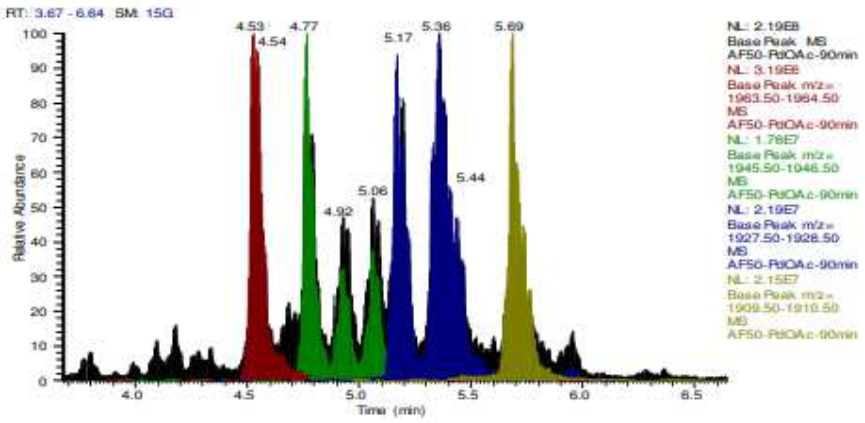

Figure A74: Overlapped UPLC-HRESIMS analysis of the crude reaction of alamethicin F50 (1), $Pd(OAc)_2$ (5 mol %) and SelectFluor (1.0 equiv.) at room temperature, after 90 min. In black, the base peak chromatogram. The extracted ion chromatograms detailed above are overlaid with each other. In red, the extracted ion chromatogram for alamethicin F50 (1). In green, the extracted chromatogram for mononitrilealamethicin F50 derivatives (6-8). In blue, the extracted chromatogram for dinitrile alamethicin F50 derivatives (3-5). In yellow, the extracted chromatogram for trinitrilealamethicin F50 derivative (2).

The conditions for dehydration of alatheicin F50 were examined with analysis by UPLC every 20 minutes. Figures A85-A87 show the formation of different analogues over time under the standard conditions (Figure A85), using a mixture of acetonitrile and dioxane (Figure A86), and in the absence of SelectFluor (Figure A87).

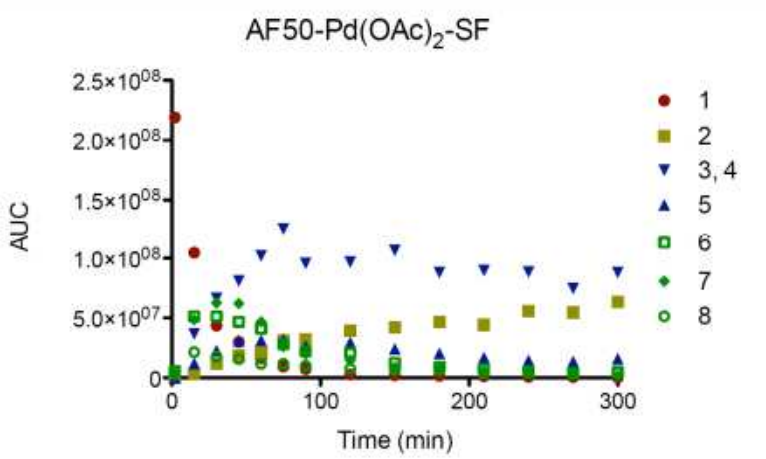

Figure A75: Analysis of the reaction between 1 (0.5 mmol), $Pd(OAc)_2$ (5 mol %) and SelectFluor (1.0 eq) in MeCN (1 mL) at room temperature. The reaction was monitored via UPLC-HRESIMS at intervals of 20 min

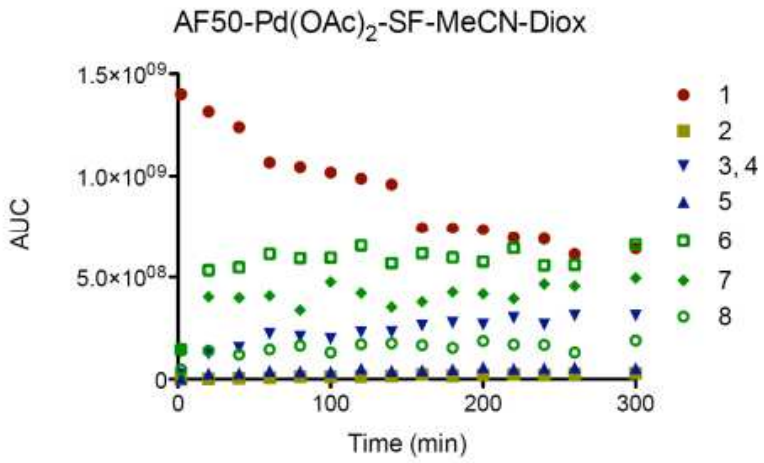

Figure A76: . Analysis of the reaction between 1 (0.5 mmol), $Pd(OAc)_2$ (5 mol %) and SelectFluor (1.0 eq) in MeCN-Dioxane 1:1 (1.0 mL). The reaction was monitored via UPLC-HRESIMS at intervals of 20 min

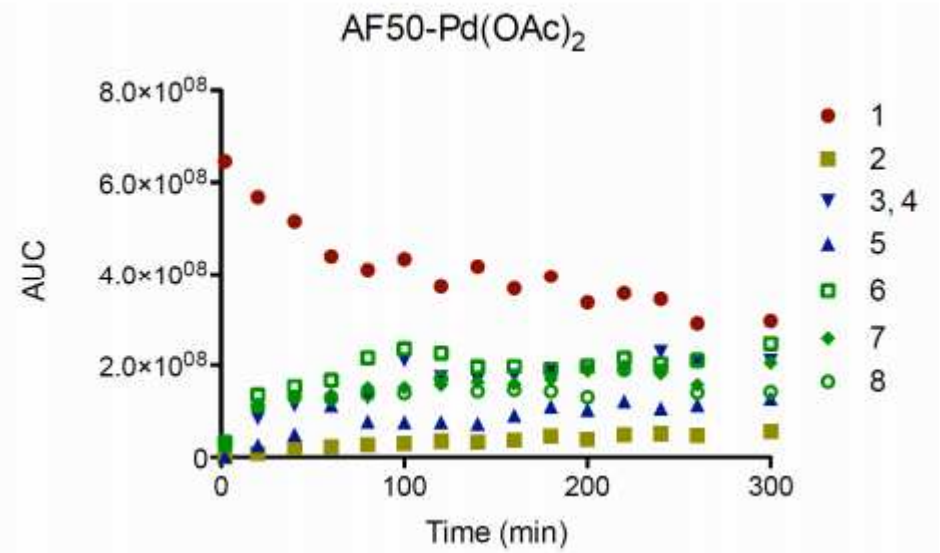

Figure A77: Analysis of the reaction between 1 (0.5 mmol) and $Pd(OAc)_2$ (5 mol %) in MeCN (1.0 mL) at room temperature. The reaction was monitored via UPLC-HRESIMS at intervals of 20 min.

Synthesis, Isolation and Characterization of Compounds 1-8

To a vial containing alamethicin F50 (10.0 mg, 0.005 mmol) in acetonitrile (1.0 M), were added palladium acetate (0.11 mg, 0.0005 mmol) and Selectfluor (1.8 mg, 0.005 mmol). The reaction mixture was stirred at room temperature for 90 min. The reaction mixture was directly subjected to preparative HPLC purification on an Atlantis T3 column, using a gradient system initiated with 80:20 MeCN-H2O (0.1% formic acid) to 100 % CH_3CN over 30 min at a flow rate of 17.0 mL/min to generate eight fractions (FI-VIII). HRESIMS/MS of each fraction, using the method described in general experimental procedures, allowed the identification and characterization of each derivative, as shown in Figures 7-14

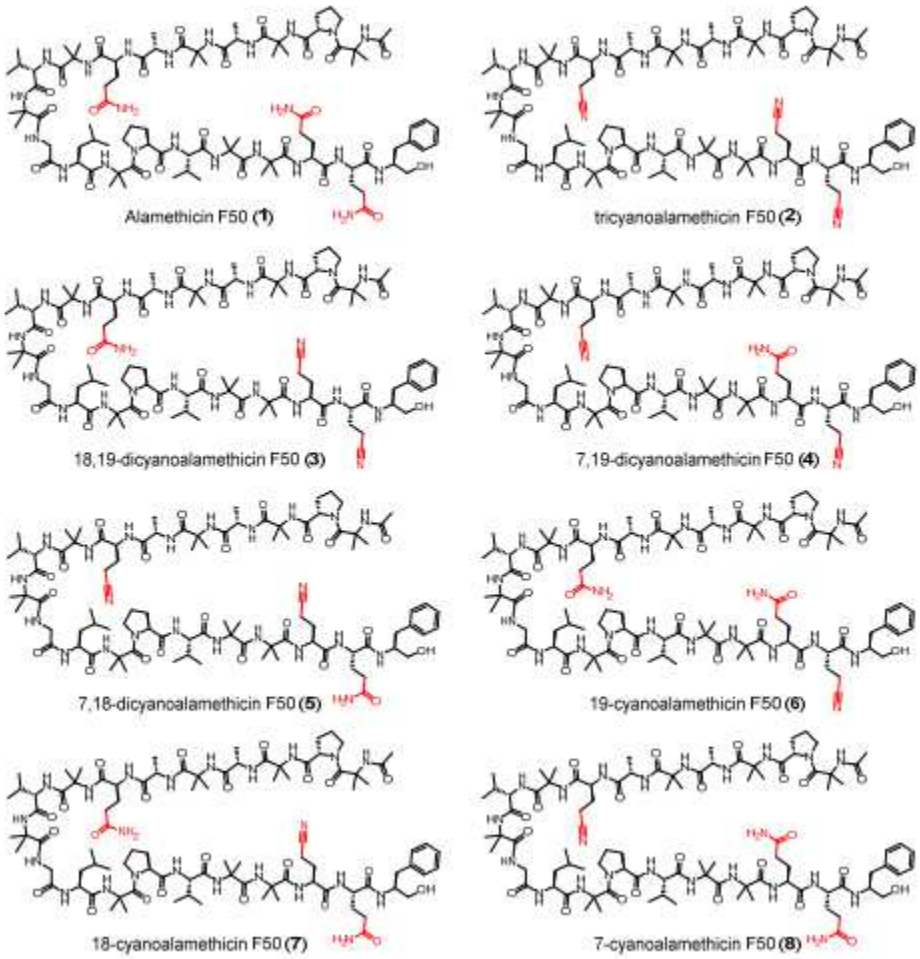

Figure A78: . Structures of alamethicin F50 (**1**, Ac-Aib[1] -Pro[2] -Aib[3] -Ala[4] -Aib[5] -Ala[6] -Gln[7] -Aib[8] -Val[9] -Aib[10]-Gly[11]- Leu[12]-Aib[13]-Pro[14]-Val[15]-Aib[16]-Aib[17]-Gln[18]-Gln[19]-Pheol[20]) and its cyano-analogues (**2-8**)

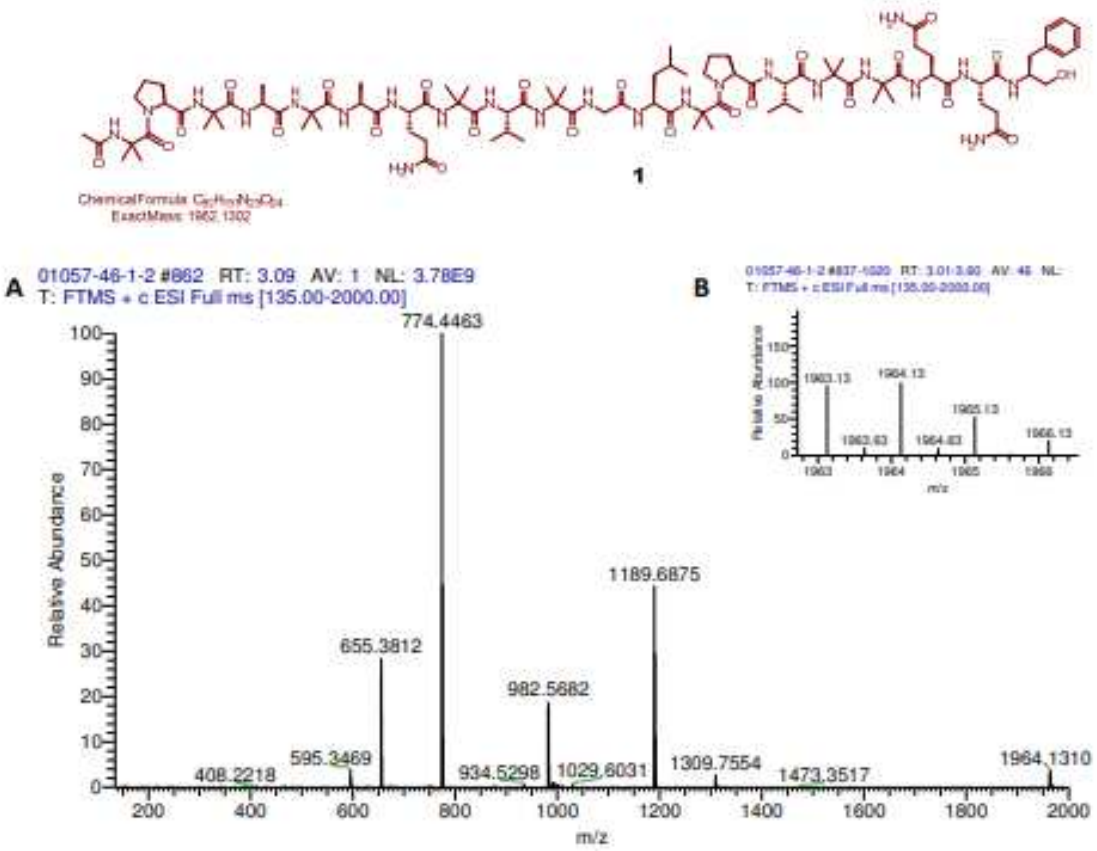

Figure A79: A) Full scan HRESIMS spectrum of compound **1**. B) Expansion of the [M + H]+ ion for alamethicin F50 (**1**) at m/z 1963.13 (Δ = -3.8 ppm). The peak at 774.44 indicates the fragment y_{7+} (-Pro^{14}-Val^{15}-Aib^{16}- Aib^{17}-Gln^{18}-Gln^{19}-Pheol^{20}). The peak at 1189.68 indicates the indicates the fragment b_{13+} (Ac-Aib^{1} -Pro^{2} -Aib^{3} -Ala^{4} -Aib^{5} - Ala^{6} -Gln^{7} -Aib^{8} -Val^{9} -Aib^{10}-Gly^{11}-Leu^{12}-Aib^{13}-).

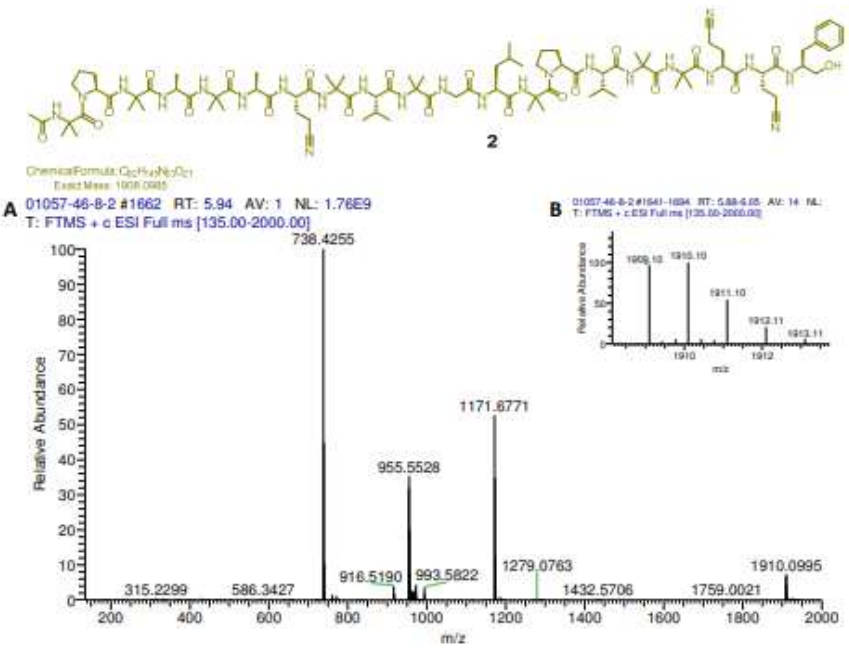

Figure A80: A) Full scan HRESIMS spectrum of compound **2** B) Expansion of the [M + H]+ ion for compound **7** at m/z 1909.10 (Δ = -3.0 ppm). The peak at 738.42 indicates the dehydration of Gln^{18} and Gln^{19} in fragment y_{7+}. The peak at 1171.67 indicates the dehydration of Gln^{7} in fragment b_{13+}.

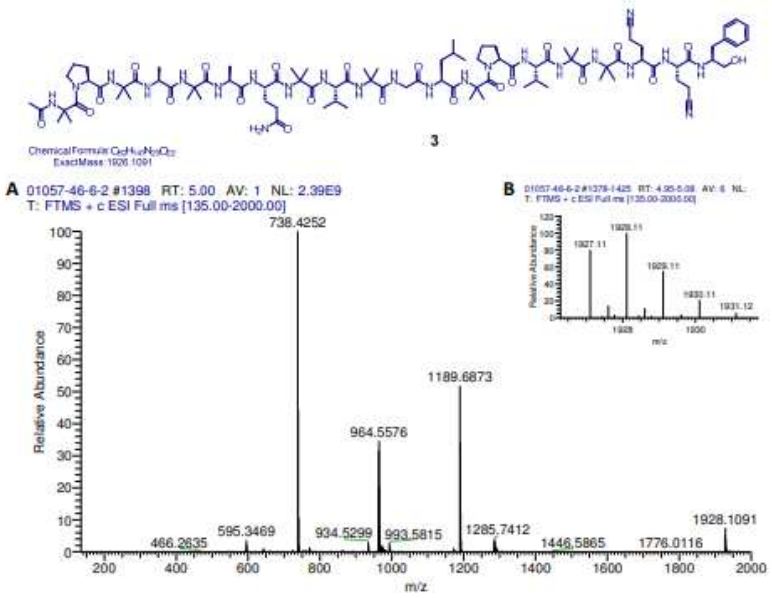

Figure A81: A) Full scan HRESIMS spectrum of compound **3**. B) Expansion of the [M + H]+ ion for compound **3** at m/z 1928.11 (Δ = -3.3 ppm). The peak at 738.42 indicates the dehydration of Gln^{18} and Gln^{19} in fragment y_{7+}.

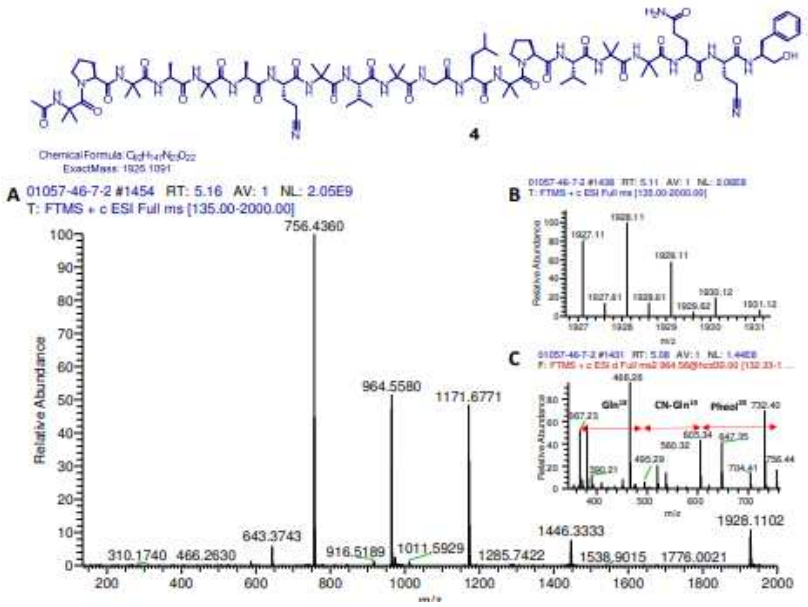

Figure A82: A) Full scan HRESIMS spectrum of compound **4**. B) Expansion of the [M + H]+ ion for compound **4** at m/z 1928.11 (Δ = -3.3 ppm). C) MS^2 of ion 964.6 indicating the losses Pheol[20], CN-Gln[19] and Gln[18] and positioning the dehydrated Gln residue in the y_{7+} fragment of the molecule. The peak at 1171.67 indicates the dehydration of Gln[7] in fragment b_{13+}

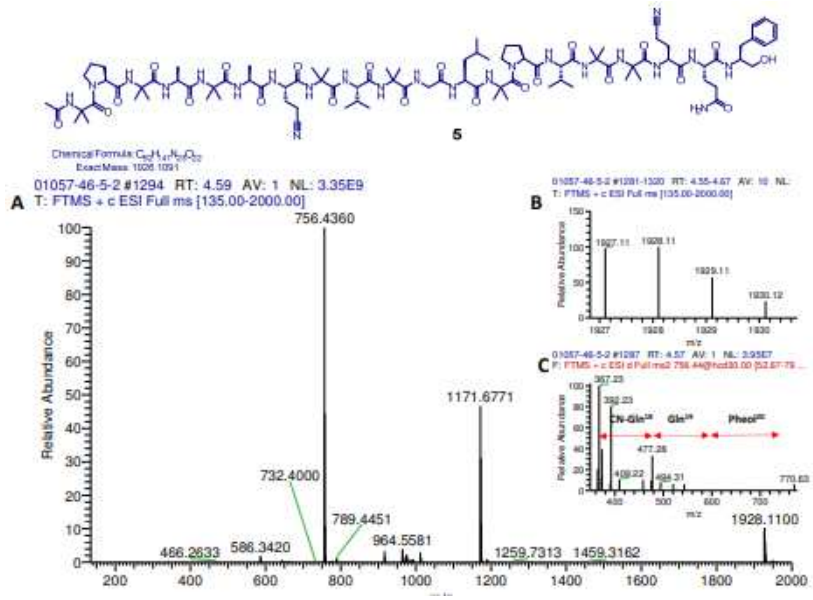

Figure A83: A) Full scan HRESIMS spectrum of compound **5**. B) Expansion of the [M + H]+ ion for compound **5** at m/z 1928.11 (Δ = -3.3 ppm). C) MS^2 of ion 756.4 indicating the losses Pheol[20], Gln[19] and CN-Gln[18] and positioning the dehydrated Gln residue in the fragment y_{7+} of the molecule. The peak at 1171.67 indicates the dehydration of Gln[7] in fragment b_{13+}

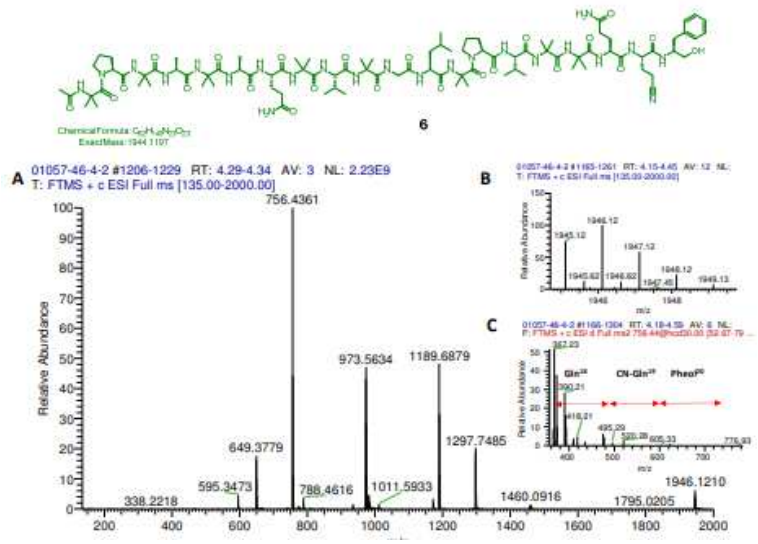

Figure A84: A) Full scan HRESIMS spectrum of compound **6**. B) Expansion of the [M + H]+ ion for compound **6** at m/z 1945.12 (Δ = -3.6 ppm). C) MS^2 of the ion 756.4 indicating the losses Pheol[20], CN-Gln[19] and Gln[18] and positioning the dehydrated Gln residue in the fragment y_{7+} of the molecule.

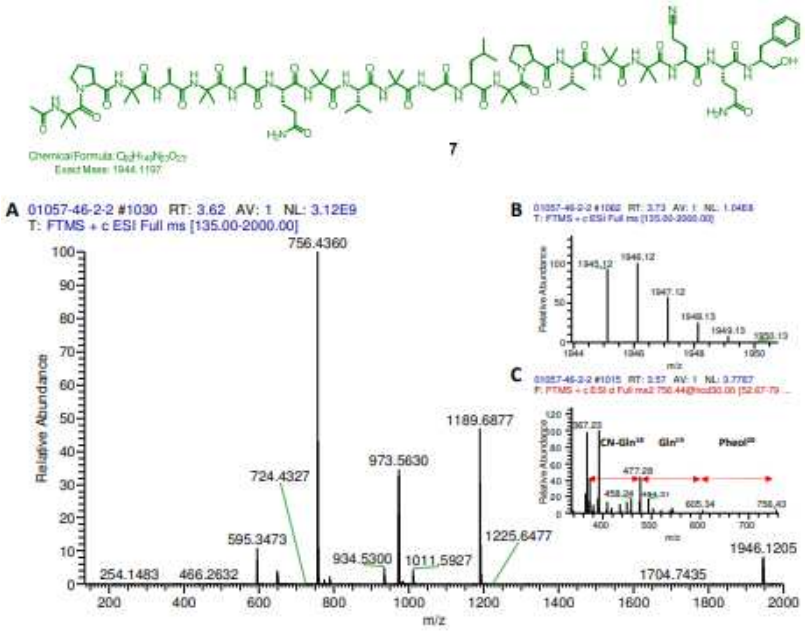

Figure A85: A) Full scan HRESIMS spectrum of compound **7**. B) Expansion of the [M + H]+ ion for compound **7** at m/z 1945.12 (Δ = -3.6 ppm). C) MS^2 of the ion 756.4 indicating the losses Pheol[20], Gln[19] and CN-Gln[18] and positioning the dehydrated Gln residue in the y_{7+} fragment of the molecule.

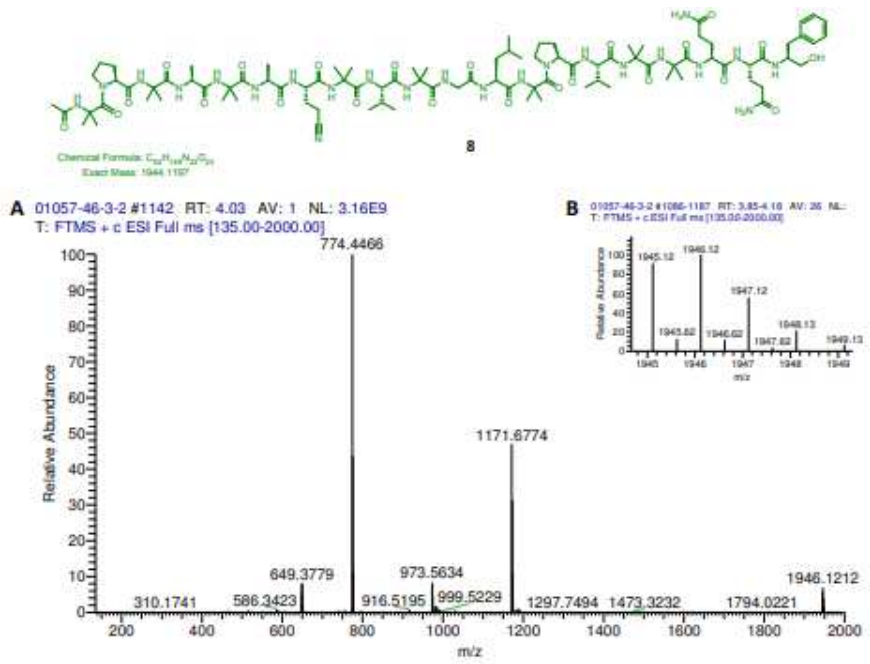

Figure A86: Full scan HRESIMS spectrum of compound **8**. B) Expansion of the [M + H]+ ion for compound **8** at m/z 1945.12 (Δ = -3.6 ppm). The peak at 1171.67 indicates the dehydration of Gln^7 in fragment b_{13+} .

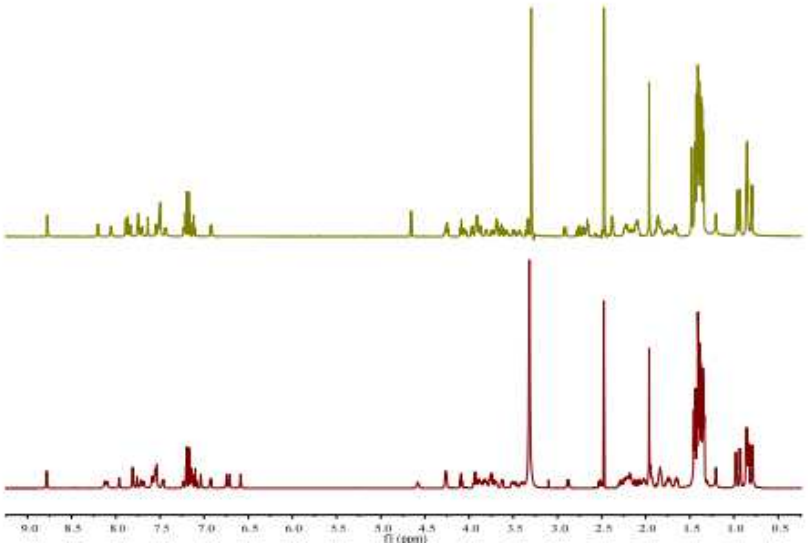

Figure A87: ^{1}H NMR spectra of compounds **1** (bottom) and **2** (top), recorded at 700 MHz in DMSO-d_6

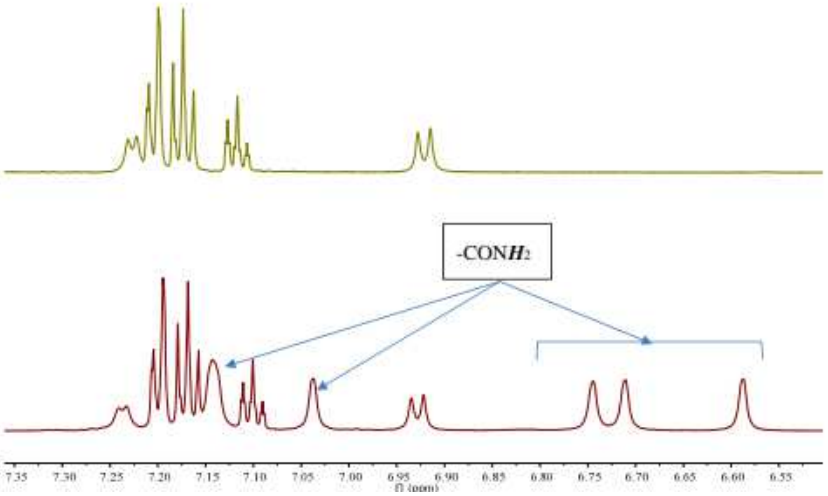

Figure A88: Expansion of the ^{1}H NMR amide region of compounds **1** (bottom) and **2** (top), recorded at 700 MHz in DMSO-d_6

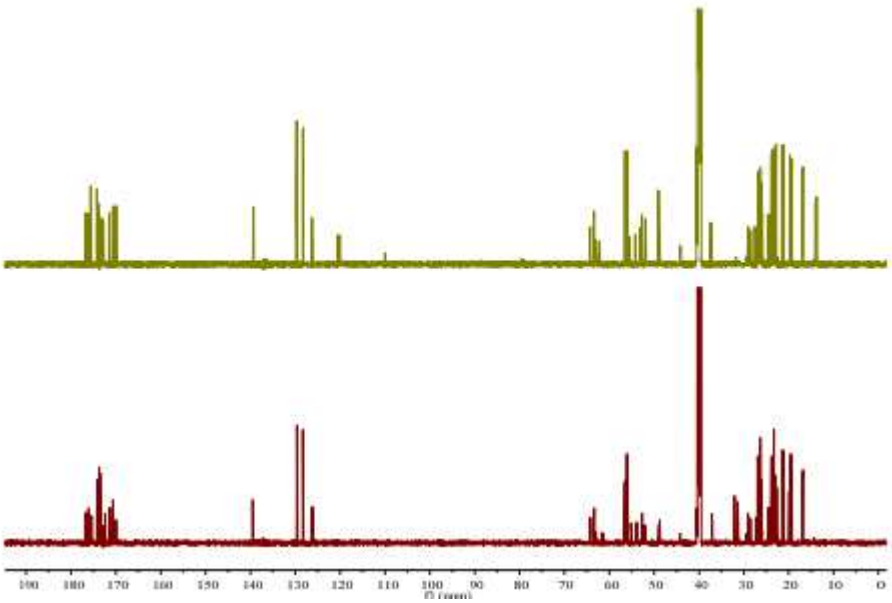

Figure A89: ^{13}C NMR spectra of compounds **1** (bottom) and **2** (top), recorded at 175 MHz in DMSO-d_6

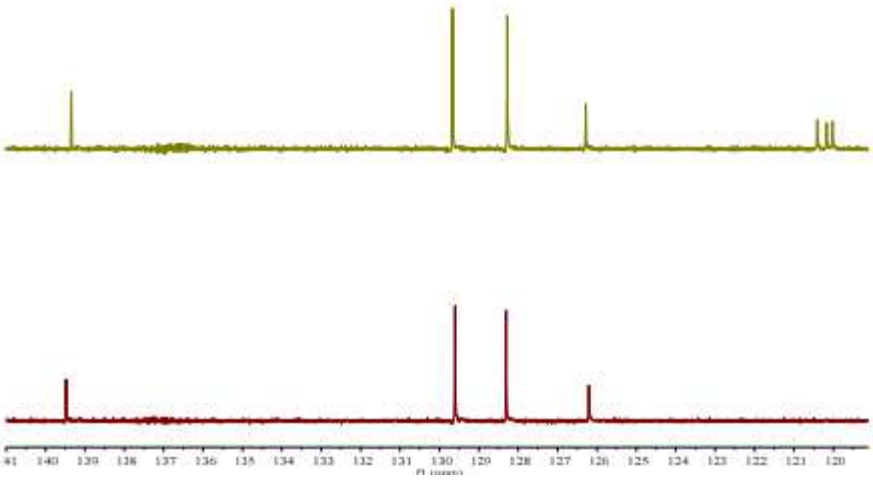

Figure A90: Expansion of the ^{13}C NMR of compounds **1** (bottom) and **2** (top), recorded at 175 MHz in DMSO-d_6, showing the carbons attributed to the aromatic moiety in **1**, the aromatic ring and nitrile carbons (120 – 121 ppm) in **2**.

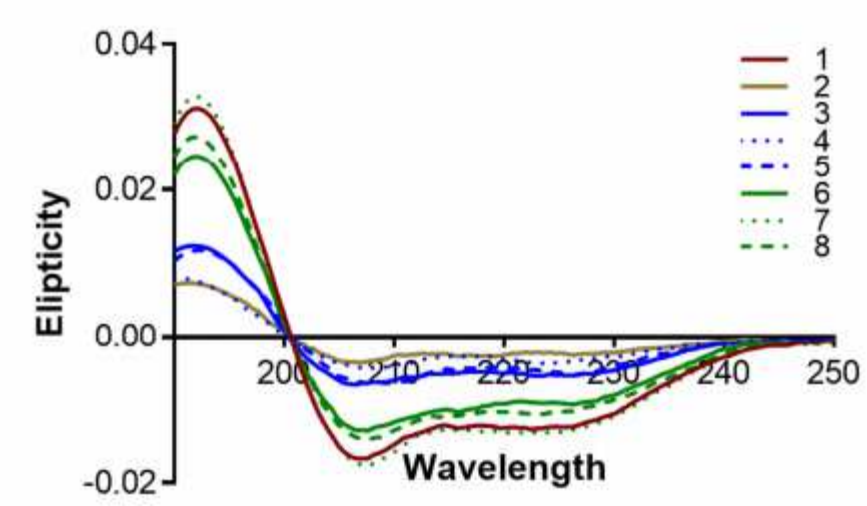

Figure A91: Full spectra overlay of far UV/CD spectra for alamethicin F50 (**1**) and its dehydrated analogues (**2-8**)

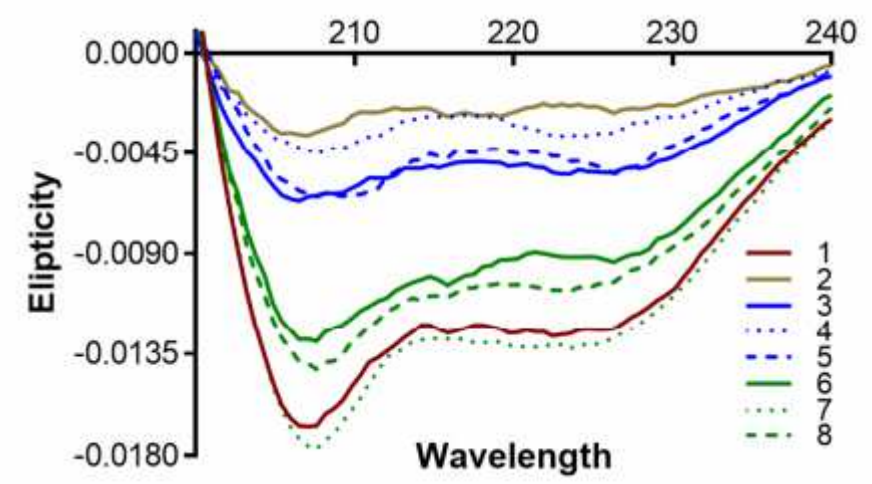

Figure A92: . Zoomed in image of far UV/CD spectra for alamethicin F50 (**1**) and its dehydrated analogues (**2-8**).

Cytotoxicity Assay

Human melanoma cancer cells MDA-MB-435, human breast cancer cells MDA-MB-231, and human ovarian cancer cells OVCAR3 were purchased from the American Type Culture Collection (Manassas, VA, USA). The cell lines were propagated at 37 °C in 5% CO_2 in RPMI 1640 medium, supplemented with fetal bovine serum (10%), penicillin (100 units/mL), and streptomycin (100 µg/mL). Cells in log phase of growth were harvested by trypsinization followed by two washes to remove all traces of enzyme. A total of 5,000 cells were seeded per well of a 96-well clear, flat-bottom plate (Microtest 96, Falcon) and incubated overnight (37 °C in 5% CO_2). Samples dissolved in DMSO were then diluted and added to the appropriate wells (several concentrations; total volume: 100µL; DMSO: 0.5%). The cells were incubated in the presence of test substance for 72 h at 37 °C and evaluated for viability with a commercial absorbance assay (CellTiter 96 AQueous One Solution Cell Proliferation Assay, Promega Corp, Madison) that measured viable cells. IC50 values were determined as the concentration required to reduce cellular proliferation by 50% relative to the untreated controls following 72 h of continuous exposure. Paclitaxel (taxol) was used as a positive control.